

UC San Diego

Research Theses and Dissertations

Title

Life History, Abundance, and Distribution of the Spotted Ratfish, *Hydrolagus coliei*

Permalink

<https://escholarship.org/uc/item/5t94c30s>

Author

Barnett, Lewis A.K.

Publication Date

2008-06-01

Peer reviewed

LIFE HISTORY, ABUNDANCE, AND DISTRIBUTION
OF THE SPOTTED RATFISH, *Hydrolagus colliei*

A Thesis

Presented to

The Faculty of Moss Landing Marine Laboratories
And the Institute of Earth Systems Science and Policy
California State University, Monterey Bay

In Partial Fulfillment

Of the Requirements for the Degree

Master of Science

In Marine Science

By

Lewis Abraham Kamuela Barnett

June 2008

© 2008
Lewis Abraham Kamuela Barnett

ALL RIGHTS RESERVED

APPROVED FOR THE DEPARTMENT OF MARINE SCIENCE

Dr. Gregor M. Cailliet, Advisor
Moss Landing Marine Laboratories

Dr. David A. Ebert
Moss Landing Marine Laboratories
Pacific Shark Research Center

Dr. James T. Harvey
Moss Landing Marine Laboratories

Dr. Enric Cortés
NOAA Fisheries, Southeast Fisheries Science Center

APPROVED FOR THE UNIVERSITY

LIFE HISTORY, ABUNDANCE, AND DISTRIBUTION
OF THE SPOTTED RATFISH, *Hydrolagus colliei*

Lewis Abraham Kamuela Barnett
California State University, Monterey Bay
2008

Size at maturity, fecundity, reproductive periodicity, distribution, and abundance were estimated for the spotted ratfish, *Hydrolagus colliei*, off the coast of California, Oregon, and Washington (USA). Skeletal muscle concentrations of the steroid hormones testosterone (T) and estradiol (E₂) predicted similar, but slightly smaller sizes at maturity than morphological criteria. Stage of maturity for males was estimated identically using internal organs or external secondary sexual characters, thus allowing non-lethal maturity assessments. Peak parturition occurred from May through October, with increased concentrations of E₂ and progesterone (P₄) in skeletal muscle of females correlating with ovarian recrudescence during November through February. Extrapolation of the hypothesized 6 to 8 mo egg-laying season to observed mean parturition rates of captive specimens yielded an estimated annual fecundity of 19.5 to 28.9 egg cases. Differences in fecundity among higher taxonomic classifications of chondrichthyans were detected, with chimaeriform fishes more fecund than myliobatiform, squaliform, and rhinobatiform fishes. Delta-lognormal generalized linear models (GLMs) and cluster analysis indicated the presence of two distinct stocks of *H. colliei* on the U.S. West Coast. Abundance of the continental slope, and northern continental shelf and upper slope populations did not vary between 1977 and 1995, but increased from 1995 to 2006. Abundance trends in the southern shelf and upper slope region were not as straightforward, with increasing abundance from 1977 to 1986, and lesser abundance thereafter, with the exception of an

increase between 1992 and 1995. Although the life history, movement patterns, and aggregative behavior of *H. colliei* indicated that it may be vulnerable to population depletion by excess fisheries mortality, temporal abundance trends indicated that their population size has increased significantly within the last decade. The paradigm that all chondrichthyans are particularly susceptible to exploitation, therefore, may not apply to chimaeroids. The hypothesis that the dorsal-fin spine of *H. colliei* is a reliable structure for age estimation was tested by analyzing growth characteristics and imaging with polarized light microscopy and micro-computed tomography. Variation among individuals in the relationship between spine width and distance from the spine tip indicated the technique of transverse sectioning may impart imprecision and bias to age estimates. The number of growth band pairs observed by light microscopy in the inner dentine layer was not a good predictor of body size. Mineral density gradients, indicative of growth zones, were not observed in the *H. colliei* dorsal-fin spine, but were present in hard parts used for age determination of the Patagonian toothfish (*Dissostichus eleginoides*), roughtail skate (*Bathyraja trachura*), and spiny dogfish (*Squalus acanthias*). The absence of mineral density gradients in the dorsal-fin spine of *H. colliei* decreases the likelihood that the bands observed by light microscopy represent a record of growth with consistent periodicity.

Acknowledgments

I thank my advisor Gregor Cailliet and co-advisor David Ebert for their great assistance, guidance, and support. Additional thanks to my colleagues Wade Smith and Joe Bizzarro for their superb advice and the wealth of knowledge and experience they readily give. Committee members Jim Harvey and Enric Cortés provided many helpful comments, improving my writing and synthesis skills. Mike Graham instigated many intriguing scientific discussions, and was always available for questions at a moment's notice. Jason Cope (NOAA Fisheries, Northwest Fisheries Science Center, Seattle Laboratory) and E.J. Dick (NOAA Fisheries, Southwest Fisheries Science Center, Santa Cruz Laboratory) offered unparalleled assistance toward my education in generalized linear modelling.

This project was made possible by cooperation and assistance in sample collection provided by the NOAA Fisheries, Northwest Fishery Science Center, especially Keith Bosley, Victor Simon, Erica Fruh, Melanie Johnson, and Beth Horness; Mark Zimmermann of the NOAA Fisheries, Alaska Fisheries Science Center; Allen Cramer, Sylvia Pauly, Kristen Green, and Jon Cusick of the West Coast Groundfish Observer Program (a cooperative effort between NOAA Fisheries, Pacific States Marine Fisheries Commission, and the states of Washington, Oregon, and California); Don Pearson, Kevin Stierhoff, and Josh Bauman from the NOAA Fisheries, Southwest Fisheries Science Center, Santa Cruz Laboratory; and Lee Bradford, Kurt Brown, and Jason Felton of the R/V John H. Martin. Gilbert Van Dykhuisen (formerly of the Monterey Bay Aquarium) graciously provided meticulously-collected data on the captive

mating and spawning of spotted ratfish. Dan Howard (NOAA Fisheries, Cordell Bank National Marine Sanctuary) stimulated several interesting discussions and eagerly supplied submersible data, and spotted ratfish coffee mugs.

Special thanks to my colleagues in the ichthyology laboratory at MLML (especially Aaron Carlisle, Chris Rinewalt, Tonatiuh Trejo, Matt Levey, Daniele Ardizzzone, Ashley Greenley, Simon Brown, Shaara Ainsley, Diane Haas, Ashley Neway, Jasmine Fry, Cassandra Brooks, Kristen Green, and Mariah Boyle), for thoughtful discussions, dissection assistance, entertainment on protracted van rides, laughter, and foosball matches. I'm extremely appreciative of the Moss Landing Marine Labs (MLML) front office staff, particularly Toni Fitzwater, Donna Kline, Kenneth Coale, and John Machado. Thanks to Joan Parker and the library staff (especially Laurie Hall, Shaara Ainsley, Rosemary Romero, Simon Brown, and Ashley Neway) for procuring obscure documents at my request, and not hassling me too much when I tried to interlibrary loan items that were available within our own confines. My sanity owes its continued existence to my friends, most notably Alison Myers, Chris Scianni, Phil Hoos, Ronnie Hoos, Charlie Endris, Jon Walsh, Berkeley Kauffman, and Cori Gible. Without these people distracting me from the rigors of graduate school, I would have burned out much earlier, yet likely graduated sooner. I'm incredibly grateful for the emotional support, patience, and love given by my girlfriend, Joëlle. She has kept my mind open, and her influence has stoked my appreciation of so many things in life.

I owe my values, sense of humor, and love for the outdoors to my parents, Dave and Barbara. Any and all of my successes in life can be attributed to my upbringing. This work is dedicated to my mother, for teaching me the joys of reading and the nuances

of caring. Thanks to my brother, Rabinder, for continuing to dispense brotherly advice, despite my resistance to follow much of it. To the rest of my family, Norm, Rita, Jean, Gail, Al, Jan, Mike, Deb, Greg, Zach, Chloë, Polly, Emily, Laurie, Paul, Susan, Madeline, Lola, Paloma, Chris, and Miki, my sincere gratitude for being so loving, close, and supportive.

This study was supported by funds from NOAA/NMFS to the National Shark Research Consortium, Pacific Shark Research Center, and in part by the National Sea Grant College Program of the U.S. Department of Commerce's National Oceanic and Atmospheric Administration under NOAA Grant no. NA04OAR4170038, project number R/F-199, through the California Sea Grant College Program and in part by the California State Resources Agency. Other funding was acquired from the Dr. Earl H. Myers and Ethel M. Myers Oceanographic and Marine Biology Trust; Western Division of the American Fisheries Society Eugene Maughan Graduate Student Scholarship; David and Lucile Packard Research and Travel Award; John H. Martin Scholarship; San Jose State University Professional Development Awards; Kim Peppard Memorial Scholarship; and a PADI Foundation Grant.

Table of Contents

List of Tables.....	xii
List of Figures.....	xiii
List of Appendices.....	xviii
Chapter 1: Maturity, fecundity, and reproductive cycle.....	1
Introduction.....	2
Materials and Methods.....	5
Reproductive Status.....	9
Reproductive Seasonality.....	11
Results.....	14
Maturity.....	15
Effects of differing sample collection methods.....	17
Reproductive Seasonality.....	18
Fecundity.....	20
Discussion.....	21
Maturity.....	21
Reproductive Seasonality.....	23
Fecundity.....	28
Literature Cited.....	33
Tables.....	51
Figures.....	56

Chapter 2: Abundance and distribution.....	78
Introduction.....	79
Materials and Methods.....	81
Natural Mortality.....	87
Results.....	88
Selectivity and the Distribution of Ontogeny and Sex.....	88
Natural Mortality.....	89
Spatial and Temporal Trends.....	89
Discussion.....	91
Selectivity and the Distribution of Ontogeny and Sex.....	91
Natural Mortality.....	93
Spatial and Temporal Trends.....	93
Conclusions.....	97
Literature Cited.....	99
Tables.....	108
Figures.....	109
Appendix.....	119
Chapter 3: Assessment of the dorsal-fin spine for chimaeroid (Holocephali: Chimeriformes) age estimation.....	127
Introduction.....	128
Materials and Methods.....	130
Age and Growth Determination.....	130

Computed Tomography.....	132
Results.....	133
Growth.....	133
Physiology of Hard Parts.....	135
Discussion.....	136
Growth.....	136
Physiology of Hard Parts.....	138
Conclusions.....	140
Literature Cited.....	141
Figures.....	146

List of Tables

Chapter 1: Maturity, Fecundity, and reproductive cycle

Table 1.....	51
Length of spawning season and depth of demersal chondrichthyan species used in comparative analyses, each estimated as the midpoint of the range from the literature. Data are either from original sources, or sources compiled in the Pacific Shark Research Center's (PSRC) Life History Data Matrix of eastern North Pacific chondrichthyan: http://psrc.mlml.calstate.edu/ . Chimaeroids included are from multiple ocean basins and elasmobranchs are from the eastern North Pacific.	
Table 2.....	52
Fecundity and maximum length of chondrichthyan species used in comparative analyses. Fecundity was estimated as the midpoint of the range from the literature, or the average if available (sources are from citations in Musick and Ellis 2005 or the Pacific Shark Research Center's (PSRC) Life History Data Matrix of eastern North Pacific chondrichthyan: http://psrc.mlml.calstate.edu/ , unless otherwise stated).	
Table 3.....	54
Results of <i>t</i> -tests comparing temporal trends in hormone concentration between sampling periods in June and September as measured from skeletal muscle and plasma.	
Table 4.....	55
Results of paired <i>t</i> -tests comparing hormone concentrations of skeletal muscle sampled from the same individual immediately after capture and three hours after capture.	

Chapter 2: Abundance and Distribution

Table 1.....	108
Model selection criteria for each delta-GLM, sorted by AIC score of the binomial fit. Final models are in bold.	

List of Figures

Chapter 1: Maturity, Fecundity, and reproductive cycle

Figure 1.....	56
Spatial distribution of samples collected from 2003 to 2007 off California, Oregon, and Washington (between 32.6° to 48.4° N and 117.3° to 125.6° W).	
Figure 2.....	57
Length-weight regression for both sexes combined.	
Figure 3.....	58
Ratio of inner clasper length to snout-vent length, displayed as a function of snout-vent length for individuals defined by the morphological criteria as juveniles (filled circles), adolescents (open circles), and adults (gray triangles).	
Figure 4.....	59
Linear regression of inner clasper length on testis length.	
Figure 5.....	60
Comparison of testis length to width, displaying isometric growth of internal and external sex organs.	
Figure 6.....	61
Comparison of the maturity estimates made from the morphological criteria and frontal tenaculum criteria. Error bars represent 95% confidence intervals. A dotted line with a slope of one and intercept of zero is shown for reference.	
Figure 7.....	62
Ratio of oviducal gland width to snout-vent length, displayed as a function of snout-vent length for individuals defined by the morphological criteria as juveniles (filled circles), adolescents (open circles), adults (gray triangles), and gravid adults (black triangles).	
Figure 8.....	63
Maturity ogives (A) for males (empty triangles) and females (filled circles), based on the morphological criteria; (B) for females using the morphological criteria (empty triangles) and estradiol concentration (filled circles); (C) for males using the morphological criteria (empty triangles) and testosterone concentration (filled circles); (D) for females north (filled circles) and south (empty triangles) of Point Conception; (E) for males north (filled circles) and south (empty triangles) of Cape Mendocino. Broken lines are 95% confidence bands.	
Figure 9.....	64
Comparison of mean steroid hormone concentrations from paired samples of muscle and plasma. Error bars represent 95% confidence intervals.	

Figure 10.....	65
Comparison of mean steroid hormone concentrations from muscle sampled immediately (before) and three hours later (after). Error bars represent 95% confidence intervals.	
Figure 11.....	66
Proportion of adult females in gravid reproductive state, by month. Sample sizes are in parentheses.	
Figure 12.....	67
Mean number of mature ova per female by month. Error bars represent 95% confidence intervals. Sample sizes are in parentheses. Letters indicate significant differences among months.	
Figure 13.....	68
Mean number of fully developed ova per female, standardized by total body mass, by month. Error bars represent 95% confidence intervals. Sample sizes are in parentheses.	
Figure 14.....	69
Mean female 11KT muscle concentration by month. Error bars represent 2 SEs. Sample sizes are in parentheses. Letters indicate significant differences among months.	
Figure 15.....	70
Mean female P ₄ muscle concentration by month. Error bars represent 2 SEs. Sample sizes are in parentheses. Letters indicate significant differences among months.	
Figure 16.....	71
Mean female E ₂ muscle concentration by month. Error bars represent 2 SEs. Sample sizes are in parentheses. Letters indicate significant differences among months.	
Figure 17.....	72
Mean female T muscle concentration by month. Error bars represent 2 SEs. Sample sizes are in parentheses.	
Figure 18.....	73
Mean oviducal gland index by month. Error bars represent 95 % confidence intervals. Sample sizes are in parentheses. Letters indicate significant differences among months.	
Figure 19.....	74
Mean female gonadosomatic index by month. Error bars represent 95% confidence intervals. Samples sizes are in parentheses. Letters indicate significant differences among months.	
Figure 20.....	75
Mean male gonadosomatic index by month. Error bars represent 95% confidence intervals. Samples sizes are in parentheses. Letters indicate significant differences among months.	

Figure 21.....76
Number of fully developed ova (20 mm diameter or greater) per reproductively active adult female, as a function of somatic body weight.

Figure 22.....77
Maximum ovum diameter per adult female as a function of snout-vent length. Filled circles represent reproductively active individuals (those with maximum ovum diameter of 16 mm or greater), and open circles represent inactive individuals (those with maximum ovum diameter of less than 16 mm).

Chapter 2: Abundance and Distribution

Figure 1.....109
Start-of-haul locations for (A) the AFSC triennial trawl surveys (1977 to 2004), and (B) the NWFSC West Coast Groundfish Surveys (2003 to 2006). Samples shown here are those restricted to the latitudinal range used for abundance analysis (36.5° to 48.5° N).

Figure 2.....110
Proportion of positive tows by 50 m depth bin (each bin comprises 50 m from the given x-axis label).

Figure 3.....111
Start-of-haul locations for the 2005 and 2006 NWFSC West Coast Groundfish Surveys. Hauls with zero catch are in grey and those with positive catch are in black.

Figure 4.....112
Proportion of male ratfish by depth. Linear regression lines are shown for each degree of latitude, but raw data are not shown for the sake of clarity.

Figure 5.....113
Survey selectivity function for the NWFSC West Coast Groundfish Survey, from the years 2005 and 2006 ($n = 7,020$).

Figure 6.....114
Length-frequencies by depth for males and females between the latitudinal regions (A) 39.5° to 48.5° N, (B) 36.5° to 39.5° N, (C) 34.5° to 36.5° N, and (D) 32.6° to 34.5° N.

Figure 7.....115
GLM-standardized CPUE estimates from the continental slope (250 to 500 m depth) between the latitudes of 36.5° to 48.5° N (A), the continental shelf and upper slope (50 to 250 m depth) between the latitudes of 39.5° to 48.5° N (B), and 36.5° to 39.5° N (C). Error bars represent SEs. Dotted lines represent the geometric mean CPUE. Open squares represent geometric mean CPUE from the NWFSC survey, standardized by the GLM-standardized 2004 triennial trawl CPUE.

Figure 8.....116
Standardized CPUE estimates for the entire survey area by 0.5° latitude bin (each bin comprises 0.5° north from the given x-axis label). Error bars represent SEs. A dotted line represents the geometric mean CPUE.

Figure 9.....117
Groundfish landings off California, Oregon, and Washington from 1981 to 2007 (PacFIN 2008).

Figure 10.....118
Bubble plot of raw CPUE data by depth and latitude. Size of the bubbles correspond to the relative CPUE, with zero catches in gray.

Chapter 3: Assessment of the dorsal-fin spine for chimaeroid (Holocephali: Chimeriformes) age estimation

Figure 1.....146
Comparison of snout-vent length to (A) total dorsal-fin spine length, (B) distance between the dorsal-fin spine tip and the apex of the pulp cavity, and (C) dorsal-fin spine width at the apex of the pulp cavity.

Figure 2.....147
Comparison of distance from dorsal-fin spine tip and spine width among individuals ($n = 28$). Lines represent linear regressions for each individual.

Figure 3.....148
Photomicrograph of a transversely sectioned dorsal-fin spine (A) anterior dentine portion, and (B) posterior face, viewed with transmitted light. SL = spine lumen; IL = inner dentine layer; OL = outer dentine layer. Scale = 0.5 mm.

Figure 4.....149
Photomicrograph of a transversely sectioned dorsal-fin spine viewed with polarized, transmitted light. Scale = 0.5 mm.

Figure 5.....150
Comparison of the number of dorsal-fin spine band pairs to (A) snout-vent length, and (B) total mass for females ($n = 16$).

Figure 6.....151
 μ CT image of the (A) transverse plane of a second dorsal fin spine, and (B) the longitudinal plane of a vertebra from *S. acanthias*. Arrows indicate density gradients that may represent distinct growth zones. Scale = 0.5 mm.

Figure 7.....	152
<p>μCT image of the (A) transverse plane of a vertebra, and (B) the longitudinal plane of a caudal thorn (just anterior to the thorn tip) from <i>B. trachura</i>. Arrows indicate density gradients that may represent distinct growth zones. Scale = 0.5 mm.</p>	
Figure 8.....	153
<p>μCT image of the transverse plane of a <i>D. eleginoides</i> otolith, just posterior to the focus. Arrows indicate density gradients that may represent distinct growth zones. Scale = 0.5 mm.</p>	
Figure 9.....	154
<p>μCT images of the <i>H. colliei</i> dorsal-fin spine, in the longitudinal (dorso-ventral) plane (A), and in the transverse plane, depicting dentine canals leading to the posterior (B) and anterior (C) spine exterior. Scale = 0.5 mm.</p>	
Figure 10.....	155
<p>μCT images of the <i>H. colliei</i> neural arch and vertebrae, from the transverse plane (A), and the longitudinal plane (B and C). Scale = 0.5 mm.</p>	

List of Appendices

Chapter 2: Abundance and Distribution

Generalized linear model diagnostic graphs.....	118
Figure 1.....	119
Quantile residuals against each explanatory variable for the binomial GLMs. Dotted line indicates the null pattern.	
Figure 2.....	120
Standardized deviance residuals against each explanatory variable for the positive GLMs. Dotted line indicates the null pattern.	
Figure 3.....	121
Quantile-quantile plots of the quantile residuals from the binomial GLMs, with a line fit through the first and third quantiles.	
Figure 4.....	122
Quantile-quantile plots of the standardized deviance residuals from the binomial GLMs, with a line fit through the first and third quantiles.	
Figure 5.....	123
Quantile residuals against fitted values for the binomial GLMs, with a Loess smoother (span = 2/3). Dotted line indicates the null pattern.	
Figure 6.....	124
Standardized deviance residuals against fitted values for the positive GLMs, with a Loess smoother (span = 2/3). Dotted line indicates the null pattern.	
Figure 7.....	125
Proportion of positive tows predicted by the binomial model against the proportion of positive tows observed. Cells with less than five observations were excluded from the analysis. Dotted line is a 1:1 reference.	

Chapter 1

Maturity, fecundity, and reproductive cycle

Introduction

Hydrolagus colliei (Lay and Bennett, 1839) is a member of the monophyletic class Chondrichthyes (Didier 1995; Grogan and Lund 2004; Maisey 1984; Maisey 1986; Schaeffer 1981), which includes the subclasses Holocephali (chimaeras or ratfishes) and Elasmobranchii (sharks and rays). Holocephalans are differentiated from elasmobranchs by numerous morphological characters, most notably a palatoquadrate fused to the neurocranium and non-replaceable teeth fused into three pairs of hypermineralized tooth plates (Didier 1995; Lund and Grogan 1997; Maisey 1986). Holocephalans are evolutionarily significant, with ancestors originating at least 300 million years ago (Grogan and Lund 2004).

Holocephalans occur in marine environments worldwide except polar seas. There are 37 species in the single order Chimaeriformes (Barnett et al. 2006; Compagno 2005; Moura et al. 2005; Quaranta et al. 2006), with ~ ten new species awaiting formal description (Dominique Didier, Millersville University, pers. comm.). Members of the order Chimaeriformes are commonly called chimaeroids or chimaeras, however, only the former term will be used in this paper, as the latter refers only to members of the genus *Chimaera*.

The impetus for researching the life history of chondrichthyans has been well documented during the past three decades. The majority of chondrichthyans have k-selected life history characteristics such as lesser growth rate, greater longevity, later age at first maturation and less reproductive output than most teleosts (review in Cailliet and Goldman 2004; Holden 1974). These biological characteristics, combined with their tendency to aggregate in large groups (Klimley 1987; Springer 1967; Steven 1933;

Strasburg 1958) may make chondrichthyans more susceptible to overfishing than most teleosts (Bonfil 1994; Cailliet 1990; Hoenig and Gruber 1990; Holden 1973; Stevens et al. 2000; Walker 1998). Fishes that inhabit the deep waters of the continental slope or beyond may exhibit k-selected life-history characteristics that are more extreme than their shallow-dwelling relatives, potentially making these species even more vulnerable to overexploitation (Anon 1997; Cailliet et al. 2001; Clarke et al. 2003; Gordon 1999; Roberts 2002). These obstacles to sustainable harvest are compounded by vast under-reporting of chondrichthyan catch (Bonfil 1994), and misidentification and intentional combination of taxonomic categories in catch statistics (Dulvy et al. 2000).

Hydrolagus colliei is found from southeast Alaska (Wilimovsky 1954) to the tip of Baja and within the northern Gulf of California (Grinols 1965). Its bathymetric distribution is quite broad, along the shelf and slope from the intertidal (Cross 1981; Dean 1906) to 913 m depth (Alverson et al. 1964). Although there is not currently a directed fishery for *H. colliei*, they are captured and discarded by recreational fishermen, as well as commercial bottom trawl and longline fisheries.

Chimaeroids are oviparous, forming egg cases that encapsulate individual embryos (Dean 1906). One or two egg cases are extruded onto the seafloor during parturition (Veronica Franklin, Monterey Bay Aquarium, pers. comm.). Gestation is estimated at 9 to 12 mo for *H. colliei* (Dean 1906) and 5 to 12 mo for the elephantfish, *Callorhinchus milii* (Didier et al. 1998; Gorman 1963), both with similar stages of embryological development. Development of *H. colliei* embryos collected by Dean (1906) off California indicated that egg case deposition occurs year-round, with a maximum in late summer or early fall. Sathyanesan (1966) found a similar pattern off

northwestern Washington, where gravid females were present in summer and winter, yet mature ova were more abundant and *in utero* egg cases more prevalent in females during summer. The lack of clear seasonality of reproduction also was evident in *Hydrolagus barbouri*, which produces eggs throughout the year and displays no distinct spawning season (Kokuho et al. 2003).

Estimation of fecundity may be difficult because offspring production in many chimaeroids is continuous (Dean 1906; Kokuho et al. 2003; Sathyanesan 1966).

Chimaeroids are serial indeterminant spawners, making it difficult to determine duration of spawning season, because vitellogenic oocytes are found in the ovary in various stages of development for protracted and often poorly defined time periods. Spawning frequency also is particularly difficult to determine, because it is not easy to acquire many fresh specimens for histological analysis of post-ovulatory follicles because of their offshore distribution and the use of fishery-dependent sampling methods. Sperm storage occurs in the chimaeroid oviducal gland (Smith et al. 2004), indicating that the timing of mating is not necessarily coincident with the timing of parturition. To obtain a better resolution of the seasonal reproductive cycle, concentrations of the steroid hormones testosterone (T), 11-ketotestosterone (11KT), estradiol (E₂), and progesterone (P₄) were analyzed in adult females. These are representatives of the primary hormones involved in reproduction of fishes (Borg 1994; Pankhurst 2008). This is the first study to assess steroid hormone concentrations for a species in the order Chimaeriformes.

The purpose of this project was to assess the reproductive biology of the spotted ratfish, *Hydrolagus colliei* (Lay and Bennett, 1839), as it relates to life history evolution and present and potential direct or indirect harvest of the species. Life history data for

many eastern North Pacific chondrichthyans is lacking, yet it is necessary for proper population assessment. This study provides estimates of the fecundity and seasonality of parturition of *H. colliei*. These data provide a baseline of life history information for chimaeroids, and are used to quantitatively test the hypotheses that fecundity is greater in oviparous than viviparous chondrichthyan lineages and that length of reproductive season increases with increasing depth range.

Materials and Methods

Specimens were collected from the continental slope and shelf of California, Oregon, and Washington, with the greatest number of samples off Monterey Bay, California (Fig. 1). Monterey Bay samples were collected from monthly trawl and long-line surveys from October, 2003 to April, 2005 (conducted by NOAA NMFS, Southwest Fisheries Science Center, Santa Cruz Laboratory). Trawls conducted by the Northwest Fishery Science Center West Coast Groundfish Survey between May and October during 2004 to 2007 provided specimens from numerous locations off the coast of California, Oregon, and Washington.

To define stage of reproductive development I measured various morphometrics. Lengths were measured to the nearest mm and mass to the nearest gram. External measurements of precaudal length (PCL), snout-vent length (SVL), and inner clasper length were recorded following Didier and Rosenberger (2002). I measured total mass, liver mass, gonad mass, seminal vesicle mass, testes length, testes width, oviducal gland width, and uterus width. The number of mature ova (those greater than 6 mm diameter with yellow coloration; Stanley 1961), fully developed ova (those greater than 20 mm

diameter; Stanley 1961), and diameter of the largest ovum were recorded from each ovary.

Blood was extracted into lithium heparinized microcentrifuge tubes from a subset of males and females via cardiac puncture shortly after capture. Blood samples were put on ice for 1-3 h, then centrifuged at $\sim 1,300$ g for 10 min. Plasma was pipetted off into microcentrifuge tubes and stored frozen at -18° C for later analysis. Skeletal muscle tissue was excised from the dorsum, just posterior to the uterine openings.

Before hormone assay, plasma samples were thawed, centrifuged at $14,000$ g for 5 min, and 500 μ l of plasma was transferred to 12×75 mm borosilicate vials. Ether extractions were conducted. Briefly, 2 ml diethyl ether was added to each borosilicate vial, and the sample was vortexed for 4 min on a multi-tube vortexer. The ether and aqueous phases were allowed to separate for 3 min, and the aqueous phase was then fast-frozen in a methanol-dry ice bath for 2 min before decanting the ether phase into a new 12×75 mm borosilicate vial. The procedure was repeated on the remaining aqueous phase, and the second ether sample was decanted into the same vial as the first. Ether was evaporated under a gentle stream of nitrogen in a 37° C water bath. Extracts were resuspended in 2 ml 0.1 M phosphate buffer for assay (1: 4 dilution).

Two muscle samples of ~ 500 mg were used for the T/11KT (mean \pm SE: 517 ± 1 mg) and the E_2/P_4 assays (mean \pm SE: 515 ± 2 mg). These muscle samples were excised from a large piece of tissue on dry ice, weighed, transferred directly to 1 to 2 ml borate buffer in a 12×75 mm borosilicate vial, and homogenized for 30 sec. Homogenate was transferred to a 16×125 mm borosilicate vial and 4 ml diethyl ether was added to the sample followed by vortexing for 4 min on a multi-tube vortexer. The ether and aqueous

phases were allowed to separate for 2 min, followed by centrifugation at 5,6000 g for 1 min at 4° C to pellet lipids in the tissue mass, and fast-freezing of the aqueous layer in a methanol-dry ice bath for 2 min before decanting the ether phase. As with the plasma, this procedure was repeated, ether layers were combined, and ether was evaporated. Hormone pellets were stored at -20° C until reconstitution in 250 µl 0.1 M phosphate buffer and assay. Reconstitution volume was determined from pilot assays, which I used to evaluate the volume necessary to fall within the linear range of the T/11KT and E₂/P₄ standard curves.

Plasma and muscle samples from males were assayed for T and 11KT, and samples from females were assayed for T, 11KT, E₂, and P₄. Samples were analyzed for P₄ and E₂ using coated-tube and double antibody radioimmunoassay kits, respectively (Siemens Medical Solutions Diagnostics, Los Angeles, CA). Samples were analyzed for T with double antibody radioimmunoassay kits from Diagnostic Systems Laboratories (Webster, TX), and for 11KT with enzyme-immunoassay kits (Cayman Chemicals, Ann Arbor, MI). Manufacturer's protocols were strictly followed. A control sample was generated from 20, 500 mg muscle samples processed in the same manner as described above, resuspended in 300 µl 0.1 M phosphate buffer, and pooled (6 ml). Aliquots (6, 1 ml samples) were used for intra- and inter-assay controls. Testosterone was quantified in two separate assays with intra-assay coefficients of variation (CVs) of 2.86% and 3.56%, and inter-assay CV of 4.21%. 11-Ketotestosterone was assayed on 7, 96-well plates with intra-assay CVs of 9.22%, 20.4%, 12.9%, 11.9%, 15.5%, and 15.7%, and an inter-assay CV of 16.7%. Estradiol was quantified in two separate assays with intra-assay CVs of

10.3% and 4.5%, and inter-assay CV of 8.3%. Progesterone was quantified in one assay with an intra-assay CV of 9.9%.

Each kit was validated for *H. coliei* muscle steroids by generating serial dilutions of the control sample (see previous paragraph) and assessing parallelism with the standard curve using a *t*-test. Significant parallelism was achieved for all hormones except progesterone (11KT: $t = 0.025$, $df = 8$, $p = 0.98$; T: $t = 1.614$, $df = 6$, $p = 0.2$; E₂: $t = 1.95$, $df = 6$, $p = 0.1$; P₄: $t = 7.08$, $df = 8$, $p < 0.001$); the serial dilution curve for P₄ exhibited a steep negative slope relative to the standard curve. Recovery was assessed by spiking the control sample with each kit standard, and by determining the relationship between expected (based on known control concentration) and observed concentrations. Slopes of all observed vs. expected regressions approximated 1.0, indicating good recovery (11KT: $F = 80.63$, $df = 1, 7$, $p < 0.001$, $\beta_1 = 1.05$, minimum recovery = 69%; T: $F = 5928.7$, $df = 1, 6$, $p < 0.001$, $\beta_1 = 1.26$, minimum recovery = 96%; E₂: $F_{1,6} = 15.06$, $df = 1, 6$, $p = 0.012$, $\beta_1 = 0.75$, minimum recovery = 111%; P₄: $F = 63.24$, $df = 1, 6$, $p = 0.0002$, $\beta_1 = 0.71$, minimum recovery = 58.4%). Sensitivities of the assays were 1.3 pg/ml for 11KT, 0.05 ng/ml for T, 1.4 pg/ml for E₂, and 0.02 ng/ml for P₄.

Weight-at-length data were analyzed with both sexes combined, because there were no sex-specific trends. A non-linear regression was fit using the model that produced the greatest adjusted R^2 value, a two-parameter power function:

$$W = aL^b$$

Where W is weight in kg, L is snout-vent length in mm, a and b are estimated iteratively.

Reproductive Status

Stage of reproductive development was determined based on macroscopic assessment of development of the epididymis, claspers, ovaries, oviducal gland, and thickness of the uterine wall (after Ebert 1996; Gorman 1963; Stanley 1961; Walmsley-Hart et al. 1999). I refer to this as the morphological criteria. The stages are defined as follows:

Males

1. Embryo: developing within egg case
2. Juvenile: no coiling of epididymis; post-pelvic claspers extremely short, uncalcified, and soft
3. Adolescent: epididymis enlarged, with few coils; post-pelvic claspers beginning to elongate but not completely calcified
4. Adult: epididymis with many, tight coils; post-pelvic claspers elongated, completely calcified and rigid

Females

1. Embryo: developing within egg case
2. Juvenile: uterus narrow with thin epithelial wall; oviducal gland marked by a minor widening of the oviduct; oocytes barely visible and whitish
3. Adolescent: oviducal gland slightly swollen and differentiated from uterus but without visibly contrasting tissue zones; uterine wall thin; oocytes small (≤ 6 mm diameter) and whitish

4. Adult: oviducal gland fully developed with bulbous bullet-shape and sharply contrasting tissue zones; uterine wall thick, especially proximal to uterine openings where it is muscular and resistant to compression; oocytes large (> 6 mm diameter), yellow, and vascularized
5. Gravid Adult: fully or partially developed egg case present in uteri

During the assessment of maturity status of males using the morphological criteria, a correspondence was observed between the stages of maturity defined above, and distinct stages of frontal tenaculum development as defined below:

1. Juvenile: frontal tenaculum not yet erupted
2. Adolescent: frontal tenaculum erupted, yet not fully developed, with hooks uncalcified or not present
3. Adult: frontal tenaculum fully developed with calcified hooks

This correspondence was tested by regressing maturity stages estimated using the frontal tenaculum criteria on stages estimated using the morphological criteria, testing the hypothesis that $\beta_1 = 1$ (1:1 agreement of maturity stage) with a *t*-test.

To verify maturity status in males, the ratio of inner clasper length to body length was plotted against body length. For females, the ratio of oviducal gland width to body length was plotted against body length. An abrupt change in the proportion of these ratios to body length was assumed to represent onset of maturity. Testis length was plotted against inner clasper length, to test whether growth of internal and external

reproductive organs was collinear and whether abrupt increases in size, associated with maturation, were concurrent.

Length at 50% maturity was estimated using a logistic regression equation (Mollet et al. 2000; Neer and Cailliet 2001; Roa et al. 1999). To test for differences of length at maturity between sexes and geographic regions, these factors were included as main effects in a binomial logistic regression. Geographic regions were defined as north or south of Point Conception or Cape Mendocino, two coastal promontories which create oceanographic anomalies. Planned pairwise comparisons among regions were performed with an experiment-wise error rate of $\alpha = 0.0125$. To identify the temporal relationship of steroid hormone production and onset of maturity, estimates of size at median maturity derived from the morphological criteria were compared with estimates derived from the concentration of T in the skeletal muscle of males and E₂ from females. To create a steroid hormone criterion, maturity status was assigned to individuals based on a threshold concentration, assumed to indicate the onset of maturity. Threshold concentrations were estimated by identifying an abrupt increase of steroid hormone concentration with snout-vent length. Analysis of Residual Sums of Squares (ARSS) was used to determine whether the logistic regression equations used to predict length at maturity differed between morphological and hormone maturity criterion (Chen et al. 1992).

Reproductive Seasonality

Wet weights of the liver, gonads, and oviducal glands were measured to the nearest gram, and expressed as a ratio of total mass as the hepatosomatic (HSI),

gonadosomatic (GSI), and oviducalsomatic indices (OGI), respectively. These indices, calculated from a sample representative of all seasons, were plotted against month of capture to determine whether temporal parturition patterns occurred, thus increasing precision of fecundity estimates. Such indices alone, however, may not provide enough evidence to estimate periodicity of parturition, as for batoids (Maruska et al. 1996). Steroid hormone analysis, therefore, was used to verify reproductive seasonality in females.

Temporal trends in steroid hormone concentrations of plasma and skeletal muscle were compared with a series of *t*-tests. During two surveys off southern Oregon in early June and early September, 2006, paired samples of plasma and skeletal muscle were sampled from each individual. Temporal differences in levels of each hormone were tested separately within plasma and muscle, to verify that trends were similar between the two, as they are in the teleost fish *Mycteroperca microlepis* (Heppell and Sullivan 2000). Among individuals from both sampling periods, correlation between plasma and muscle hormone concentration was tested for each hormone separately.

A pilot test was used to determine whether the variable delay of sampling or freezing of specimens subsequent to capture was a source of measurement error in the greater study. For a subset of individuals, muscle tissue was sampled immediately after capture, and again after specimens remained at ambient sea surface temperature for three h. Paired *t*-tests were performed separately for each hormone to detect whether hormone concentrations were affected by the difference in length of time between capture and sampling or freezing of specimens.

Seasonal changes in OGI, the number of mature ova per female, and tissue concentrations of steroid hormones were tested with ANOVA. Assumptions of normality and were tested with Kolmogorov-Smirnoff tests, and homoscedacity with Levene's tests. Post-hoc multiple comparison tests were performed using Hotchberg's GT2 test, because sample sizes were greatly uneven. Kruskal-Wallis tests were used to compare seasonal changes in the number of fully developed ova per female, HSI, and GSI, because of heteroscedacity. For these non-parametric statistics, post-hoc multiple comparisons tests were performed using the Nemenyi-Damico-Wolfe-Dunn test (Hollander and Wolfe 1999; Hothorn et al. 2006). Least-squares regression analyses were used to test the hypothesis that length of spawning season of demersal chondrichthyan species increases with increasing midpoint of bathymetric range (Table 1; data for chimaeroid species from multiple ocean basins and elasmobranchs from the eastern North Pacific).

To estimate a maximum annual fecundity (the number of offspring produced per year), the observed rate of parturition (egg cases deposited / week) from each of two captive *H. colliei* at the Monterey Bay Aquarium was multiplied by the number of weeks in a year. To estimate a realized annual fecundity, the maximum annual fecundity was multiplied by the estimate of the proportion of the year the wild adult population is spawning, as determined with steroid hormones, indices of organ weights, and presence of *in utero* egg cases and mature ova in adult females. Descriptions of mating and egg-laying of captive *H. colliei* were provided from personal observations of Gilbert Van Dykhuizen, of the Monterey Bay Aquarium. Fecundity of chimaeroid species ($n = 2$) was quantitatively compared with that of other chondrichthyans (Table 2) with a series of randomization tests ($\alpha = 0.05$). Mean fecundity was compared between viviparous

species and oviparous species with a *t*-test. Fecundity for each species was estimated as the midpoint of the range reported in the literature, or the average if available. Before testing, least-squares linear regression analyses were used to test for increasing fecundity with increasing maximum size (TL, or DW when TL not available) among species within each species group. Groups with significant effects of size on fecundity were split into separate groups by a size threshold that minimized within-group variance in fecundity. The randomization test solved the problem of heteroscedacity by comparing observed mean differences among species groups to a null distribution of 100,000 mean differences, each generated by bootstrapping two samples, each with two replicates, from the pooled fecundities and calculating the difference between means. The latter analysis was performed in the statistical computing environment R, version 2.4.1 (R Development Core Team 2007). All comparisons among taxa were based on the classification system of Compagno (1999).

Differences between oocyte size distribution of left and right ovaries of mature females were tested with a Kolmogorov-Smirnov test. The number of mature oocytes, and maximum ovum size per adult female were tested for potential increase with body length, using least-squares regression.

Results

The relationship between body weight and length was described by the equation $W(kg) = 2.459 \times 10^{-7} (SVL)^{2.755}$ ($R^2 = 0.939$; Fig. 2). Snout-vent length was not measured for all individuals. A linear regression of SVL on PCL, however, provided a good fit (males: $n = 237$, $SVL = 0.556(PCL) - 1.358$, $R^2 = 0.987$; females: $n = 474$, $SVL =$

0.576(PCL) - 4.097, $R^2 = 0.988$), therefore, the resulting sex-specific linear equations were used to predict the missing SVL values.

Maturity

An abrupt increase in the ratio of inner clasper length to snout-vent length with increasing snout-vent length corresponded well with onset of maturity ($n = 252$; Fig. 3), with few exceptions. The timing and scale of the abrupt increase in inner clasper length were similar to those of testis length ($t = 63.062$, $df = 213$, $p < 0.001$, $R^2 = 0.949$; Fig. 4). Testis length was a suitable proxy for testicular growth, as testes grew isometrically in length and width ($t = 63.208$, $df = 222$, $R^2 = 0.947$, $p < 0.001$; Fig. 5). Male maturity assessments using the frontal tenaculum development criterion were not significantly different from assessments using the morphological criteria ($t = 1.450$, $df = 213$, $R^2 = 0.973$, $p = 0.2$; Fig. 6). These results indicate that accurate estimates of maturity can be deduced from male external morphology, and therefore do not necessarily require lethal sampling techniques.

The purpose of the frontal tenaculum and prepelvic claspers was revealed during two observations of mating at the Monterey Bay Aquarium (Gilbert Van Dykhuizen, pers. comm.). Males used their frontal tenaculum to grapple the pectoral fin of the female, and subsequently the prepelvic clasper was attached to the female's ventrum, corroborating previous observations (Didier and Rosenberger 2002). A single bifid clasper was inserted into the female, with each terminal lobe swelling to 2 cm in diameter after insertion into one of the two uterine openings. The mating pairs swam around the tank in a normal swimming posture, side by side, while copulating for ~ 37 to 120 min.

During parturition, egg cases took 18 to 30 h to completely emerge from the uterine openings, then remained attached to the uterus by a thin filament for 3 to 6 d before deposition.

Abrupt increases in the ratio of oviducal gland width to snout-vent length with increasing snout-vent length corresponded well with onset of maturity, as determined by morphological criteria ($n = 476$; Fig. 7). Uterus width also increased with maturity, but is not displayed. A large, gelatinous mass was found in the accessory genital gland (also termed “receptaculum seminis” or “digitiform gland”) of 89% of adult females ($n = 198$) and only 5% of sub-adult females ($n = 91$).

Length at maturity varied significantly between sexes ($\chi^2 = 219.098$, $df = 1$, $p < 0.001$) and regions ($\chi^2 = 25.296$, $df = 2$, $p < 0.001$). For individuals from the entire survey area, size at 50% maturity (Fig. 8a) was 202.8 mm SVL for females (95% CI: 199.0 - 206.4, $R^2 = 0.995$, $n = 530$) and 157.2 mm SVL for males (95% CI: 154.1 - 160.4, $R^2 = 0.996$, $n = 278$). *Post-hoc* sex-specific comparisons indicated that female size at maturity differed between the region south of Point Conception and the two regions to the north (south vs. central: $\chi^2 = 6.650$, $df = 1$, $p = 0.010$; south vs. north: $\chi^2 = 6.937$, $df = 1$, $p = 0.008$), whereas male size at maturity differed between the region north of Cape Mendocino and the two regions to the south (north vs. central: $\chi^2 = 15.175$, $df = 1$, $p < 0.001$; north vs. south: $\chi^2 = 21.922$, $df = 1$, $p < 0.001$). Separate logistic curves were fit for each sex and region for which length at maturity varied. Size at 50% maturity was greater for females captured north of Point Conception (202.5 mm SVL; 95% CI: 198.2 - 206.7) than south (189.8 mm SVL; 95%CI: 186.4 - 191.3; Fig. 8d). Size at 50% maturity

was greater for males captured north of Cape Mendocino (163.1 mm SVL; 95% CI: 157.8 - 168.2) than south (147.3 mm SVL; 95% CI: 145.4 - 148.8; Fig. 8e).

Length at maturity was significantly different between maturity criterion within the subset of females assayed for estradiol ($F = 5.518$, $df = 3, 24$, $p = 0.01$), but did not differ within the subset of males assayed for testosterone ($F = 1.774$, $df = 3, 10$, $p = 0.2$). Female size at maturity indicated by estradiol concentration (185.3 mm SVL; 95% CI: 180.7, 189.9) was less than indicated by the morphological criteria (192.7 mm SVL; 95% CI: 190.0, 195.5; Fig. 8b). There was a trend of smaller size at maturity estimated by testosterone concentration (153.5 mm SVL; 95% CI: 147.9, 159.3) than the morphological criteria (159.7 mm SVL; 95% CI: 155.0, 164.3; Fig. 8c).

Smallest mature specimens were 190 mm SVL for females and 149 mm SVL for males. Maximum and minimum sizes for each sex were north of Cape Mendocino. Minimum size (male: 46 mm SVL; female: 41 mm SVL) is believed to be near size at birth. Maximum size for males was 208 mm SVL (496 mm TL) and 283 mm SVL (633 mm TL) for females. Maximum size previously was reported as 965 mm TL (Miller and Lea 1972), indicating this population has decreased dramatically in body size, that original records were overestimated, or simply that the record represents an anomalous individual.

Effects of differing sample collection methods

Temporal trends were similar between plasma and muscle for all hormones except P₄ (Fig. 9); however, none of the trends were significant (Table 1). There was a significant positive correlation of hormone concentration between plasma and muscle

samples for T ($\chi^2 = 9.626, r = 0.65, p = 0.002$), 11KT ($\chi^2 = 6.673, r = 0.563, p = 0.01$), and P₄ ($\chi^2 = 5.028, r = 0.457, p = 0.025$), but not for E₂ ($\chi^2 = 1.516, r = 0.261, p = 0.2$).

Concentrations were greater in plasma than muscle. Hormone concentrations of muscle samples taken immediately after capture were not significantly different from samples taken three hours later from the same individuals (Table 2); however, there was a slight trend of decreasing concentration with time of sampling for E₂ and P₄ (Fig. 10).

Reproductive Seasonality

Gravid females were detected in January, and May through October (Fig. 11). The size-frequency distribution of oocytes did not differ between left and right ovaries (Kolmogorov-Smirnov: $Z = 0.955, p = 0.3$), therefore, total number of ova per female was used for analyses. The number of mature ova per female varied among months (ANOVA: $F = 4.543, df = 7, 167, p < 0.001$; Fig. 12); significantly greater in late summer and early fall than all other time periods (Hochberg GT2: $df = 167, p \leq 0.034$). The number of fully developed ova, 20 mm diameter or greater (Stanley 1961), varied dramatically among months (Kruskal-Wallis: $\chi^2 = 20.322, df = 10, p = 0.026$; Fig. 13). The seasonal presence of fully developed ova and *in utero* egg cases indicated 6-8 mo of parturition per year.

Concentration of 11KT in muscle of females varied among months (ANOVA: $F = 6.404, df = 6, 110, p < 0.001$; Fig. 14); significantly greater in April than any other month (Hochberg GT2: $df = 110, p \leq 0.001$). Concentration of P₄ in muscle of females varied among months (ANOVA: $F = 2.991, df = 10, 114, p = 0.002$; Fig. 15); significantly greater in January than June and September (Hochberg GT2: $df = 114, p \leq 0.003$).

Concentration of E₂ in muscle of females also varied among months (ANOVA: $F = 2.732$, $df = 10, 140$, $p = 0.004$; Fig. 16); significantly greater in November than March, May, and September (Hochberg GT2: $df = 140$, $p \leq 0.017$). Concentration of T in muscle of females did not vary significantly among months (ANOVA: $F = 2.042$, $df = 7, 120$, $p = 0.055$; Fig. 17), but there was a slight trend of greater concentrations in summer than fall.

Mean OGI varied among months (ANOVA: $F = 2.958$, $df = 7, 156$, $p = 0.006$; Fig. 18); significantly less in January than July, August, September, and October (Hochberg GT2: $df = 156$, $p \leq 0.045$). Mean GSI varied among months for females (Kruskal-Wallis: $\chi^2 = 32.523$, $df = 10$, $p < 0.001$; Fig. 19); significantly greater in October than in February, March, or November (Nemenyi-Damico-Wolfe-Dunn test: $p \leq 0.019$). Mean GSI also varied among months for males (Kruskal-Wallis: $\chi^2 = 39.279$, $df = 9$, $p < 0.001$; Fig. 20), greatest in January through March, and least in May, June, and July (Nemenyi-Damico-Wolfe-Dunn test: $p \leq 0.016$). Mean HSI did not vary among months for females (Kruskal-Wallis: $\chi^2 = 16.205$, $df = 10$, $p = 0.094$) or males (Kruskal-Wallis: $\chi^2 = 11.534$, $df = 9$, $p = 0.241$).

Duration of spawning season increased with depth distribution for all chondrichthyan groups combined ($t = 3.262$, $df = 24$, $R^2 = 0.278$, $p = 0.003$). This relationship was not present within viviparous ($t = 0.651$, $df = 14$, $p = 0.5$) and oviparous ($t = 1.352$, $df = 10$, $p = 0.2$) groups, however, nor within specific chondrichthyan taxonomic orders (chimaeroids: $t = 0.464$, $df = 4$, $p = 0.7$; carcharhinoids: $t = 1.579$, $df = 6$, $p = 0.2$).

Fecundity

Two captive *H. colliei*, taken from Puget Sound, WA, deposited 18 and 20 egg cases, respectively, while monitored for 24 consecutive weeks from December 1996 to June 1997 at the Monterey Bay Aquarium (Gilbert Van Dykhuizen, pers. comm.). Annual fecundity was 19.5 to 28.9. The number of fully developed ova, 20 mm diameter or greater (Stanley 1961), increased with adult female somatic weight ($r = 0.394$, $df = 54$, $p = 0.003$; Fig. 21). Additionally, for reproductively active females, the maximum ovum diameter increased with snout-vent length ($t = 3.833$, $df = 159$, $R^2 = 0.079$, $p < 0.001$). For the latter analysis, females were considered reproductively active if their ovaries contained at least one follicle of 16 mm diameter or greater, a threshold that became apparent when maximum ovum size was compared with snout-vent length (ANCOVA: interaction term = maximum ovum size*snout-vent length; $F = 7.734$, $df = 1, 203$, $p = 0.006$; Fig. 22).

Fecundities differed between oviparous and viviparous species ($t = 10.433$, $df = 83$, $p < 0.001$); mean fecundity of viviparous species was less (8.1; SE = 0.94) than mean fecundity of oviparous species (50.1; SE = 6.2). Fecundity decreased with size within the order Squaliformes ($t = 2.312$, $df = 12$, $p = 0.039$), and therefore was separated into large (TL > 60 cm) and small (TL < 60 cm) categories. There was no significant relationship between fecundity and body size of other taxonomic orders. When these same species were grouped by higher taxonomic level, the oviparous chimaeriform fishes had greater fecundity than the viviparous lamniform (marginally significant; $p = 0.052$), myliobatiform ($p = 0.008$), rhinobatiform ($p = 0.021$), and squaliform fishes (small: $p =$

0.044; large: $p = 0.021$), and similar fecundity to the oviparous rajiforms ($p = 0.15$) and the carcharhiniforms ($p > 0.9$), with both reproductive modes represented.

Discussion

Maturity

Size at maturity and maximum size were greater in northern than southern regions. This latitudinal pattern is commonly observed in fishes (Carlson and Parsons 1997; Heibo et al. 2005; Lombardi-Carlson et al. 2003; Parsons 1993; Yamaguchi et al. 2000). Spatial differences in size at maturity often are caused by temperature (Parsons 1993; Walker 2007; Yamaguchi et al. 2000), photoperiod (Parsons 1993), and food abundance (Yamaguchi et al. 2000). Such variance also can result from differential fishing intensity, with greater exploitation rates causing smaller size at maturity through density-dependent compensation or simply artificial selection for smaller sizes (Conover and Munch 2002; Edeline et al. 2007; Olsen et al. 2004; Roff 2002; Sosebee 2005; Stearns 1992). Unfortunately, catch of *H. colliei* is typically not reported, so it is not possible to test the latter hypothesis. However, there are greater temperatures and fewer nutrients on the seafloor of the shelf and upper slope south of Point Conception than north, and to a lesser extent, south of Cape Mendocino than north (Tolimieri 2007). Differential temperature and food availability, therefore, likely are the primary factors causing a latitudinal gradient in size at maturity of *H. colliei*. It also is possible that differences in size may be the product of multiple discrete breeding populations (or metapopulations), as indicated for the Port Jackson Shark, *Heterodontus portusjacksoni*

(Tovar-Avila et al. 2007). There is insufficient evidence, however, to evaluate the latter hypothesis.

Recent studies have indicated that assays of the steroid hormones T and E₂ in plasma serves as an accurate, non-lethal method of determining size at maturity for chondrichthyans (Sulikowski et al. 2004). In this study, however, steroid hormone maturity criteria predicted significantly smaller size at maturity than morphological criteria for females, and a similar, yet insignificant trend for males. The differences were not great in magnitude, but the results indicated that accuracy of maturity estimates from hormone data was not perfect, and perhaps biased toward identification of smaller size at maturity. In the teleost fish *Mycteroperca microlepis* neither E₂ nor T from plasma or muscle were consistent indicators of maturity (Heppell and Sullivan 2000).

It is logical that hormones related to maturity should increase before morphological maturity, as T is correlated with development of intromittent organs (Schreibman et al. 1986), and 11KT is correlated with expression of secondary sexual physiological characters (Borg 1987; Borg et al. 1993; de Ruiter and Mein 1982; Hishida and Kawamoto 1970; Idler et al. 1961; Pottinger and Pickering 1985). The synchronous development of the frontal tenaculum and internal reproductive organs also was observed, albeit qualitatively, in the elephant fish *Callorhynchus milii* (Gorman 1963). Gorman (1963), however, also reported that prepelvic claspers were only present in adult males, but they were omnipresent in *H. colliei* males. The gelatinous mass of the accessory genital gland, which contains desquamated epithelial cells (Stanley 1963), was found in 89% of mature females. The function of this secretion is unknown, but also was present in nearly all mature females in a previous study (Stanley 1963).

The *in situ* observations of mating behavior recorded from captive *H. colliei* resolved questions regarding the copulation and parturition process. It was previously hypothesized that the frontal tenaculum was used for grappling the base of the female's dorsal fin during copulation (Dean 1903). The duration of the parturition process, combined with observed captive parturition rates, is consistent with Dean's (1903) 3 to 5 d estimate of duration of egg-case formation based on the progression of fertilization.

Stylasterias spp., *Neptunia* spp., and *Icelinus filamentosus* were observed on egg cases in aquaria, perhaps attempting to predate upon them. In natural systems, elasmobranch egg cases are preyed upon primarily by gastropods (Cox and Koob 1993; Lucifora and Garcia 2004), but are occasionally eaten by fishes and other marine vertebrates (Bor and Santos 2003). Predation rates of egg-cases by gastropods are 2 to 45% for skates (Hoff 2007), and 14 to 40% for a mixed group of skates and sharks off South Africa (Smith and Griffiths 1997).

Reproductive Seasonality

Fluctuations of T, 11KT, E₂, and P₄ are related to many important reproductive events in oviparous fishes. 11-Ketotestosterone is correlated with pre-vitellogenic oocyte growth (Matsubara et al. 2003), oocyte maturation (Semenkova et al. 2006), and ovulation (Semenkova et al. 2006) in females, and sexual behavior in males (Borg 1987; Kindler et al. 1991). Greater concentration in April is consistent with the apparent function of 11KT in pre-parturition stages of reproduction. If the correlation with sexual behavior is consistent for females, the observed peak also may be related to mating activity. Although there was no clear physical evidence of mating activity, Dean (1903)

indicated that mating takes place shortly before parturition, based on the presence of fresh mating scars on gravid females.

Testosterone is correlated with ovary recrudescence (Sumpter and Dodd 1979), oocyte maturation (Semenkova et al. 2006), oviposition (Sumpter and Dodd 1979), and encapsulation (Rasmussen et al. 1999), greatest just before increases in progesterone associated with oviposition and egg capsule formation (Koob et al. 1986). Testosterone is synthesized by developing follicles and luteal tissue, whereas estradiol is primarily synthesized by developing follicles (Callard et al. 1993). The observed seasonal fluctuation of T was not very distinct, but the increase during May through August may be consistent with its role in oviposition and encapsulation.

Estradiol is correlated with ovarian recrudescence (Sulikowski et al. 2004; Sumpter and Dodd 1979), increased oviducal gland weight (Sulikowski et al. 2004), follicle size (Sulikowski et al. 2004), elevated plasma vitellogenin (Craik 1978; 1979; Ho et al. 1980; Takemura and Kim 2001; Woodhead 1969), oviposition (Sumpter and Dodd 1979), and induction and maintenance of structural proteins and enzymes in the oviducal glands (Dodd and Goddard 1961; Koob et al. 1986). Relative levels of E₂ to P₄ influence oviduct contraction, with P₄ acting as an inhibitor (Abrams-Motz and Callard 1989). Estradiol may enhance sensitivity to relaxin, which may facilitate oviposition, gestation, and parturition by allowing increased dilation of the reproductive tract (Koob et al. 1984) and perhaps controlling smooth muscle action required for these processes (Callard et al. 1993). Conversely, P₄ seems to inhibit the function of relaxin (Sorbera and Callard 1989). In *H. colliei*, E₂ was greatest in November, and least from March through

October, indicating that its primary role may be preovulatory, particularly ovarian recrudescence.

In oviparous chondrichthyans, P_4 may increase extensibility and vascularization of the uterine wall (Koob and Callard 1999) immediately before ovulation and encapsulation (Koob and Hamlett 1998). Progesterone and its receptors may restrict rates of folliculogenesis through a variety of pathways (Callard et al. 1995), including inhibition of E_2 -induced vitellogenin gene transcription in the liver (Perez and Callard 1993). Progesterone is correlated with parturition (Sulikowski et al. 2004) and final oocyte maturation (Semenkova et al. 2006). Progesterone is primarily synthesized by luteal tissue (Callard et al. 1993; Fileti and Callard 1988). In this study, P_4 was greatest in January, and decreased through fall. This pattern is incongruous with the other indicators of reproductive activity and the typical physiological effects of P_4 on oviparous chondrichthyans. The peak may be related to mating, however, as Heupel et al. (1999) observed a peak in P_4 just before the mating season in the viviparous shark *Hemiscyllium ocellatum*.

Steroid hormone cycles of oviparous chondrichthyans have been generalized as a synchronous cycle wherein E_2 and P_4 increase during follicular growth (preovulation) and decrease during luteal development (Callard et al. 1991), with greatest levels of E_2 slightly preceding those of P_4 (Koob et al. 1986). This pattern was evident for *H. colliei*; however, these maxima preceded maximum ovulatory activity by as long as 5 mo, a greater duration than anticipated, especially considering the role of P_4 in encapsulation (Koob et al. 1986) and increased extensibility of the reproductive tract to accommodate

egg cases (Koob and Hamlett 1998). This discrepancy may represent the difference between population and individual hormone cycles.

I found *H. colliei* had a discrete reproductive cycle, contradicting previous studies (Dean 1906; Sathyanesan 1966). Duration and timing of the parturition season of *H. colliei* was similar to that of *Chimaera phantasma* (Malagrino et al. 1981) and *Chimaera monstrosa* (Vu-Tan-Tue 1972). It also was similar to callorhynchids (Bell 2003; Di Giacomo and Perier 1994; Freer and Griffiths 1993b; Gorman 1963; review in McClatchie and Lester 1994), which make inshore migrations for egg deposition and have a shallower bathymetric range than chimaerids.

Discrete spawning periods are temporally regulated by social cues (Whittier and Crews 1987), and environmental cues such as temperature (Danilowicz 1995; Goulet 1995; Hilder and Pankhurst 2003; Whittier and Crews 1987), photoperiod (Jobling 1995; Whittier and Crews 1987), lunar phase (Robertson et al. 1990; review in Robertson 1991), illumination (Whittier and Crews 1987), and food abundance (Tyler and Stanton 1995; Whittier and Crews 1987). In temperate zones, the most common cue is photoperiod, with some influence of temperature (Jobling 1995; Whittier and Crews 1987). Length of reproductive season is greater in tropical than temperate zones (Jobling 1995). Duration of reproductive season also may be correlated with the amount of primary productivity (Whittier and Crews 1987).

The current paradigm regarding reproductive seasonality in the marine environment is that animals that inhabit deeper depths are less likely to have seasonal cycles of reproductive output (Parsons and Grier 1992; Wourms 1977). Although this relationship was present when analyzing all chondrichthyans combined, it was not

apparent when oviparous and viviparous species were analyzed separately, indicating an artefact of reproductive mode. The effect also was not significant within the chimaeroids or carcharhinoids. It is not surprising that this generalization is faulty. Recent researchers have shown that productivity from coastal upwelling can have a major influence on benthic communities as deep as 4,100 m (Ruhl and Smith 2004). These new insights indicate that the evolution of discrete versus continuous reproductive cycles is a much more complex process than previously thought.

Hydrolagus colliei has a constant or endogenous reproductive cycle (Whittier and Crews 1987). In the former situation, the gonads are always prepared for reproduction, but sexual behavior is cued by environmental conditions, and in the latter situation, reproductive activity is seasonal, but has minimal environmental regulation. Under these criteria, *H. colliei* has constant cycle, because parturition of the wild population coincides with dramatic annual environmental changes in thermocline depth and primary productivity. Captive *H. colliei* at the Monterey Bay Aquarium have extruded egg cases during all seasons, which also may be evidence for the environmental regulation of reproductive activity. Alternatively, reproductive activity could be regulated by social cues, with captive individuals remaining constantly reproductively active due to the perpetual proximity of males, a situation that is not probable in some wild chondrichthyan populations (Economakis and Lobel 1998). Further evidence for an endogenous cycle regulated by social cues is provided by Bell (2003), in which captive female *Callorhynchus milii*, in the absence of males, retained their annual reproductive cycle while temperature and photoperiod were kept relatively stable.

Fecundity

The simple method of fecundity estimation by extrapolation of observed parturition rates was used instead of methods of Holden (1975) because assumptions of Holden's methods likely were violated. Holden (1975) used the proportion of gravid individuals sampled from the wild population as a proxy for the proportion of the population depositing egg-cases during a given period of time. A primary assumption of this method is that the gravid population is being appropriately sampled. This assumption is likely not met for *H. colliei*, as parturition in this species occurs primarily on or around seamounts. These regions are poorly represented in surveys because they comprise an exceptionally small area of the seafloor and their rocky, rugose surface cannot be sampled with trawl gear. Holden's (1975) alternative method of estimating fecundity relies upon the following assumptions: (1) all mature ova produced by an adult female during a given year are formed before the onset of parturition, and therefore are simultaneously present in the ovary; (2) this group of mature ova will all be placed in egg cases and extruded during the current spawning season; and (3) no ovum resorption occurs. It is doubtful that these assumptions are met for *H. colliei*, in which ovum resorption and/or follicle atresia were commonly observed. The number of mature and fully developed ova in females and female GSI do not decrease gradually toward the end of the spawning season (Figs. 12, 13, 19), as would be expected if the former two assumptions were met.

Fecundity of *H. colliei* is similar to that estimated for *Callorhinchus milii* (16-24; Bell 2003), but much greater than that estimated for *Chimaera monstrosa* (mean = 6; Moura et al. 2004). The latter discrepancy, however, could be caused in part by the

method of fecundity estimation. Moura et al. (2004) estimated fecundity by calculating the mean number of fully developed ova per adult female. Similarly, Tovar-Avila et al. (2007) estimated fecundity for *Heterodontus portjacksoni*, a shark with single oviparous reproductive mode, as the mean number of oocytes $\geq 75\%$ of ovulatory size in adult female sharks in the months before the parturition season. The latter method provided similar estimates to that derived by extrapolation of captive parturition rates (Tovar-Avila 2006). In *H. colliei*, however, the mean number of oocytes greater than 10 mm diameter ($\geq \sim 35\text{-}50\%$ of ovulatory size) per female captured before the egg-laying season was only 10 (range = 1-36; $\sigma = 9.04$; $n = 32$), less than half the mean fecundity estimated from captive parturition rates. This discrepancy indicates that the method of simply enumerating maturing ova may be inadequate for chimaeroids, and other chondrichthyans with single oviparity that display rapid vitellogenesis (e.g. Holden et al. 1971) and protracted production of mature ova.

Fecundity estimation for chondrichthyans with single oviparity is a difficult and uncertain process, with extrapolation of captive parturition rates often providing the most accurate fecundity estimates. In my study, fecundity of *H. colliei* was 19.5-28.9, but it may be much less, as some of the egg cases deposited in captivity were ruptured or not completely formed during parturition. Additionally, only 10% of egg cases deposited in captivity were fertile ($n = 38$). The phenomenon of “gel eggs,” or egg cases without an ovum and containing only egg jelly, may be another factor reducing fecundity in natural populations. Although gel eggs have not been observed in chimaeroids, Hoff (2007) reported that gel eggs composed nearly 5% of all *in utero* egg cases in Bering Sea skates.

Incorporation of embryonic survival, therefore, will greatly improve fecundity estimates derived from extrapolation of captive parturition rates.

The number of fully developed ova increased with adult female somatic weight, providing marginally significant evidence for increased fecundity with size. This effect occurs in another chimaeroid, *Callorhinchus milii* (Bell 2003), and other organisms, including skates (Matta 2006), sharks (Simpfendorfer 1992; Yano 1995), and rockfishes (Bobko and Berkeley 2004; Boehlert et al. 1982; Cooper et al. 2005). There also is some evidence for increasing maximum ovum size with maternal body size. Larger females may provide more nutrients to their young, potentially increasing offspring fitness (Berkeley et al. 2004a). Increased embryo, egg, egg case, or yolk sac size and/or nutrient content with larger maternal size occurs in many fishes, including skates (Hoff 2007), sharks, and rockfish (Berkeley et al. 2004a). Increased number and fitness of offspring with increased maternal size is an important biological component in conservation planning (Berkeley et al. 2004b). Although there are many chondrichthyans with one of the two maternal size effects observed in *H. colliei*, there are few species that exhibit both (Cortes 2000). There seems to be a tradeoff between the number of offspring and offspring size within and among chondrichthyan populations (review in Cortes 2000), indicating the existence of a specific ratio of the two that would maximize fitness (Roff 2002).

Previously oviparity was considered the plesiomorphic state of chondrichthyans (Compagno 1990; Dulvy and Reynolds 1997; Wourms 1977; Wourms and Lombardi 1992), but a recent review indicated that viviparity is the ancestral state (Musick and Ellis 2005). Musick and Ellis (2005) revisited the ideas of Holden (1973) and hypothesized

that oviparity evolved to increase fecundity in small-bodied species, which have too little coelomic space to produce many live offspring per litter. Support for this hypothesis is provided by the trend for fecundity in oviparous than viviparous species of small body size, a phenomena that was previously disputed (Wourms and Lombardi 1992). In this study, fecundity was quantitatively compared among chondrichthyan lineages to provide more explanatory power for these hypotheses by incorporating interpretation of fecundity evolution into the evolution of reproductive modes.

A current paradigm indicates that viviparous species of chondrichthyans are less fecund than their oviparous counterparts. To quantitatively test this theory, I compared fecundities for oviparous and viviparous species from the orders Carcharinhiformes ($n = 20$), Rajiformes ($n = 12$), Rhinobatiformes ($n = 9$), Myliobatiformes ($n = 19$), Torpediniformes ($n = 2$), Chimaeriformes ($n = 2$), Squaliformes ($n = 14$), Lamniformes ($n = 4$), Rhiniformes ($n = 1$) and Orectolobiformes ($n = 2$). It should be noted that the two rajiforms with multiple oviparity, *Raja binoculata* and *Raja pulchra*, were considered outliers because of their potential to produce many more offspring than other rajiforms (Ebert and Davis 2007), and therefore were excluded from analyses. Mean fecundity of viviparous species was less than mean fecundity of oviparous species. When those same species were grouped by higher taxonomic level, the oviparous chimaeriform fishes had greater fecundity than the viviparous lamniform, squaliform, and rhinobatiform fishes, but similar fecundity to the oviparous rajiforms and the mixed carcharhiniforms. There was a trend of greater mean fecundity for Rajiformes (56.4) than Chimaeriformes (22.1). These results indicate that the oviparous Chimaeriformes evolved greater fecundity than their viviparous elasmobranch relatives, but perhaps lesser fecundity than the more

derived oviparous species within the order Rajiformes. With the Chimaeriformes added into the analysis of evolution of fecundity, more evidence is provided that supports the hypothesis of viviparous plesiomorphy in chondrichthyans, as argued by Musick and Ellis (2005).

Literature Cited

- Abrams-Motz V, Callard IP (1989) Seasonal variations in oviduct myometrial activity, extensibility and tensile strength in *Chrysemys picta*. *General and Comparative Endocrinology* 72: 453-460
- Alverson DL, Pruter AT, Ronholt LL (1964) A study of demersal fishes and fisheries of the northeastern Pacific Ocean. H.R. MacMillan Lectures in Fisheries. Institute of Fisheries, University of British Columbia, Vancouver
- Anon (1997) Report of the study group of elasmobranch fishes. ICES CM 1997/G:2
- Barnett LAK, Dagit DD, Long DJ, Ebert DA (2006) *Hydrolagus mccoskeri* sp. nov., a new species of chimaeroid fish from the Galápagos Islands (Holocephali: Chimaeriformes: Chimaeridae). *Zootaxa* 1328: 27-38
- Bell JD (2003) Fisheries and reproductive biology of the elephant fish, *Callorhinchus milii*, in south-east Australia. Bachelor of Environmental Science (honours). Deakin University
- Berkeley SA, Chapman C, Sogard SM (2004a) Maternal age as a determinant of larval growth and survival in a marine fish, *Sebastes melanops*. *Ecology* 85: 1258-1264
- Berkeley SA, Hixon MA, Larson RJ, Love MS (2004b) Fisheries sustainability via protection of age structure and spatial distribution of fish populations. *Fisheries* 29: 23-32
- Bobko SJ, Berkeley SA (2004) Maturity, ovarian cycle, fecundity, and age-specific parturition of black rockfish (*Sebastes melanops*). *Fishery Bulletin* 102: 418-429
- Boehlert GW, Barss WH, Lamberson PB (1982) Fecundity of the widow rockfish, *Sebastes entomelas*, off the coast of Oregon. *Fishery Bulletin* 80: 881-884

- Bonfil R (1994) Overview of world elasmobranch fisheries. FAO Technical Paper 341
- Bor PHF, Santos MB (2003) Findings of elasmobranch eggs in the stomachs of sperm whales and other marine organisms. *Journal of the Marine Biological Association of the U.K.* 83: 1351-1353
- Borg B (1987) Stimulation of reproductive behaviour by aromatizable and non-aromatizable androgens in the male three-spined stickleback, *Gasterosteus aculeatus* L. In: Kullander SOK, Fernholm B (eds) Proc. 5th Congr. Eur. Ichthyol. Stockholm. Swedish Museum of Natural History, Stockholm, pp 269-271
- Borg B (1994) Androgens in teleost fishes. *Comparative Biochemistry and Physiology Part C: Comparative Pharmacology and Toxicology* 109: 219-245
- Borg B, Antonopoulou E, Andersson E, Carlberg T, Mayer I (1993) Effectiveness of several androgens in stimulating kidney hypertrophy, a secondary sexual character, in castrated male three-spined stickleback, *Gasterosteus aculeatus*. *Canadian Journal of Zoology* 71: 2327-2329
- Cailliet GM (1990) Elasmobranch age determination and verification: an updated review. In: Pratt Jr HL, Gruber SH, Taniuchi T (eds) *Elasmobranchs as living resources: advances in the biology, ecology, systematics, and the status of the fisheries.* NOAA Technical Report 90, pp 157-165
- Cailliet GM, Andrews AH, Burton EJ, Watters DL, Kline DE, Ferry-Graham LA (2001) Age determination and validation studies of marine fishes: do deep-dwellers live longer? *Experimental Gerontology* 36: 739-764

- Cailliet GM, Goldman KJ (2004) Age determination and validation in chondrichthyan fishes. In: Carrier JC, Musick JA, Heithaus MR (eds) Biology of sharks and their relatives. CRC Press, Boca Raton, FL, pp 399-448
- Callard IP, Etheridge K, Giannoukos G, Lamb T, Perez L (1991) The role of steroids in reproduction in female elasmobranchs and reptiles. *Journal of Steroid Biochemistry and Molecular Biology* 40: 571-575
- Callard IP, Fileti LA, Koob TJ (1993) Ovarian steroid synthesis and the hormonal control of the elasmobranch reproductive tract. *Environmental Biology of Fishes* 38: 175-185
- Callard IP, Putz O, Paolucci M, Koob TJ (1995) Elasmobranch reproductive life-histories: endocrine correlates and evolution. *Proceedings of the International Symposium on the Reproductive Physiology of Fish*, Austin, TX, pp 204-208
- Carlson JK, Parsons GR (1997) Age and growth of the bonnethead shark, *Sphyrna tiburo*, from northwest Florida, with comments on clinal variation. *Environmental Biology of Fishes* 50: 331-341
- Chen Y, Jackson DA, Harvey HH (1992) A comparison of von Bertalanffy and polynomial functions in modelling fish growth data. *Canadian Journal of Fisheries and Aquatic Sciences* 49: 1228-1235
- Clarke MW, Kelly CJ, Connolly PL, Molloy JP (2003) A life history approach to the assessment and management of deepwater fisheries in the northeast Atlantic. *Journal of Northwest Atlantic Fishery Science* 31: 401-411
- Compagno LJV (1990) Alternative life-history styles of cartilaginous fishes in time and space. *Environmental Biology of Fishes* 28: 33-75

- Compagno LJV (1999) Checklist of living elasmobranchs. In: Hamlett WC (ed) Sharks, skates, and rays: the biology of elasmobranch fishes. The Johns Hopkins University Press, Baltimore, Maryland
- Compagno LJV (2005) Checklist of living Chondrichthyes. In: Hamlett WC (ed) Reproductive biology and phylogeny of Chondrichthyes: sharks batoids and chimaeras. Science Publishers, Inc., Enfield, pp 503-548
- Conover DO, Munch SB (2002) Sustaining fisheries yields over evolutionary time scales. *Science* 297: 94-96
- Cooper DW, Pearson KE, Gunderson DR (2005) Fecundity of shortspine thornyhead (*Sebastolobus alascanus*) and longspine thornyhead (*S. altivelis*) (Scorpaenidae) from the northeastern Pacific Ocean, determined by stereological and gravimetric techniques. *Fishery Bulletin* 103: 15-22
- Cortes E (2000) Life history patterns and correlations in sharks. *Reviews in Fisheries Science* 8: 299-344
- Cox DL, Koob TJ (1993) Predation on elasmobranch eggs. *Environmental Biology of Fishes* 38: 117-125
- Craik JCA (1978) An annual cycle of vitellogenesis in the elasmobranch *Scyliorhinus canicula* L. *Journal of the Marine Biological Association of the United Kingdom* 58: 719-726
- Craik JCA (1979) Simultaneous measurement of rates of vitellogenin synthesis and plasma levels of estradiol in an elasmobranch. *General and Comparative Endocrinology* 38: 264-266

- Cross JN (1981) Structure of a rocky intertidal fish assemblage. Ph.D. Thesis, University of Washington
- Danilowicz BS (1995) Spatial patterns of spawning in the coral-reef damselfish *Dascyllus albisella*. *Marine Biology* 122: 145-155
- de Ruiter AJH, Mein CG (1982) Testosterone-dependent changes *in vivo* and *in vitro*. *General and Comparative Endocrinology* 47: 70-83
- Dean B (1903) An outline of the development of a chimaeroid. *Biological Bulletin* 4: 270-286
- Dean B (1906) Chimaeroid fishes and their development. Carnegie Institute Publication, Washington, D.C.
- Di Giacomo EE, Perier MR (1994) Reproductive biology of the cockfish, *Callorhynchus callorhynchus* (Holocephali: Callorhynchidae), in Patagonian waters (Argentina). *Fishery Bulletin* 92: 531-539
- Didier DA (1995) Phylogenetic systematics of extant Chimaeroid fishes (Holocephali, Chimaeroidei). *American Museum Novitates* 3119: 1-86
- Didier DA, LeClair EE, Vanbuskirk DR (1998) Embryonic staging and external features of development of the chimaeroid fish, *Callorhynchus milii* (Holocephali, Callorhynchidae). *Journal of Morphology* 236: 25-47
- Didier DA, Rosenberger LJ (2002) The spotted ratfish, *Hydrolagus colliei*: notes on its biology with a redescription of the species (Holocephali: Chimaeridae). *California Fish and Game* 88: 112-125

- Dodd JM, Goddard CK (1961) Some effects of oestradiol benzoate on the reproductive ducts of the female dogfish *Scyliorhinus caniculus*. Proceedings of the Zoological Society of London 137: 325-331
- Dulvy NK, Metcalfe JD, Glanville J, Pawson MG, Reynolds JD (2000) Fishery stability, local extinctions, and shifts in community structure in skates. Conservation Biology 14: 283-293
- Dulvy NK, Reynolds JD (1997) Evolutionary transitions among egg-laying, live-bearing and maternal inputs in sharks and rays. Proceedings of the Royal Society of London, Series B: Biological Sciences 264: 1309-1315
- Ebert DA (1996) Biology of the sevengill shark, *Notorynchus cepedianus* (Peron, 1807) in the temperate coastal waters of Southern Africa. South African Journal of Marine Science 17: 93-103
- Ebert DA, Davis CD (2007) Descriptions of skate egg cases (Chondrichthyes: Rajiformes: Rajoidei) from the eastern North Pacific. Zootaxa 1393: 1-18
- Economakis AE, Lobel PS (1998) Aggregation behavior of the grey reef shark, *Carcharhinus amblyrhynchos*, at Johnston Atoll, Central Pacific Ocean. Environmental Biology of Fishes 51: 129-139
- Edeline E, Carlson SM, Stige LC, Winfield IJ, Fletcher JM, James JB, Haugen TO, Vollestad LA, Stenseth NC (2007) Trait changes in a harvested population are driven by a dynamic tug-of-war between natural and harvest selection. Proceedings of the National Academy of Sciences 104: 15799-15804

- Fileti LA, Callard IP (1988) Corpus luteum function and regulation in the little skate, *Raja erinacea*. Bulletin of the Mount Desert Island Biological Laboratory 27: 37-39
- Freer DWL, Griffiths CL (1993) The fishery for, and general biology of, the St. Joseph *Callorhynchus capensis* (Dumeril) off the southwestern Cape, South Africa. South African Journal of Marine Science 13: 63-74
- Gordon JDM (1999) Management considerations of deepwater shark fisheries. In: Shotton R (ed) Case studies of the management of elasmobranch fisheries. FAO Fisheries Technical Paper No. 378, part 2. FAO, Rome, pp 774-818
- Gorman TBS (1963) Biological and economic aspects of the elephant fish *Callorhynchus milii* Bory in Pegasus Bay and the Canterbury Bight. New Zealand Department of Fisheries Technical Report 8
- Goulet D (1995) Temporal patterns of reproduction in the Red Sea damselfish *Amblyglyphidodon leucogaster*. Bulletin of Marine Science 57: 582-595
- Grinols RB (1965) Check-list of the offshore marine fishes occurring in the northeastern Pacific Ocean, principally off the coasts of British Columbia, Washington, and Oregon. M.S. Thesis, University of Washington
- Grogan ED, Lund R (2004) The origin and relationships of early Chondrichthyes. In: Carrier JC, Musick JA, Heithaus MR (eds) Biology of sharks and their relatives. CRC Press, Boca Raton, FL, pp 3-32
- Heibo E, Magnhagen C, Vollestad LA (2005) Latitudinal variation in life-history traits in Eurasian perch. Ecology 86: 3377-3386

- Heppell SA, Sullivan CV (2000) Identification of gender and reproductive maturity in the absence of gonads: muscle tissue levels of sex steroids and vitellogenin in gag (*Mycteroperca microlepis*). Canadian Journal of Fisheries and Aquatic Sciences 57: 148-159
- Heupel MR, Whittier JM, Bennett MB (1999) Plasma steroid hormone profiles and reproductive biology of the epaulette shark, *Hemiscyllium ocellatum*. Journal of Experimental Zoology 284: 586-594
- Hilder ML, Pankhurst NW (2003) Evidence that temperature change cues reproductive development in the spiny damselfish, *Acanthochromis polyacanthus*. Environmental Biology of Fishes 66: 187-196
- Hishida T, Kawamoto N (1970) Androgenic and male-inducing effects of 11-ketotestosterone on a teleost, the medaka (*Oryzias latipes*). Journal of Experimental Zoology 173: 279-284
- Ho S, Wulczyn G, Callard IP (1980) Induction of vitellogenin synthesis in the spiny dogfish, *Squalus acanthias*. Bulletin of the Mount Desert Island Biological Laboratory 19: 37-38
- Hoening JM, Gruber SH (1990) Life history patterns in the elasmobranchs: implications for fisheries management. In: Pratt Jr HL, Gruber SH, Taniuchi T (eds) Elasmobranchs As living resources: advances in the biology, ecology, systematics, and the status of the fisheries. NOAA Technical Report 90, pp 1-16
- Hoff GR (2007) Reproductive biology of the Alaska skate *Bathyraja parmifera*, with regard to nursery sites, embryo development and predation. Ph.D. Thesis, University of Washington

- Holden MJ (1973) Are long-term sustainable fisheries for elasmobranchs possible?
Rapports et Procès-verbaux des Réunions, Conseil International pour
L'Exploration de la Mer 164: 360-367
- Holden MJ (1974) Problems in the rational exploitation of elasmobranch populations and
some suggested solutions. In: Harden-Jones FR (ed) Sea fisheries research. Logos
Press, London, pp 117-138
- Holden MJ (1975) The fecundity of *Raja clavata* in British waters. Journal du Conseil
International pour L'Exploration de la Mer 36: 110-118
- Holden MJ, Rout DW, Humphreys CN (1971) The rate of egg laying by three species of
ray. Journal du Conseil International pour L'Exploration de la Mer 33: 335-339
- Hollander M, Wolfe DA (1999) Nonparametric statistical methods. John Wiley & Sons,
New York
- Hothorn T, Hornik K, van de Wiel MA, Zeileis A (2007) A lego system for conditional
inference. The American Statistician 60(3): 257-263
- Idler DR, Bitners II, Schmidt PJ (1961) 11-Ketotestosterone: an androgen for sockeye
salmon. Canadian Journal of Biochemistry and Physiology 39: 1737-1742
- Jobling M (1995) Environmental biology of fishes. Chapman and Hall, London
- Kindler PM, Bahr JM, Philipp DP (1991) The effect of exogenous 11-ketotestosterone,
testosterone, and cyproterone acetate on prespawning and parental care behaviors
of male bluegill. Hormones and Behavior 25: 410-423
- Klimley AP (1987) The determinants of sexual segregation in the scalloped hammerhead
shark, *Sphyrna lewini*. Environmental Biology of Fishes 18: 27-40

- Kokuho T, Nakaya K, Kitagawa D (2003) Distribution and reproductive biology of the nine-spot ratfish *Hydrolagus barbouri* (Holocephali; Chimaeridae). *Memoirs of the Graduate School of Fisheries Science, Hokkaido University* 50: 63-87
- Koob TJ, Callard IP (1999) Reproductive endocrinology of female elasmobranchs: Lessons from the little skate (*Raja erinacea*) and spiny dogfish (*Squalus acanthias*). *Journal of Experimental Zoology* 284: 557-574
- Koob TJ, Hamlett WC (1998) Microscopic structure of the gravid uterus in the little skate, *Raja erinacea*. *The Journal of Experimental Zoology* 282: 421-437
- Koob TJ, Laffan JJ, Callard IP (1984) Effects of relaxin and insulin on reproductive tract size and early fetal loss in *Squalus acanthias*. *Biology of Reproduction* 31: 231-238
- Koob TJ, Tsang P, Callard IP (1986) Plasma estradiol, testosterone, and progesterone levels during the ovulatory cycle of the skate (*Raja erinacea*). *Biology of Reproduction* 35: 267-275
- Lombardi-Carlson LA, Cortes E, Parsons GR, Manire CA (2003) Latitudinal variation in life-history traits of bonnethead sharks, *Sphyrna tiburo* (Carcharhiniformes: Sphyrnidae) from the eastern Gulf of Mexico. *Marine and Freshwater Research* 54: 875-883
- Lucifora LO, Garcia VB (2004) Gastropod predation on egg cases of skates (Chondrichthyes, Rajidae) in the southwestern Atlantic: quantification and life history implications. *Marine Biology* 145: 917-922
- Lund R, Grogan ED (1997) Relationships of the Chimaeriformes and the basal radiation of the Chondrichthyes. *Reviews in Fish Biology and Fisheries* 7: 65-123

- Maisey JG (1984) Chondrichthyan phylogeny: a look at the evidence. *Journal of Vertebrate Paleontology* 4: 359-371
- Maisey JG (1986) Heads and tails: a chordate phylogeny. *Cladistics* 2: 201-256
- Malagrino G, Takemura A, Mizue K (1981) Studies on the Holocephali-II. On the reproduction of *Chimaera phantasma* (Jordan and Snyder) caught in the coastal waters of Nagasaki. *Bulletin of the Faculty of Fisheries, Nagasaki University* 51: 1-7
- Maruska KP, Cowie EG, Tricas TC (1996) Periodic gonadal activity and protracted mating in elasmobranch fishes. *Journal of Experimental Zoology* 276: 219-232
- Matsubara M, Lokman PM, Senaha A, Kazeto Y, Ijiri S, Kambegawa A, Hirai T, Young G, Todo T, Adachi S, Yamauchi K (2003) Synthesis and possible function of 11-ketotestosterone during oogenesis in eel (*Anguilla* spp.). *Fish Physiology and Biochemistry* 28: 353-354
- Matta EM (2006) Aspects of the life history of the Alaska skate, *Bathyraja parmifera*, in the eastern Bering Sea. M.S. Thesis, University of Washington
- McClatchie S, Lester P (1994) Stock assessment of elephantfish (*Callorhinchus milii*). New Zealand Fisheries Assessment Research Document, New Zealand Ministry of Agriculture and Fisheries 94/6
- Miller DJ, Lea RN (1972) Guide to the coastal marine fishes of California. California Department of Fish and Game, University of California Sea Grant Marine Advisory Program and Division of Agricultural Sciences, Sacramento, CA.

- Mollet HF, Cliff G, Pratt HL, Jr, Stevens JD (2000) Reproductive biology of the female shortfin mako, *Isurus oxyrinchus* Rafinesque, 1810, with comments on the embryonic development of lamnoids. *Fishery Bulletin* 98: 299-318
- Moura T, Figueiredo I, Bordalo-Machado P, Almeida C, Gordo LS (2005) A new deep-water chimaerid species, *Hydrolagus lusitanicus* n. sp., from off mainland Portugal with a proposal of a new identification key for the genus *Hydrolagus* (Holocephali: Chimaeridae) in the north-east Atlantic. *Journal of Fish Biology* 67: 742-751
- Moura T, Figueiredo I, Machado PB, Gordo LS (2004) Growth pattern and reproductive strategy of the holocephalan *Chimaera monstrosa* along the Portuguese continental slope. *Journal of the Marine Biological Association of the United Kingdom* 84: 801-804
- Musick JA, Ellis JK (2005) Reproductive evolution of chondrichthyans. In: Hamlett WC (ed) *Reproductive biology and phylogeny of chondrichthyans: sharks, batoids, and chimaeras*. Science Publishers, Inc., Enfield, NH, USA, pp 45-71
- Neer JA, Cailliet GM (2001) Aspects of the life history of the Pacific electric ray, *Torpedo californica* (Ayres). *Copeia* 2001: 842-847
- Olsen EM, Heino M, Lilly GR, Morgan MJ, Brattey J, Ernande B, Dieckmann U (2004) Maturation trends indicative of rapid evolution preceded the collapse of northern cod. *Nature* 428: 932-935
- Pankhurst NW (2008) Gonadal steroids: functions and patterns of change. In: Rocha MJ, Arukwe A, Kapoor BG (eds) *Fish reproduction*. Science Publishers, Enfield, NH, pp 67-111

- Parsons GR (1993) Geographic variation in reproduction between two populations of the bonnethead shark, *Sphyrna tiburo*. *Environmental Biology of Fishes* 38: 25-35
- Parsons GR, Grier HJ (1992) Seasonal changes in shark testicular structure and spermatogenesis. *Journal of Experimental Zoology* 261: 173-184
- Perez LE, Callard IP (1993) Regulation of hepatic vitellogenin synthesis in the little skate (*Raja erinacea*): use of homologous enzyme-linked immunosorbent assay. *Journal of Experimental Zoology* 266: 31-39
- Pottinger TG, Pickering AD (1985) The effects of 11-ketotestosterone and testosterone on the skin structure of brown trout, *Salmo trutta* L. *General and Comparative Endocrinology* 59: 335-342
- Quaranta KL, Didier DA, Long DJ, Ebert DA (2006) A new species of chimaeroid, *Hydrolagus alphas* sp. nov. (Chimaeriformes: Chimaeridae) from the Galapagos Islands. *Zootaxa* 1377: 33-45
- Rasmussen LEL, Hess DL, Luer CA (1999) Alterations in serum steroid concentrations in the clearnose skate, *Raja eglanteria*: Correlations with season and reproductive status. *Journal of Experimental Zoology* 284: 575-585
- R Development Core Team (2007) R: A language and environment for statistical computing. Version 2.4.1. R Foundation for Statistical Computing, Vienna, Austria
- Roa R, Ernst B, Tapia F (1999) Estimation of size at sexual maturity: an evaluation of analytical and resampling procedures. *Fishery Bulletin* 97: 570-580
- Roberts CM (2002) Deep impact: the rising toll of fishing in the deep sea. *Trends in Ecology & Evolution* 17: 242-245

- Robertson DR (1991) The role of adult biology in the timing of the spawning of tropical reef fishes. In: Sale PF (ed) The ecology of coral reef fishes. Academic Press, New York, pp 356-386
- Robertson DR, Petersen CW, Brawn JD (1990) Lunar reproductive cycles of benthic-brooding reef fishes: reflections of larval biology or adult biology? Ecological Monographs 60: 311-329
- Roff DA (2002) Life history evolution. Sinauer Associates, Sunderland, MA
- Ruhl HA, Smith KL, Jr. (2004) Shifts in deep-sea community structure linked to climate and food supply. Science 305: 513-515
- Sathyanesan AG (1966) Egg-laying of the chimaeroid fish *Hydrolagus collei*. Copeia 1966(1): 132-134
- Schaeffer B (1981) The xenacanth shark neurocranium with comments on the elasmobranch phylogeny. Bulletin of the American Museum of Natural History 169: 3-66
- Schreibman MP, Margolis-Nunno H, Halpern-Sebold LR, Goos HJT, Perlman PW (1986) The influence of androgen administration on the structure and function of the brain-pituitary-gonad axis of sexually immature platyfish, *Xiphophorus maculatus*. Cell and Tissue Research 245: 519-524
- Semenkova TB, Canario AVM, Bayunova LV, Couto E, Kolmakov NN, Barannikova IA (2006) Sex steroids and oocyte maturation in the sterlet (*Acipenser ruthenus* L.). Journal of Applied Ichthyology 22: 340-345

- Simpfendorfer CA (1992) Biology of tiger sharks (*Galeocerdo cuvier*) caught by the Queensland Shark Meshing Program off Townsville, Australia. Australian Journal of Marine and Freshwater Research 43: 33-43
- Smith C, Griffiths C (1997) Shark and skate egg-cases cast up on two South African beaches and their rates of hatching success, or causes of death. South African Journal of Zoology 32: 112-117
- Smith RM, Walker TI, Hamlett WC (2004) Microscopic organisation of the oviducal gland of the holocephalan elephant fish, *Callorhynchus milii*. Marine and Freshwater Research 55: 155-164
- Sorbera LA, Callard IP (1989) The myometrium of the spiny dogfish, *Squalus acanthias*: a model for steroid and peptide regulation. Bulletin of the Mount Desert Island Biological Laboratory 28: 32-35
- Sosebee KA (2005) Are density-dependent effects on elasmobranch maturity possible? Journal of Northwest Atlantic Fishery Science 35: 115-124
- Springer S (1967) Social organization of shark populations. In: Gilbert PW, Mathewson RF, Rall DP (eds) Sharks, skates and rays. Johns Hopkins University Press, Baltimore, MD, pp 149-174
- Stanley HP (1961) Studies on the genital systems and reproduction in the chimaeroid fish *Hydrolagus colliei* (Lay and Bennett). Ph.D. Thesis, Oregon State University
- Stanley HP (1963) Urogenital morphology in the chimaeroid fish *Hydrolagus colliei* (Lay and Bennett). Journal of Morphology 112: 99-127
- Stearns SC (1992) The evolution of life histories. Oxford University Press, New York

- Steven GA (1933) Rays and skates of Devon and Cornwall III. The proportions of the sexes in nature and in commercial landings, and their significance to the fishery. *Journal of the Marine Biological Association of the United Kingdom* 18: 611-625
- Stevens JD, Bonfil R, Dulvy NK, Walker PA (2000) The effects of fishing on sharks, rays, and chimeras (chondrichthyans), and the implications for marine ecosystems. *ICES Journal of Marine Science* 57: 476-494
- Strasburg DW (1958) Distribution, abundance, and habits of pelagic sharks in the central Pacific Ocean. *Fishery Bulletin* 138: 335-361
- Sulikowski JA, Tsang PCW, Huntting Howell W (2004) An annual cycle of steroid hormone concentrations and gonad development in the winter skate, *Leucoraja ocellata*, from the western Gulf of Maine. *Marine Biology* 144: 845-853
- Sumpter JP, Dodd JM (1979) The annual reproductive cycle of the female lesser spotted dogfish, *Scyliorhinus canicula* L., and its endocrine control. *Journal of Fish Biology* 15: 687-695
- Takemura A, Kim BH (2001) Effects of estradiol-17[beta] treatment on *in vitro* and *in vivo* synthesis of two distinct vitellogenins in tilapia. *Comparative Biochemistry and Physiology - Part A: Molecular & Integrative Physiology* 129: 641-651
- Tolimieri N (2007) Patterns in species richness, species density, and evenness in groundfish assemblages on the continental slope of the U.S. Pacific coast. *Environmental Biology of Fishes* 78: 241-256
- Tovar-Avila J (2006) Reproduction, age validation, growth determination and effects of fishing on the Port Jackson shark (*Heterodontus portjacksoni*) in South-Eastern Australia. Ph.D. Thesis, University of Melbourne

- Tovar-Avila J, Walker TI, Day RW (2007) Reproduction of *Heterodontus portusjacksoni* in Victoria, Australia: evidence of two populations and reproductive parameters for the eastern population. *Marine and Freshwater Research* 58: 956-965
- Tyler WA, Stanton FG (1995) Potential influence of food abundance on spawning patterns in a damselfish, *Abudefduf abdominalis*. *Bulletin of Marine Science* 57: 610-623
- Vu-Tan-Tue (1972) Variations cycliques des gonades et de quelques glandes endocrines chez *Chimaera montrosa* Linne (Pisces: Holocephali). *Annales Des Sciences Naturelles comprenant la zoologie* 14: 49-94
- Walker TI (1998) Can shark resources be harvested sustainably? A question revisited with a review of shark fisheries. *Marine and Freshwater Research* 49: 553-572
- Walker TI (2007) Spatial and temporal variation in the reproductive biology of gummy shark *Mustelus antarcticus* (Chondrichthyes : Triakidae) harvested off southern Australia. *Marine and Freshwater Research* 58: 67-97
- Walmsley-Hart SA, Sauer WHH, Buxton CD (1999) The biology of the skates *Raja wallacei* and *R. pullopunctata* (Batoidea: Rajidae) on the Agulhas Bank, South Africa. *South African Journal of Marine Science* 21: 165-179
- Whittier JM, Crews D (1987) Seasonal reproduction: patterns and control. In: Norris DO, Jones RE (eds) *Hormones and reproduction in fishes, amphibians, and reptiles*. Plenum Press, New York, pp 385-409
- Wilimovsky NJ (1954) List of the fishes of Alaska. *Stanford Ichthyological Bulletin* 4: 279-294

- Woodhead PMJ (1969) Effects of estradiol and thyroxine upon the plasma calcium content of a shark *Scyliorhinus canicula*. *General and Comparative Endocrinology* 13: 310-312
- Wourms JP (1977) Reproduction and development in chondrichthyan fishes. *American Zoologist* 17: 379-410
- Wourms JP, Lombardi J (1992) Reflections on the evolution of piscine viviparity. *American Zoologist* 32: 276-293
- Yamaguchi A, Taniuchi T, Shimizu M (2000) Geographic variations in reproductive parameters of the starspotted dogfish, *Mustelus manazo*, from five localities in Japan and in Taiwan. *Environmental Biology of Fishes* 57: 221-233
- Yano K (1995) Reproductive biology of the black dogfish, *Centroscyllium fabricii*, collected from waters off western Greenland. *Journal of the Marine Biological Association of the U.K.* 75: 285-310

Table 1. Length of spawning season and depth of demersal chondrichthyans species used in comparative analyses, each estimated as the midpoint of the range from the literature. Data are either from original sources, or sources compiled in the Pacific Shark Research Center's (PSRC) Life History Data Matrix of eastern North Pacific chondrichthyans: <http://psrc.mlml.calstate.edu/>. Chimaeroids included are from multiple ocean basins and elasmobranchs are from the eastern North Pacific.

<i>Order</i>	<i>Species</i>	<i>Depth</i>	<i>Months of Parturition</i>	<i>Citations</i>
Carcharhiniformes	<i>Cephalurus cephalus</i>	541	2	PSRC
Carcharhiniformes	<i>Triakis semifasciata</i>	46	3	PSRC
Carcharhiniformes	<i>Mustelus californicus</i>	34	4.5	PSRC
Carcharhiniformes	<i>Negaprion brevirostris</i>	46	5	PSRC
Carcharhiniformes	<i>Galeorhinus galeus</i>	236	5	PSRC
Carcharhiniformes	<i>Mustelus henlei</i>	100	6.3	PSRC
Carcharhiniformes	<i>Apristurus brunneus</i>	517	8.5	PSRC
Carcharhiniformes	<i>Parmaturus xaniurus</i>	671	12	PSRC
Chimaeriformes	<i>Callorhynchus millii</i>	50	5	Gorman 1963; review in McLatchie and Lester 1994; Francis et al. 2002; Bell 2003
Chimaeriformes	<i>Chimaera phantasma</i>	260	6	Malagrino et al. 1981; Didier Dagit 2006a
Chimaeriformes	<i>Chimaera monstrosa</i>	725	6	Vu-Tan-Tue 1972; Stehmann and Bürkel 1984; Gordon and Bergstad 1992
Chimaeriformes	<i>Hydrolagus colliciei</i>	356	7	This study
Chimaeriformes	<i>Callorhynchus callorhynchus</i>	69	10.5	Menni and Lopez 1984; DiGiacomo and Perier 1994
Chimaeriformes	<i>Hydrolagus barbouri</i>	675	12	Dagit 2006b; Kokuho et al. 2003
Heterodontiformes	<i>Heterodontus francisci</i>	75	3	PSRC
Myliobatiformes	<i>Urobatis halleri</i>	46	2	PSRC
Myliobatiformes	<i>Dasyatis dipterura</i>	14	3	PSRC
Myliobatiformes	<i>Gymnura marmorata</i>	11	3.3	PSRC
Myliobatiformes	<i>Myliobatis californica</i>	54	4.25	PSRC
Orectolobiformes	<i>Ginglymostoma cirratum</i>	65	3	PSRC
Rajiformes	<i>Bathyraja aleutica</i>	450	6	PSRC
Rajiformes	<i>Raja inornata</i>	309	12	PSRC
Rajiformes	<i>Raja binoculata</i>	399	12	PSRC
Rhinobatiformes	<i>Zapteryx exasperate</i>	6	2	PSRC
Rhinobatiformes	<i>Rhinobatos productus</i>	6	2.3	PSRC
Rhinobatiformes	<i>Platyrrhinoidis triseriata</i>	69	3	PSRC
Torpediniformes	<i>Narcine entemedor</i>	50	2	PSRC
Torpediniformes	<i>Torpedo californica</i>	214	12	PSRC

Table 2. Fecundity and maximum length of chondrichthyan species used in comparative analyses. Fecundity was estimated as the midpoint of the range from the literature, or the average if available (sources are from citations in Musick and Ellis 2005 or the Pacific Shark Research Center’s (PSRC) Life History Data Matrix of eastern North Pacific chondrichthyans: <http://psrc.mlml.calstate.edu/>, unless otherwise stated).

Order	Species	Mode	Fecundity	Max Size		Citations
Carcharhiniformes	<i>Parmaturus xaniurus</i>	oviparity	23	61	TL	PSRC
Carcharhiniformes	<i>Apristurus brunneus</i>	oviparity	29	69	TL	PSRC
Carcharhiniformes	<i>Scyliorhinus rotifer</i>	oviparity	48.5	47	TL	Musick and Ellis 2005
Carcharhiniformes	<i>Scyliorhinus canicula</i>	oviparity	109.5	80	TL	Musick and Ellis 2005
Carcharhiniformes	<i>Rhizoprionodon longurio</i>	viviparity	3.5	154	TL	PSRC
Carcharhiniformes	<i>Carcharhinus porosus</i>	viviparity	5	150	TL	PSRC
Carcharhiniformes	<i>Nasolamia velox</i>	viviparity	5	150	TL	PSRC
Carcharhiniformes	<i>Mustelus henlei</i>	viviparity	5.5	100	TL	PSRC
Carcharhiniformes	<i>Carcharhinus leucas</i>	viviparity	7	324	TL	PSRC
Carcharhiniformes	<i>Carcharhinus longimanus</i>	viviparity	7.5	243	TL	PSRC
Carcharhiniformes	<i>Carcharhinus altimus</i>	viviparity	9	300	TL	PSRC
Carcharhiniformes	<i>Sphyrna tiburo</i>	viviparity	9	134	TL	PSRC
Carcharhiniformes	<i>Mustelus californicus</i>	viviparity	9.5	160	TL	PSRC
Carcharhiniformes	<i>Negaprion brevirostris</i>	viviparity	11	320	TL	PSRC
Carcharhiniformes	<i>Carcharhinus brachyurus</i>	viviparity	16	293	TL	PSRC
Carcharhiniformes	<i>Triakis semifasciata</i>	viviparity	21	198	TL	PSRC
Carcharhiniformes	<i>Sphyrna mokarran</i>	viviparity	27.5	600	TL	PSRC
Carcharhiniformes	<i>Galeorhinus galeus</i>	viviparity	29	195	TL	PSRC
Carcharhiniformes	<i>Prionace glauca</i>	viviparity	30	400	TL	PSRC
Carcharhiniformes	<i>Sphyrna zygaena</i>	viviparity	33	385	TL	PSRC
Chimaeriformes	<i>Callorhynchus millii</i>	oviparity	20	94	TL	Bell 2003
Chimaeriformes	<i>Hydrolagus colliciei</i>	oviparity	24.2	63	TL	Gorman 1963; This study
Lamniformes	<i>Lamna ditropis</i>	viviparity	3.5	305	TL	PSRC
Lamniformes	<i>Alopias vulpinus</i>	viviparity	4	667	TL	PSRC
Lamniformes	<i>Isurus paucus</i>	viviparity	5	360	TL	PSRC
Lamniformes	<i>Isurus oxyrinchus</i>	viviparity	9.5	351	TL	PSRC
Large Squaliformes	<i>Centrophorus cf. uyato</i>	viviparity	1	100	TL	Musick and Ellis 2005
Large Squaliformes	<i>Centrophorus moluccensis</i>	viviparity	2	98	TL	Musick and Ellis 2005
Large Squaliformes	<i>Squalus rancureli</i>	viviparity	3	77	TL	Musick and Ellis 2005
Large Squaliformes	<i>Squalus megalops</i>	viviparity	3	71	TL	Musick and Ellis 2005
Large Squaliformes	<i>Squalus blainvillei</i>	viviparity	3.5	95	TL	Musick and Ellis 2005
Large Squaliformes	<i>Squalus japonicus</i>	viviparity	4.08	91	TL	Musick and Ellis 2005
Large Squaliformes	<i>Centroselachus crepidater</i>	viviparity	6	90	TL	Musick and Ellis 2005
Large Squaliformes	<i>Deania profundorum</i>	viviparity	6	76	TL	Musick & Ellis 2005
Large Squaliformes	<i>Oxynotus bruniensis</i>	viviparity	7	82	TL	Musick and Ellis 2005
Myliobatiformes	<i>Manta birostris</i>	viviparity	1	910	DW	PSRC
Myliobatiformes	<i>Mobula japonica</i>	viviparity	1	248	DW	PSRC

Myliobatiformes	<i>Dasyatis longa</i>	viviparity	2	156	DW	Musick and Ellis 2005
Myliobatiformes	<i>Dasyatis dipterura</i>	viviparity	2.5	88	DW	Musick and Ellis 2005
Myliobatiformes	<i>Urobatis halleri</i>	viviparity	2.5	18	TL	PSRC
Myliobatiformes	<i>Dasyatis Sabina</i>	viviparity	2.6	37	DW	Musick and Ellis 2005
Myliobatiformes	<i>Aetobatus narinari</i>	viviparity	3	230	DW	PSRC
Myliobatiformes	<i>Dasyatis marmorata</i>	viviparity	3	440	DW	Musick and Ellis 2005
Myliobatiformes	<i>Dasyatis sayi</i>	viviparity	3.5	73	DW	Musick and Ellis 2005
Myliobatiformes	<i>Dasyatis centroura</i>	viviparity	4	220	DW	Musick and Ellis 2005
Myliobatiformes	<i>Dasyatis tortonesei</i>	viviparity	4	80	DW	Musick and Ellis 2005
Myliobatiformes	<i>Dasyatis Americana</i>	viviparity	4.2	200	DW	Musick and Ellis 2005
Myliobatiformes	<i>Potamotrygon circularis</i>	viviparity	5.8	60	DW	Musick and Ellis 2005
Myliobatiformes	<i>Dasyatis pastinaca</i>	viviparity	6	60	DW	Musick and Ellis 2005
Myliobatiformes	<i>Dasyatis violacea</i>	viviparity	6	88	DW	PSRC
Myliobatiformes	<i>Potamotrygon motoro</i>	viviparity	6.3	46	DW	Musick and Ellis 2005
Myliobatiformes	<i>Myliobatis californica</i>	viviparity	7	180	DW	PSRC
Myliobatiformes	<i>Pteroplatytrygon violacea</i>	viviparity	8.5	80	DW	Musick and Ellis 2005
Myliobatiformes	<i>Gymnura marmorata</i>	viviparity	10	100	TL	PSRC
Orectolobiformes	<i>Hemiscyllium ocellatum</i>	oviparity	22	107	TL	Compagno 2005; Musick and Ellis 2005
Orectolobiformes	<i>Ginglymostoma cirratum</i>	viviparity	35	355	TL	PSRC
Rajiformes	<i>Bathyraja parmifera</i>	oviparity	29	119	TL	Matta 2006
Rajiformes	<i>Leucoraja erinacea</i>	oviparity	30	54	TL	Musick and Ellis 2005
Rajiformes	<i>Dipturus batis</i>	oviparity	40	250	TL	Musick and Ellis 2005
Rajiformes	<i>Raja polystigma</i>	oviparity	41	53	DW	Musick and Ellis 2005
Rajiformes	<i>Raja montagui</i>	oviparity	42.5	80	DW	Musick and Ellis 2005
Rajiformes	<i>Amblyraja radiata</i>	oviparity	45	105	TL	Musick and Ellis 2005; Sulikowski et al. 2005
Rajiformes	<i>Raja eglanteria</i>	oviparity	60	79	TL	Musick and Ellis 2005
Rajiformes	<i>Raja miraletus</i>	oviparity	61	60	TL	Musick and Ellis 2005
Rajiformes	<i>Raja brachyuran</i>	oviparity	65	120	TL	Musick and Ellis 2005
Rajiformes	<i>Raja asterias</i>	oviparity	73	70	TL	Musick and Ellis 2005
Rajiformes	<i>Leucoraja naevus</i>	oviparity	90	70	TL	Musick and Ellis 2005
Rajiformes	<i>Raja clavata</i>	oviparity	100	90	TL	Musick and Ellis 2005
Rhiniformes	<i>Rhyncobatus djiddensis</i>	viviparity	4	310	TL	Musick and Ellis 2005
Rhinobatiformes	<i>Rhinobatos granulatus</i>	viviparity	4	280	SL	Musick and Ellis 2005
Rhinobatiformes	<i>Rhinobatos hynnicephalus</i>	viviparity	4.6	44	TL	Musick and Ellis 2005
Rhinobatiformes	<i>Rhinobatos lentiginosus</i>	viviparity	6	75	TL	Musick and Ellis 2005
Rhinobatiformes	<i>Rhinobatos rhinobatos</i>	viviparity	7	162	TL	Musick and Ellis 2005
Rhinobatiformes	<i>Rhinobatos cemiculus</i>	viviparity	7.5	230	TL	Musick and Ellis 2005
Rhinobatiformes	<i>Zapteryx exasperate</i>	viviparity	7.5	97	TL	Musick and Ellis 2005
Rhinobatiformes	<i>Platyrhinoides triseriata</i>	viviparity	8	91	TL	Musick and Ellis 2005
Rhinobatiformes	<i>Rhinobatos horkelii</i>	viviparity	8	130	TL	Musick and Ellis 2005
Rhinobatiformes	<i>Rhinobatos productus</i>	viviparity	10	156	TL	PSRC
Small Squaliformes	<i>Etmopterus brachyurus</i>	viviparity	2	42	TL	Compagno 2005
Small Squaliformes	<i>Etmopterus hillanus</i>	viviparity	4.5	50	TL	Musick and Ellis 2005
Small Squaliformes	<i>Euprotomicrus bispinatus</i>	viviparity	8	27	TL	Musick and Ellis 2005
Small Squaliformes	<i>Isistius brasiliensis</i>	viviparity	9	56	TL	Ebert 2003; Compagno 2005
Small Squaliformes	<i>Etmopterus granulosus</i>	viviparity	11.5	38	TL	Musick and Ellis 2005
Torpediniformes	<i>Narcine entemedor</i>	viviparity	12	93	TL	PSRC
Torpediniformes	<i>Torpedo californica</i>	viviparity	17	137	TL	PSRC

Table 3. Results of *t*-tests comparing temporal trends in hormone concentration between sampling periods in June and September as measured from skeletal muscle and plasma.

<i>Sample type</i>	<i>Hormone</i>	<i>Df</i>	<i>t</i>	<i>p-value</i>
Muscle	11KT	18	-0.17	0.87
Muscle	T	18	-0.23	0.82
Muscle	E ₂	22	1.50	0.15
Muscle	P ₄	22	0.34	0.73
Plasma	11KT	18	-0.04	0.97
Plasma	T	18	0.02	0.99
Plasma	E ₂	22	1.32	0.20
Plasma	P ₄	22	-0.38	0.71

Table 4. Results of paired *t*-tests comparing hormone concentrations of skeletal muscle sampled from the same individual immediately after capture and three hours after capture.

<i>Hormone</i>	<i>df</i>	<i>t</i>	<i>p-value</i>
KT	3	0.70	0.54
T	6	0.09	0.93
E ₂	5	0.47	0.66
P ₄	4	2.43	0.07

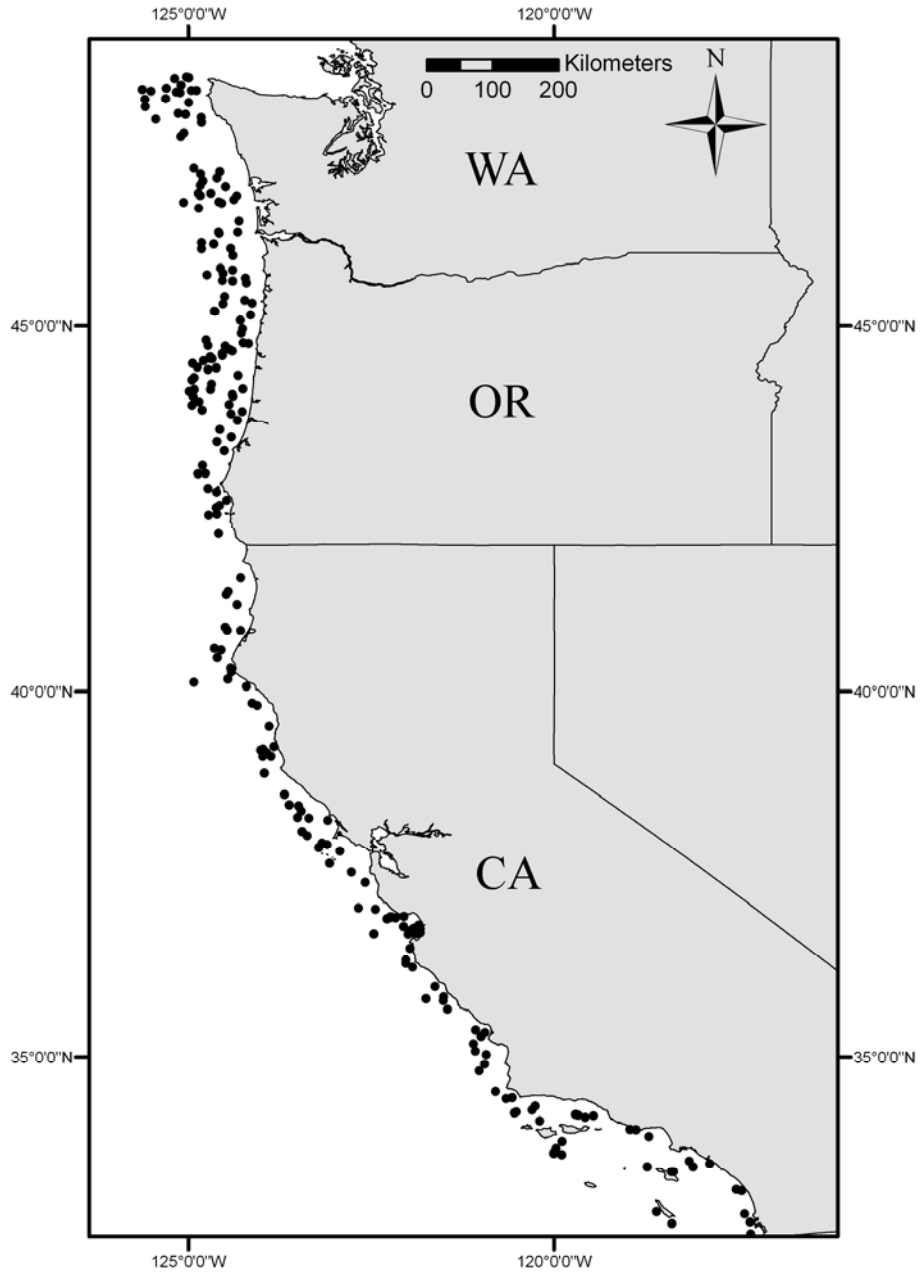


Figure 1. Spatial distribution of samples collected from 2003 to 2007 off California, Oregon, and Washington (between 32.6° to 48.4° N and 117.3° to 125.6° W).

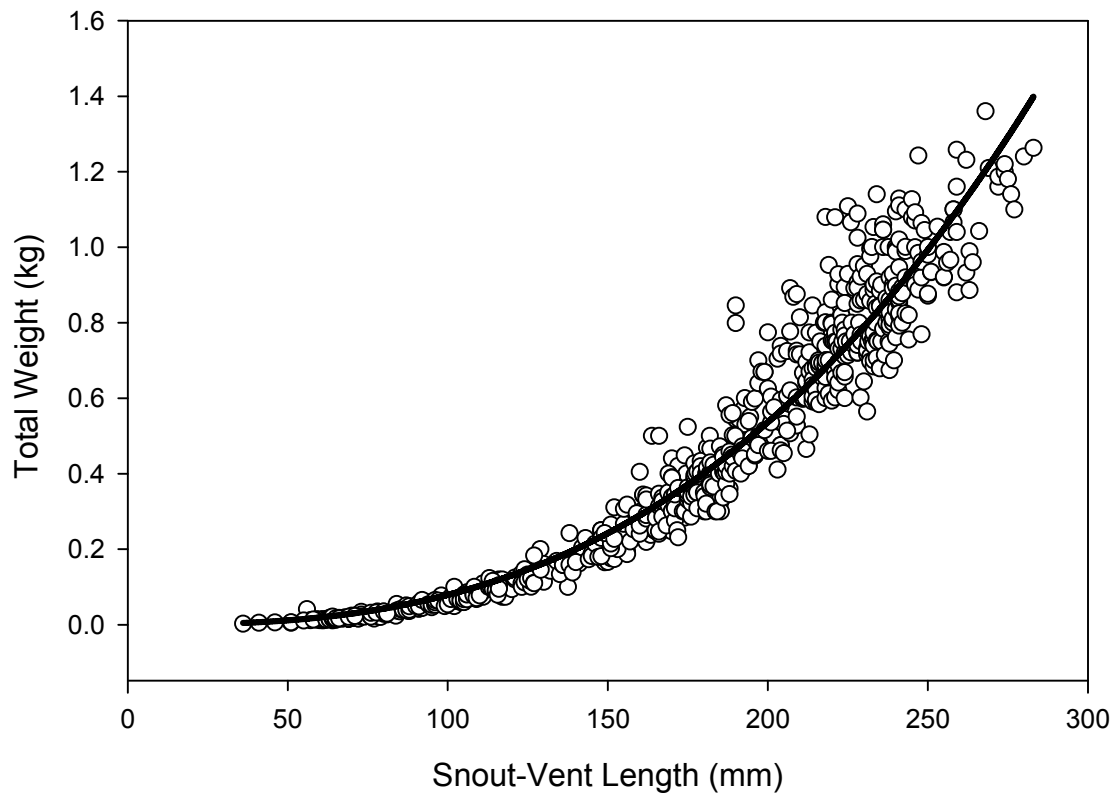


Figure 2. Length-weight regression for both sexes combined.

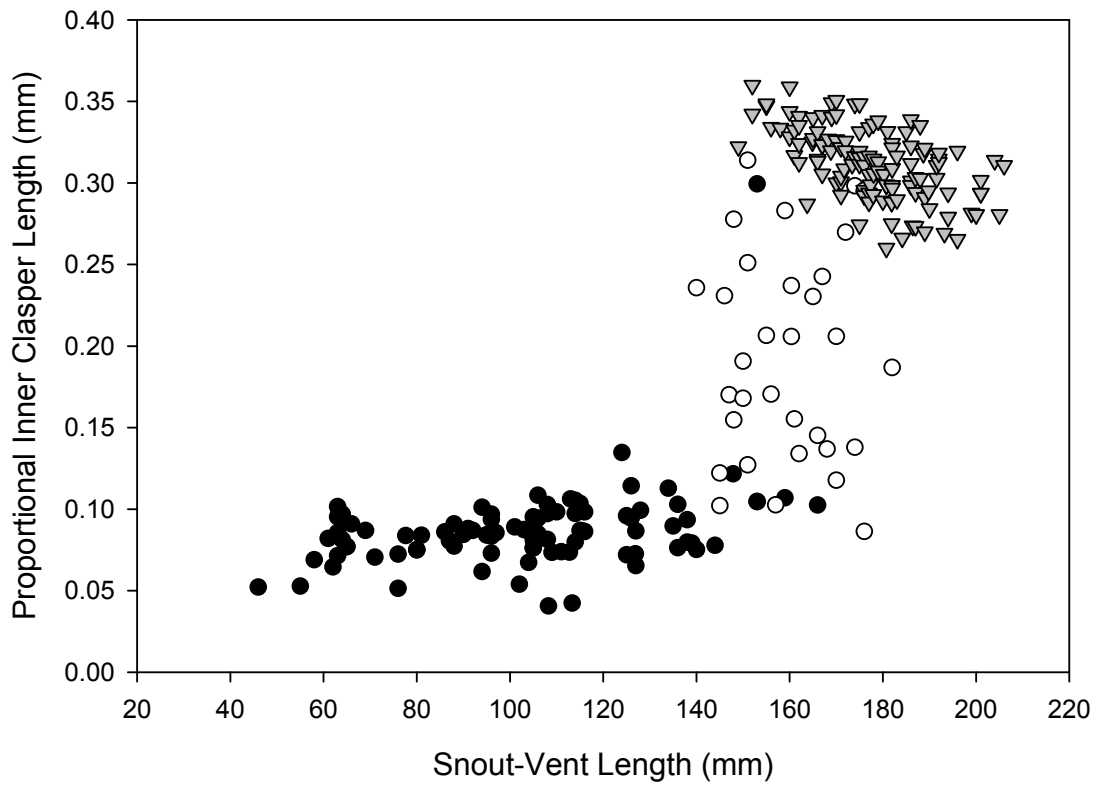


Figure 3. Ratio of inner clasper length to snout-vent length, displayed as a function of snout-vent length for individuals defined by the morphological criteria as juveniles (filled circles), adolescents (open circles), and adults (gray triangles).

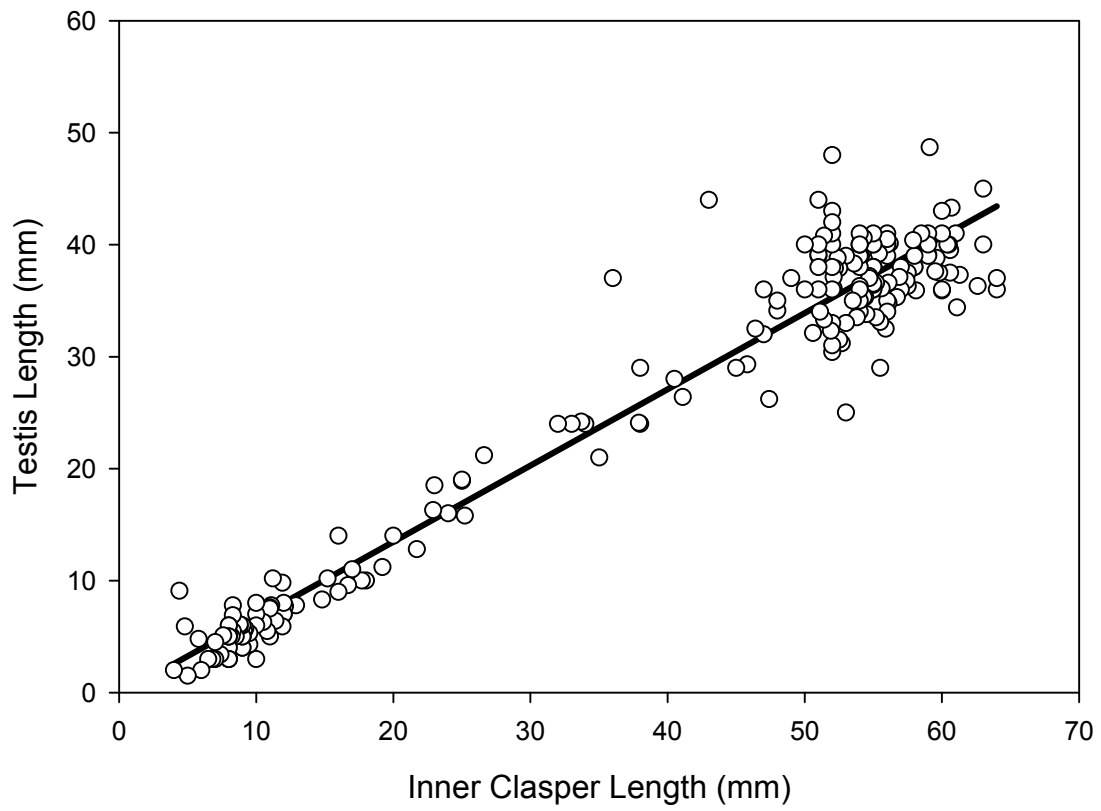


Figure 4. Linear regression of inner clasper length on testis length.

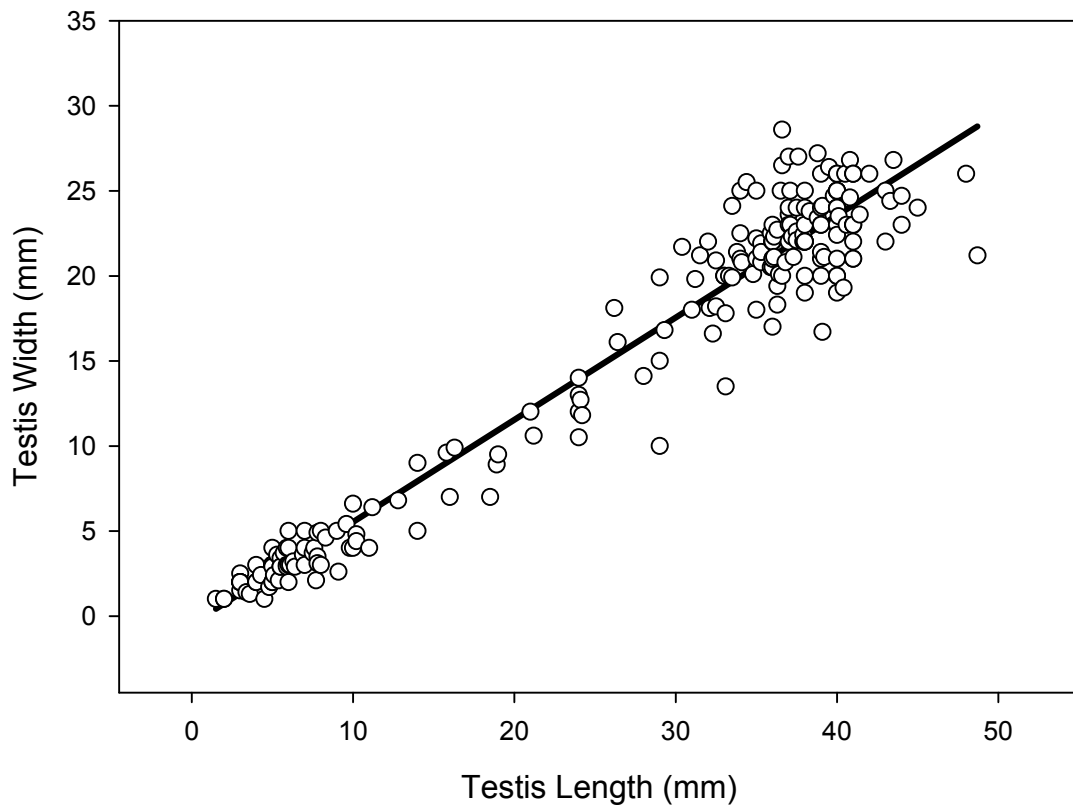


Figure 5. Comparison of testis length to width, displaying isometric growth of internal and external sex organs.

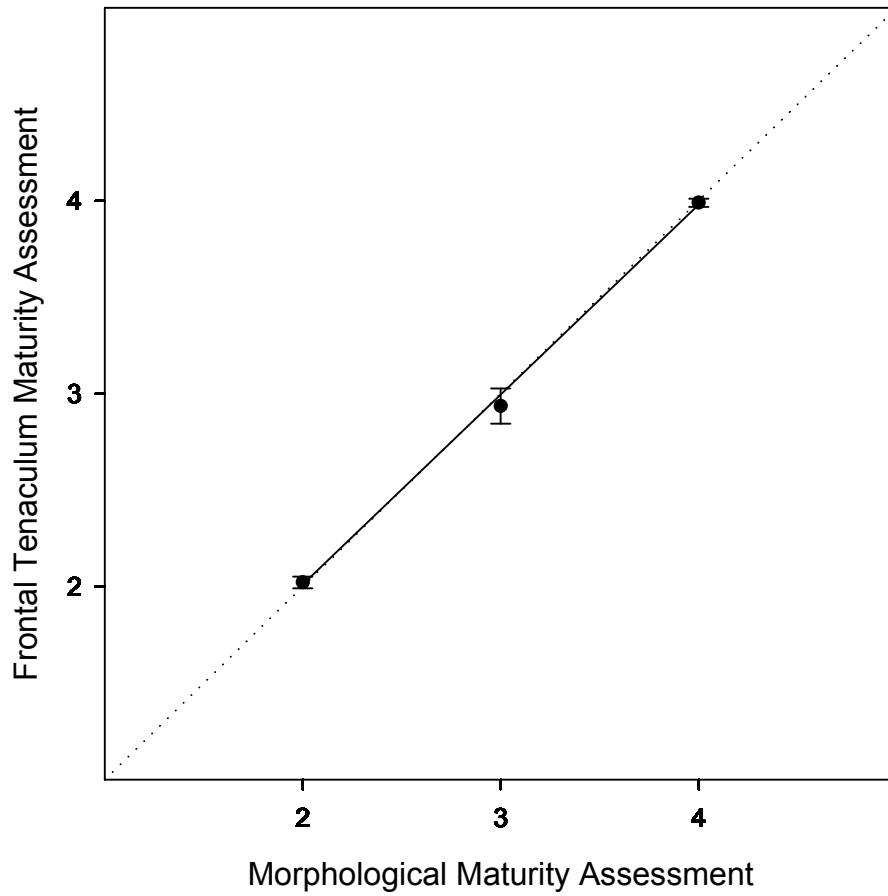


Figure 6. Comparison of the maturity estimates made from the morphological criteria and frontal tenaculum criteria. Error bars represent 95% confidence intervals. A dotted line with a slope of one and intercept of zero is shown for reference.

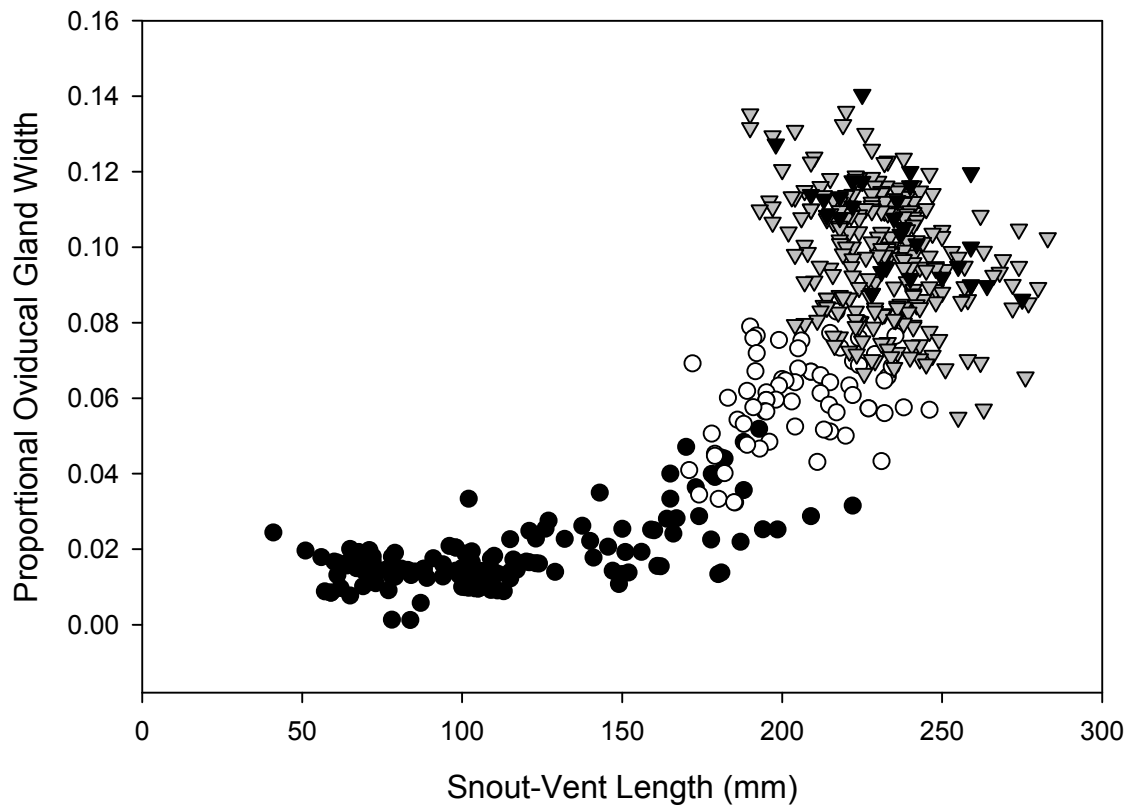


Figure 7. Ratio of oviducal gland width to snout-vent length, displayed as a function of snout-vent length for individuals defined by the morphological criteria as juveniles (filled circles), adolescents (open circles), adults (gray triangles), and gravid adults (black triangles).

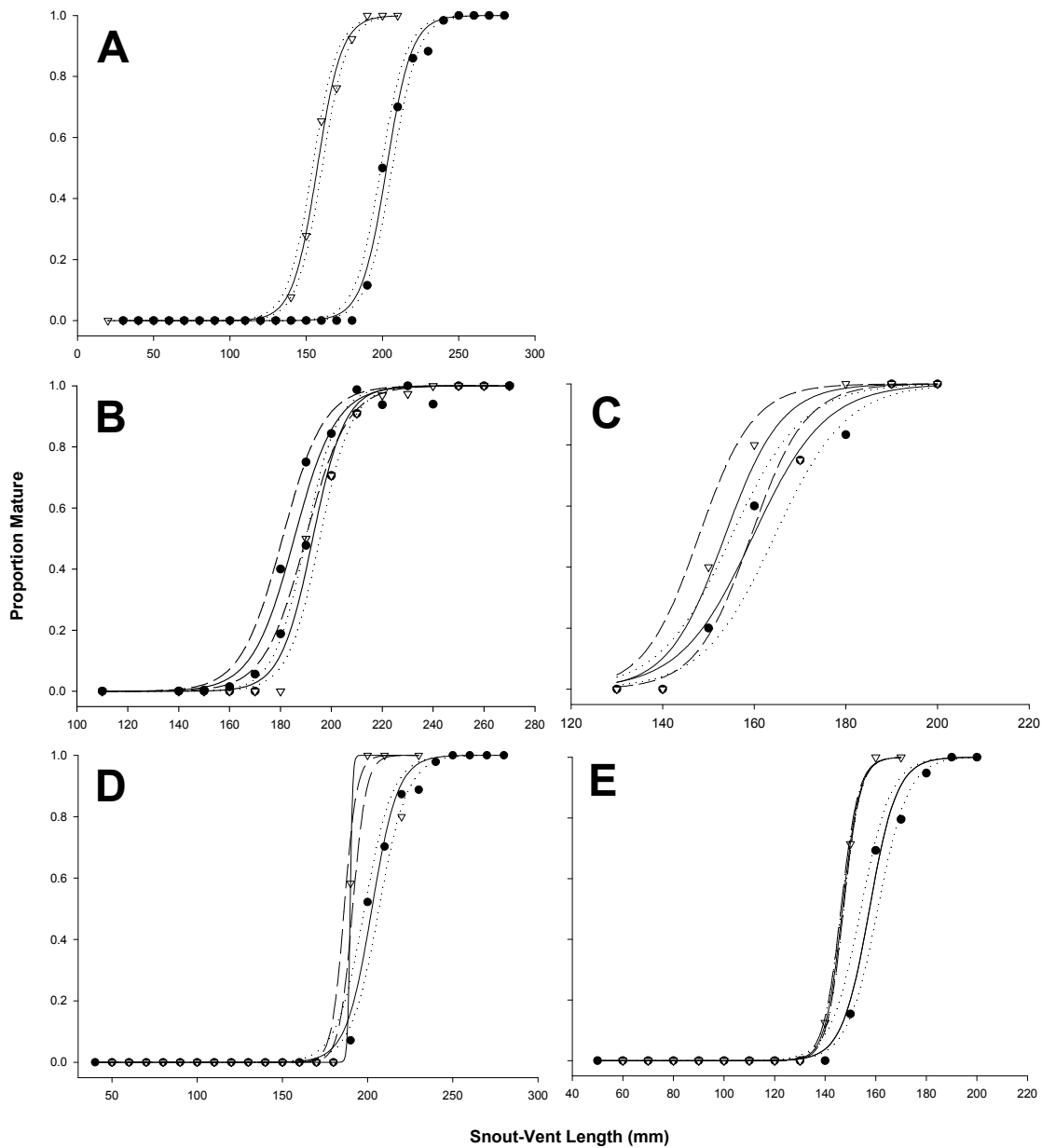


Figure 8. Maturity ogives (A) for males (empty triangles) and females (filled circles), based on the morphological criteria; (B) for females using the morphological criteria (empty triangles) and estradiol concentration (filled circles); (C) for males using the morphological criteria (empty triangles) and testosterone concentration (filled circles); (D) for females north (filled circles) and south (empty triangles) of Point Conception; (E) for males north (filled circles) and south (empty triangles) of Cape Mendocino. Broken lines are 95% confidence bands.

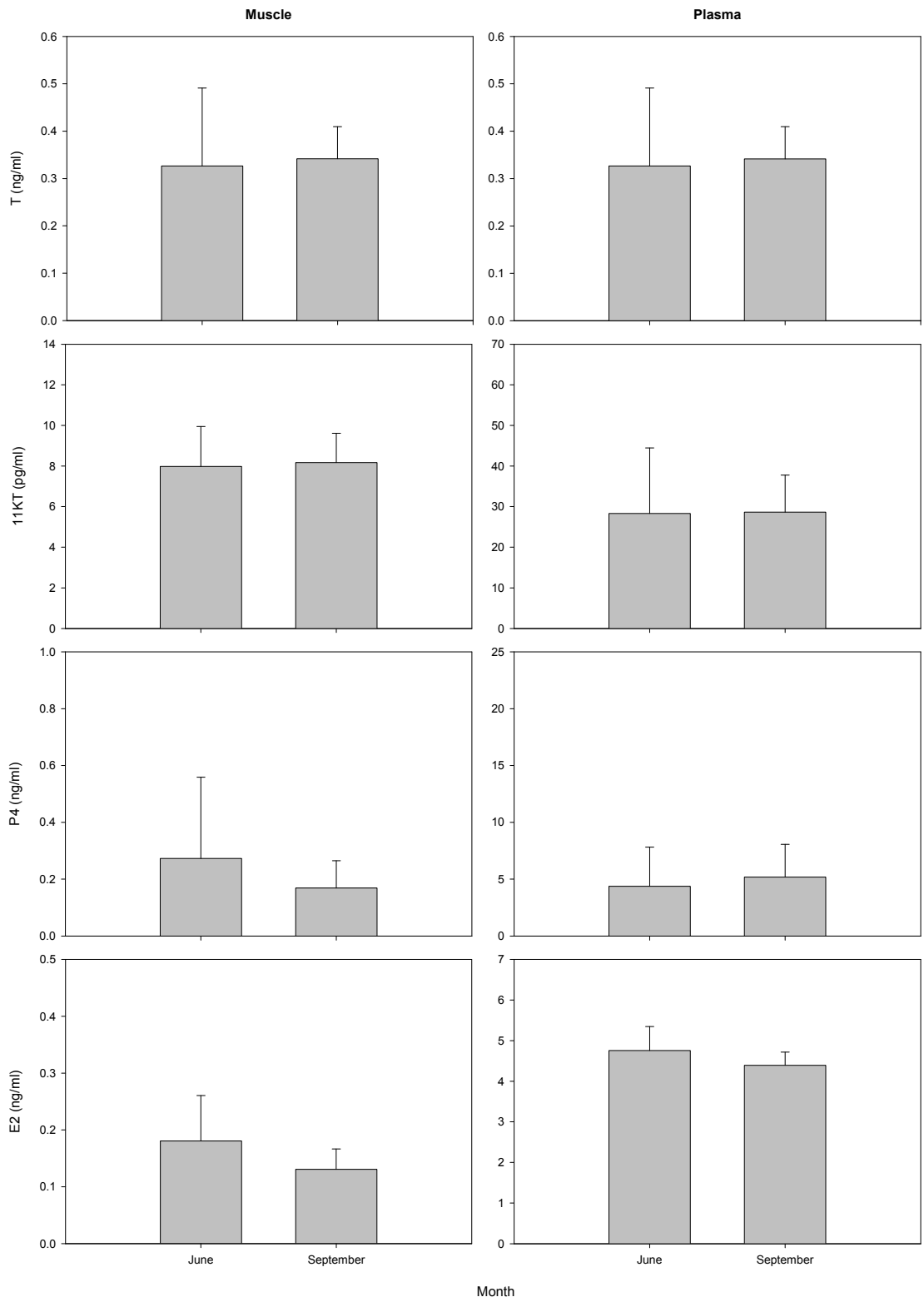


Figure 9. Comparison of mean steroid hormone concentrations from paired samples of muscle and plasma. Error bars represent 95% confidence intervals.

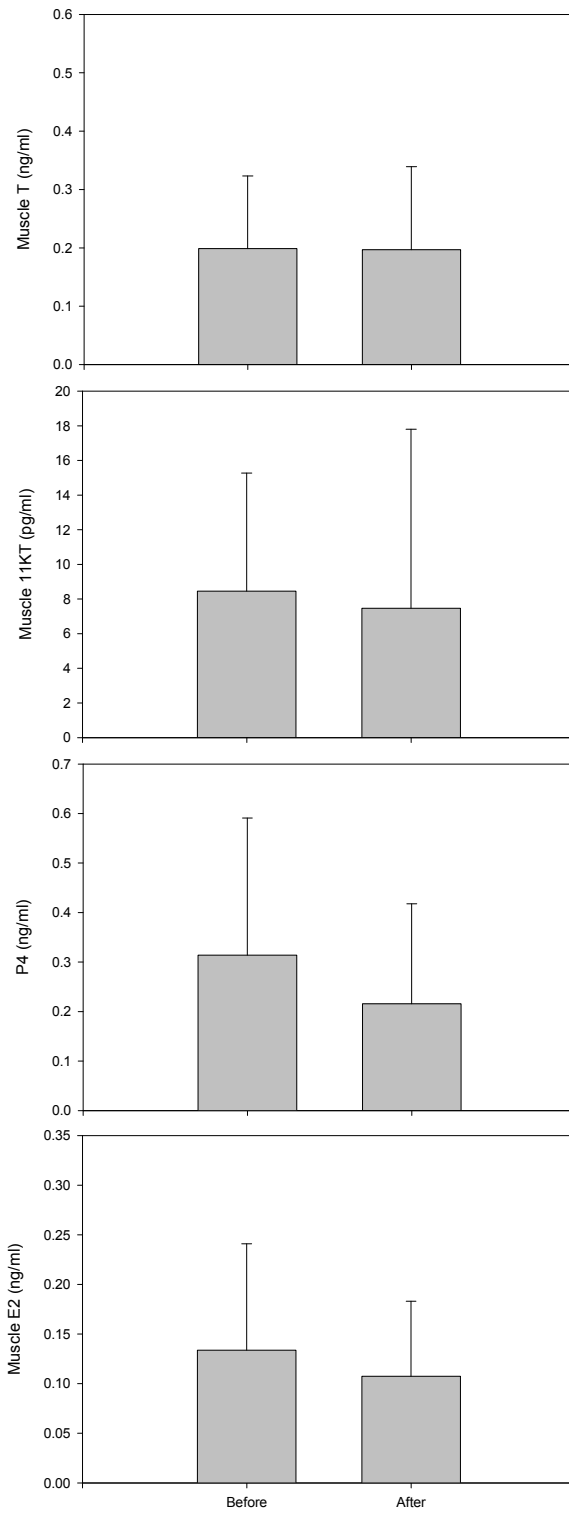


Figure 10. Comparison of mean steroid hormone concentrations from muscle sampled immediately (before) and three hours later (after). Error bars represent 95% confidence intervals.

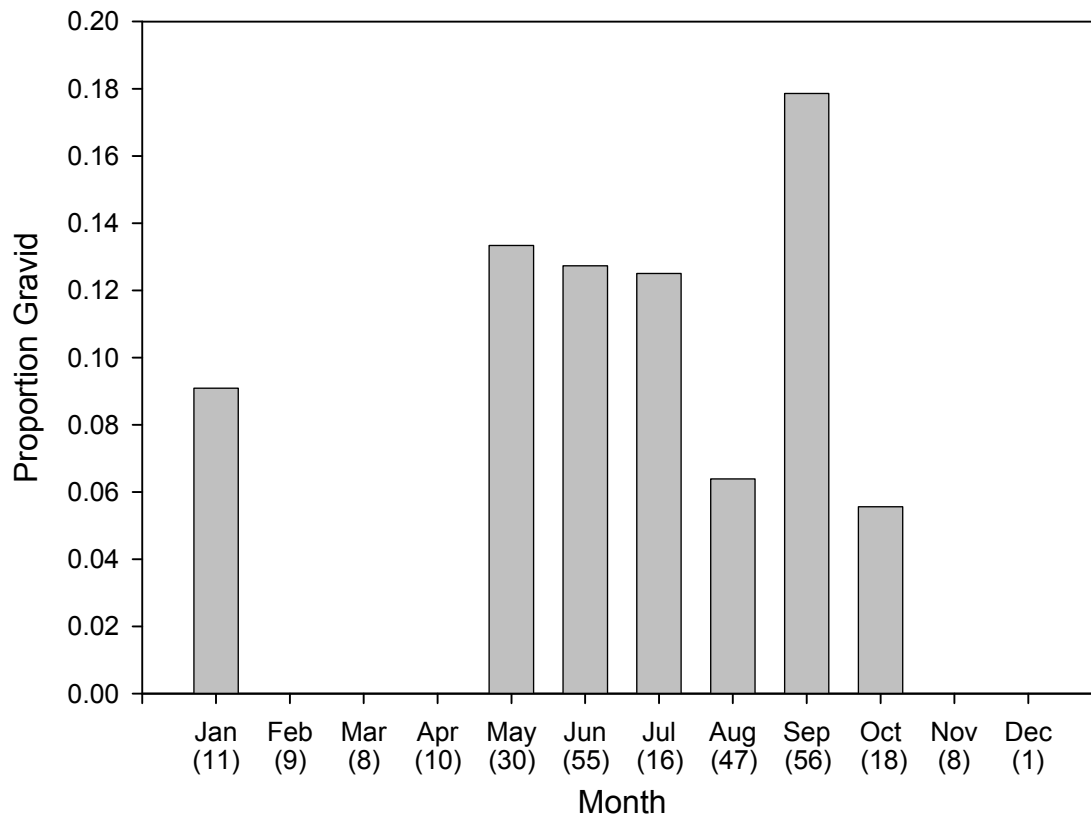


Figure 11. Proportion of adult females in gravid reproductive state, by month. Sample sizes are in parentheses.

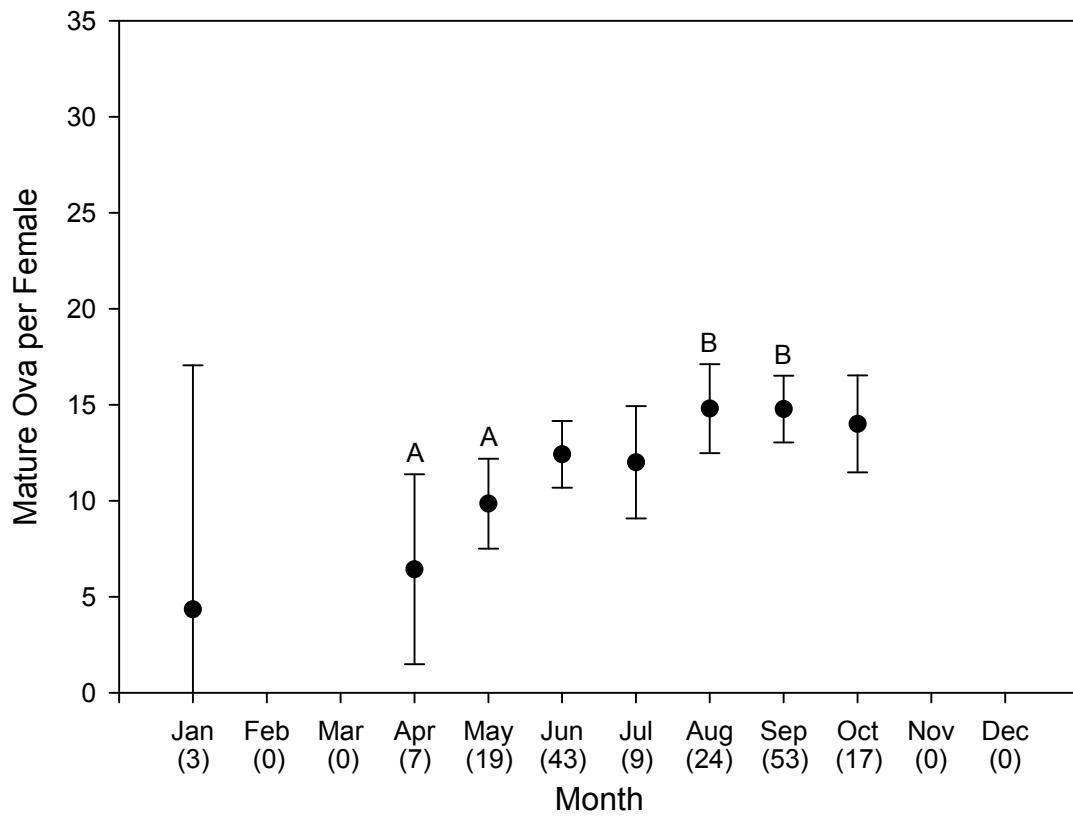


Figure 12. Mean number of mature ova per female, by month. Error bars represent 95% confidence intervals. Sample sizes are in parentheses. Letters indicate significant differences among months.

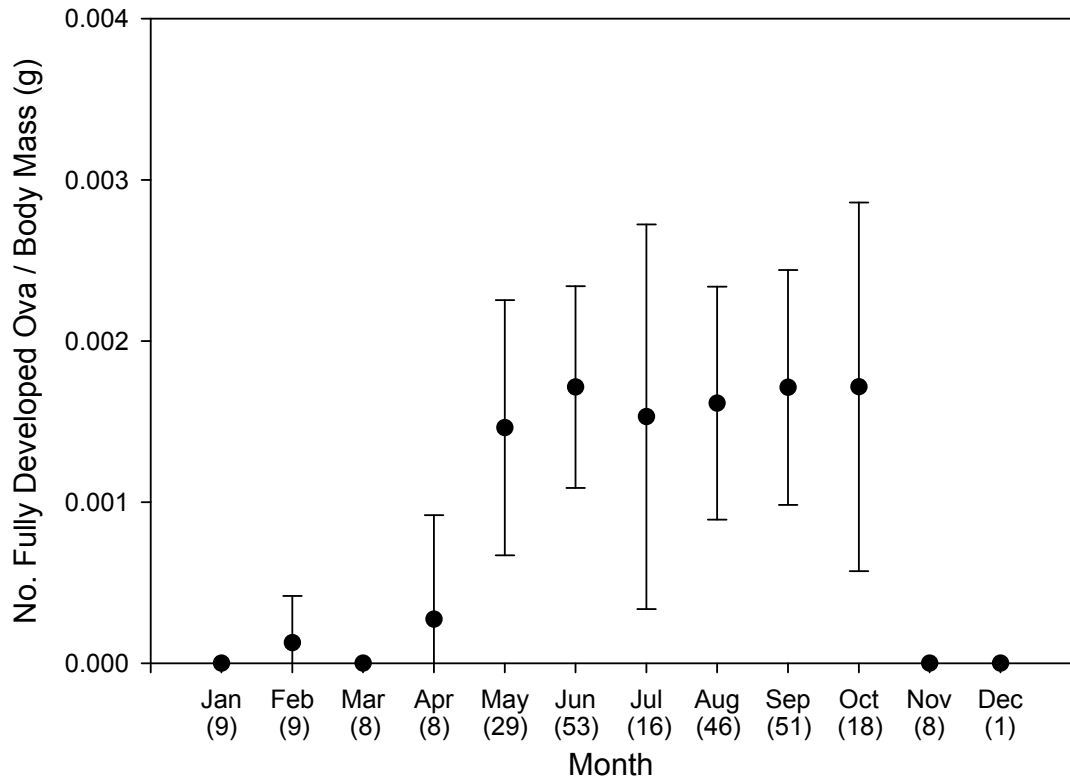


Figure 13. Mean number of fully developed ova per female, standardized by total body mass, by month. Error bars represent 95% confidence intervals. Sample sizes are in parentheses.

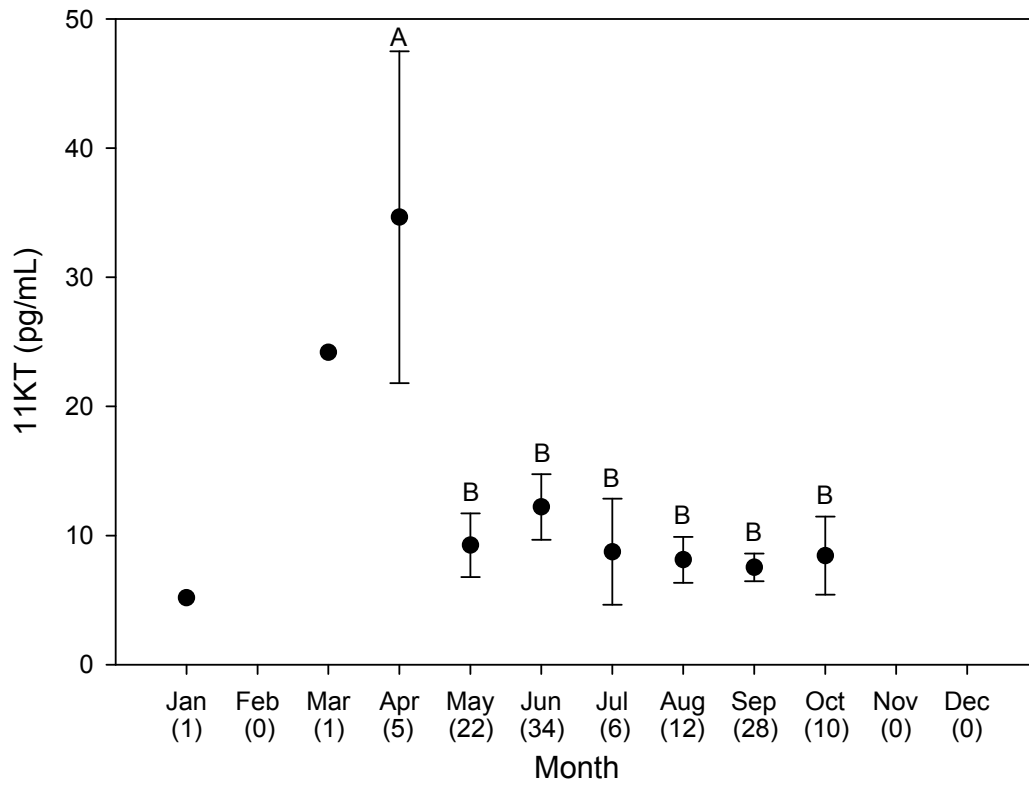


Figure 14. Mean female 11KT muscle concentration by month. Error bars represent 2 SEs. Sample sizes are in parentheses. Letters indicate significant differences among months.

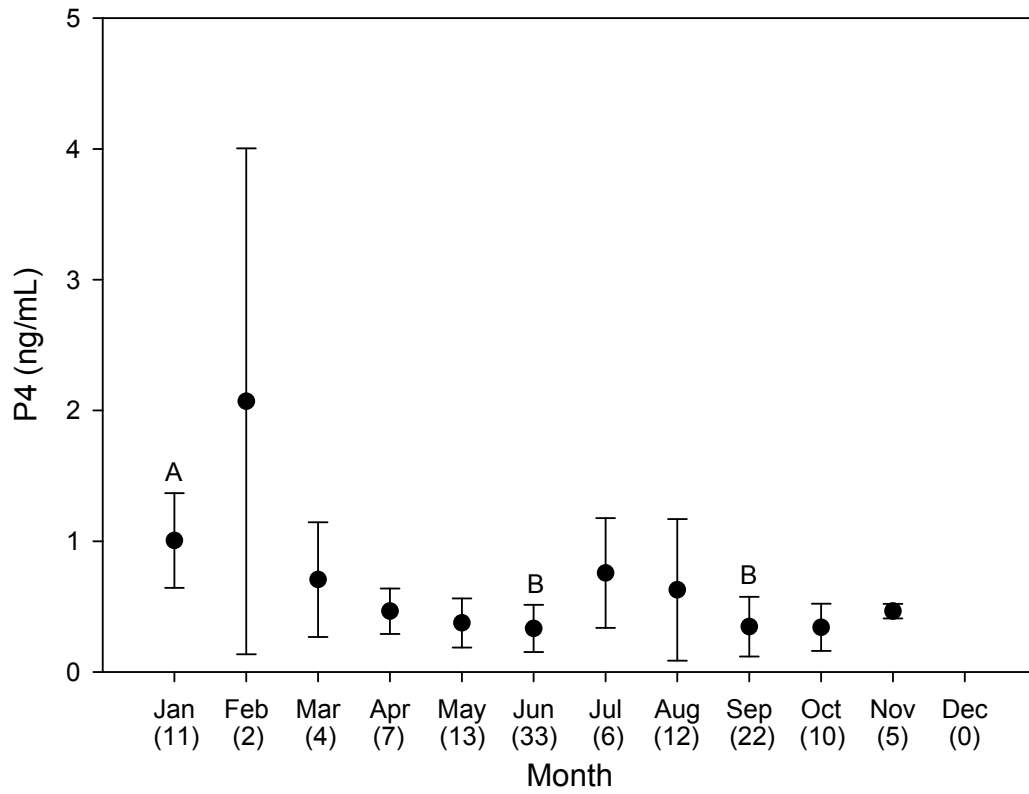


Figure 15. Mean female P₄ muscle concentration by month. Error bars represent 2 SEs. Sample sizes are in parentheses. Letters indicate significant differences among months.

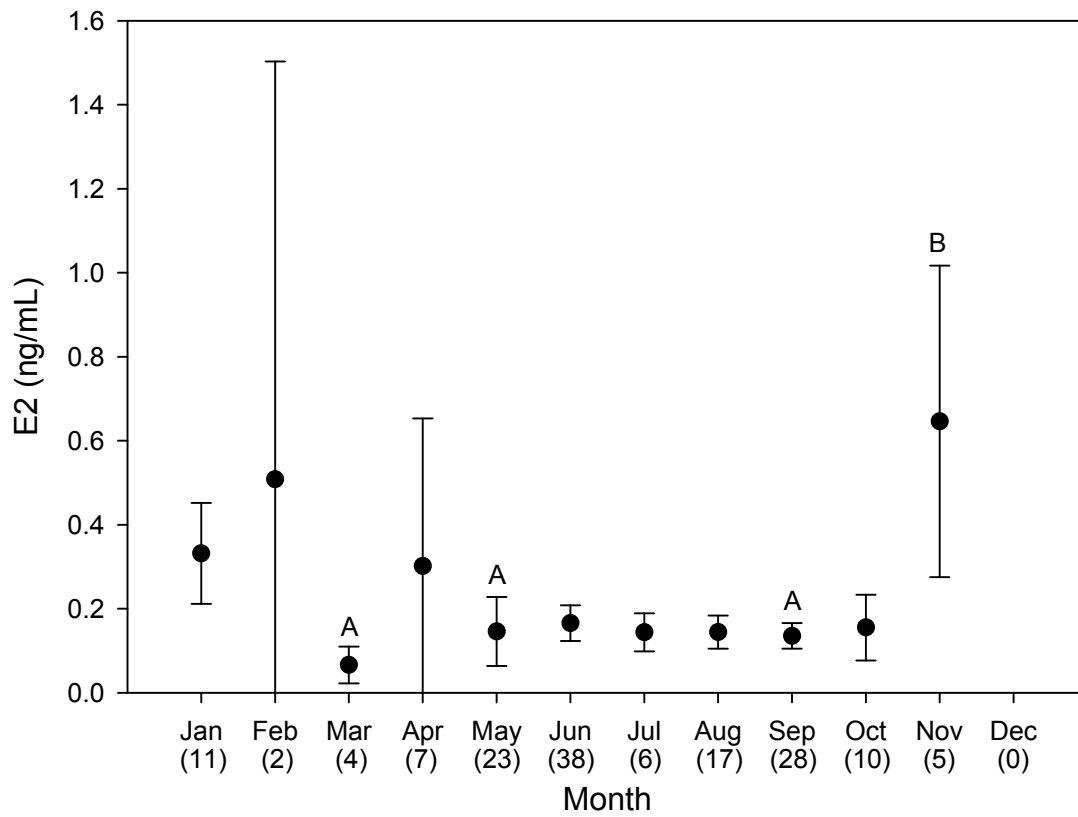


Figure 16. Mean female E₂ muscle concentration by month. Error bars represent 2 SEs. Sample sizes are in parentheses. Letters indicate significant differences among months.

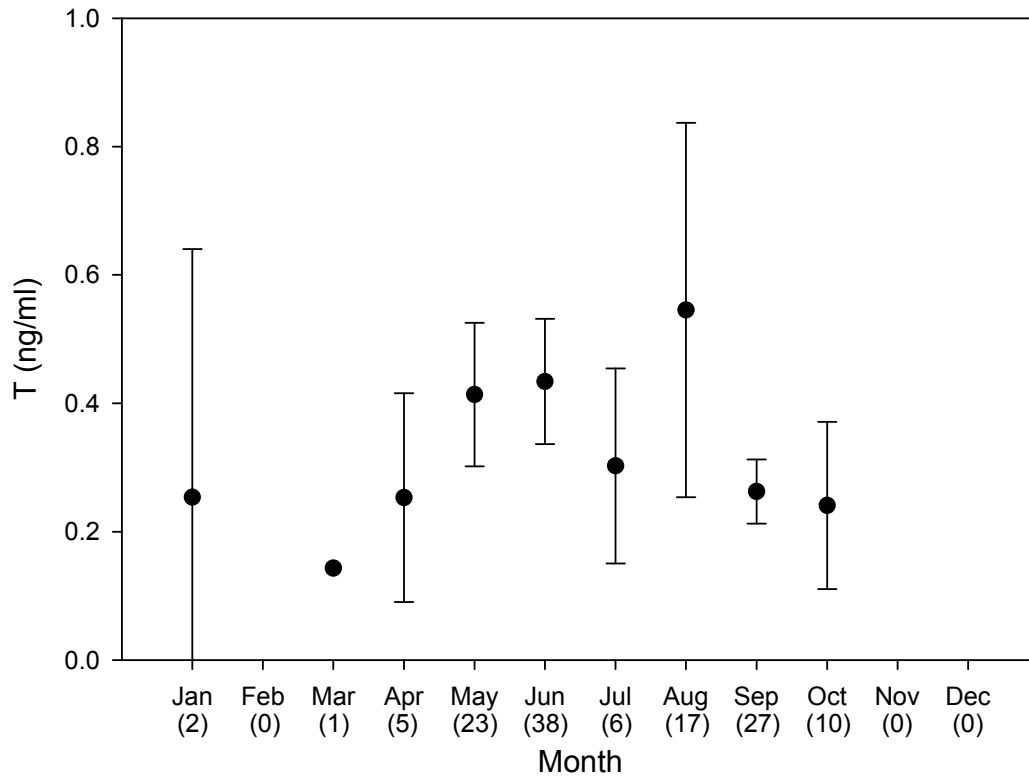


Figure 17. Mean female T muscle concentration by month. Error bars represent 2 SEs. Sample sizes are in parentheses.

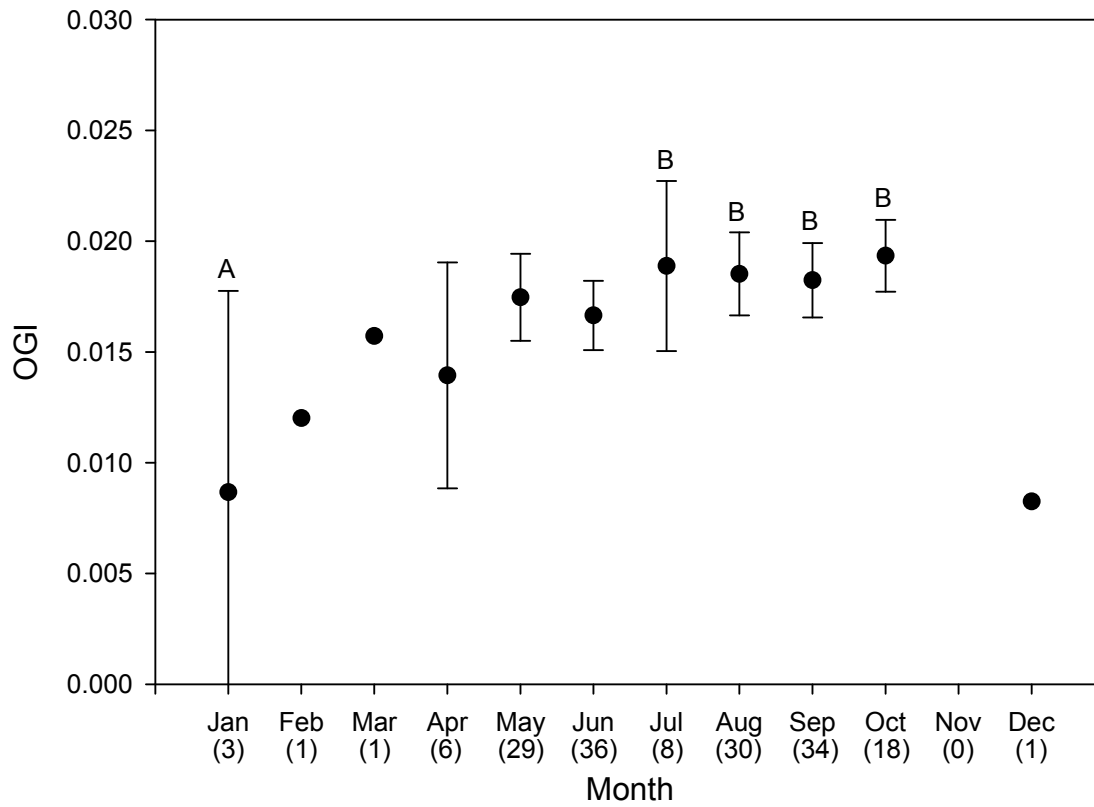


Figure 18. Mean oviducal gland index by month. Error bars represent 95 % confidence intervals. Sample sizes are in parentheses. Letters indicate significant differences among months.

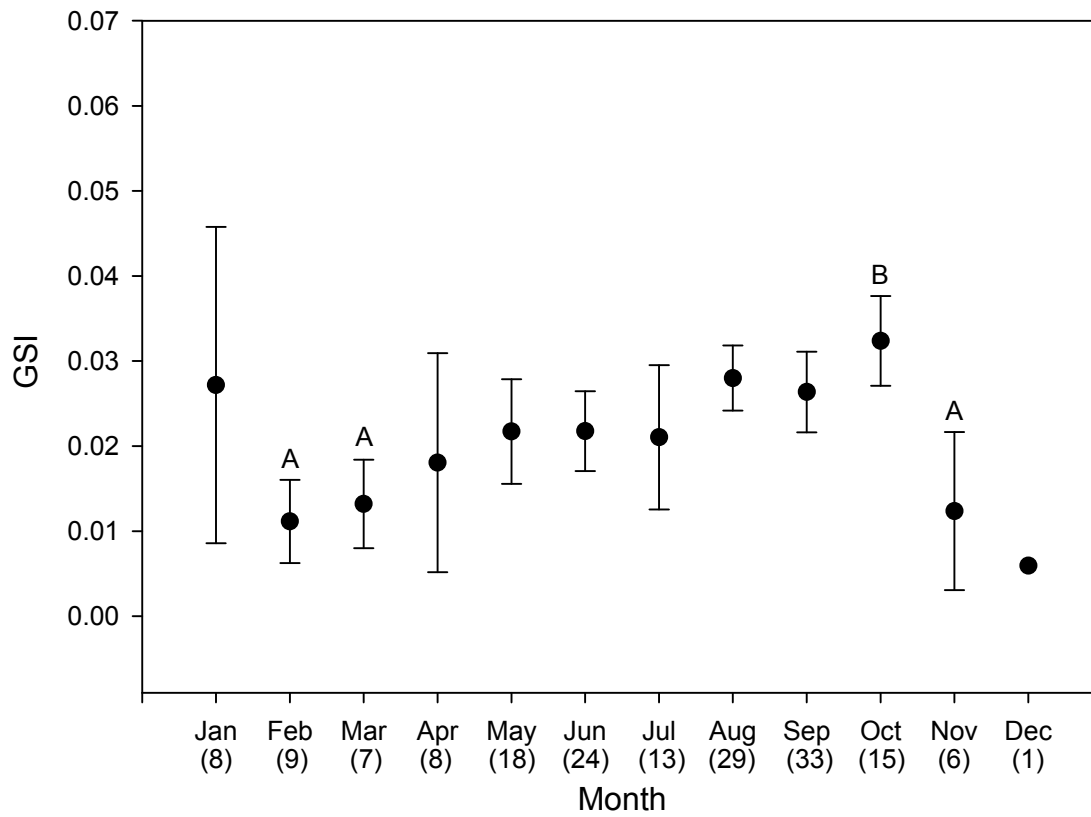


Figure 19. Mean female gonadosomatic index by month. Error bars represent 95% confidence intervals. Samples sizes are in parentheses. Letters indicate significant differences among months.

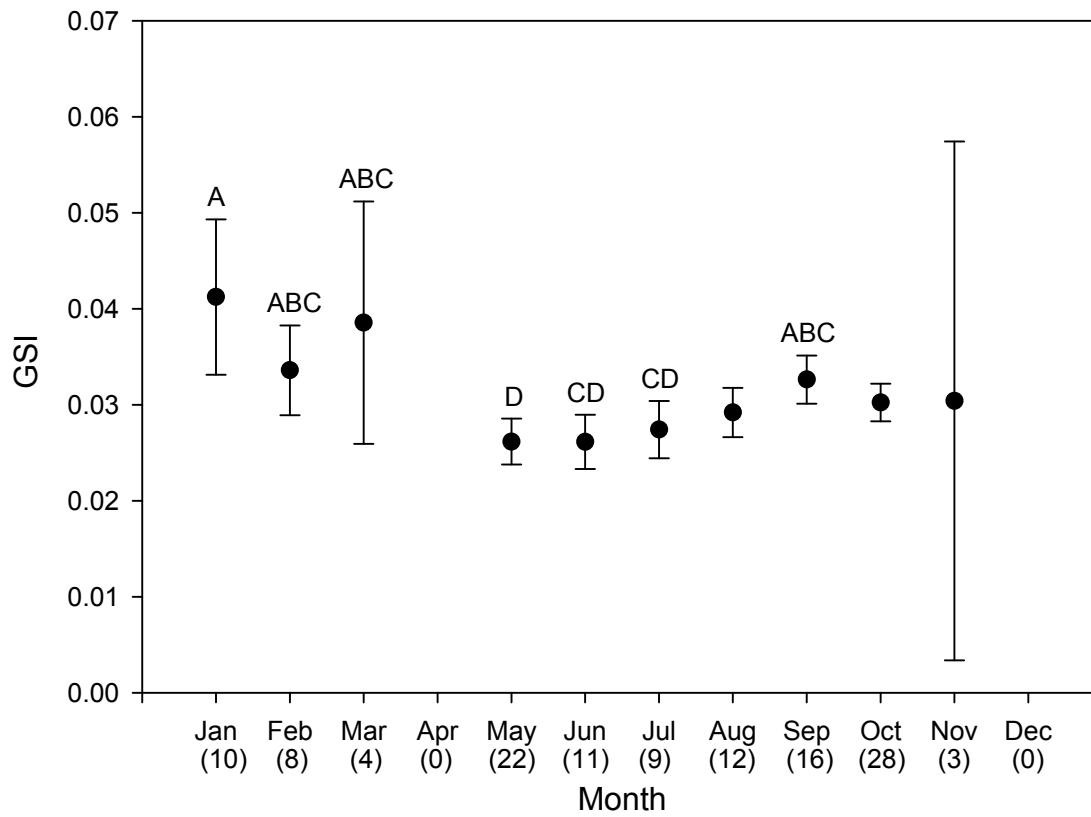


Figure 20. Mean male gonadosomatic index by month. Error bars represent 95% confidence intervals. Samples sizes are in parentheses. Letters indicate significant differences among months.

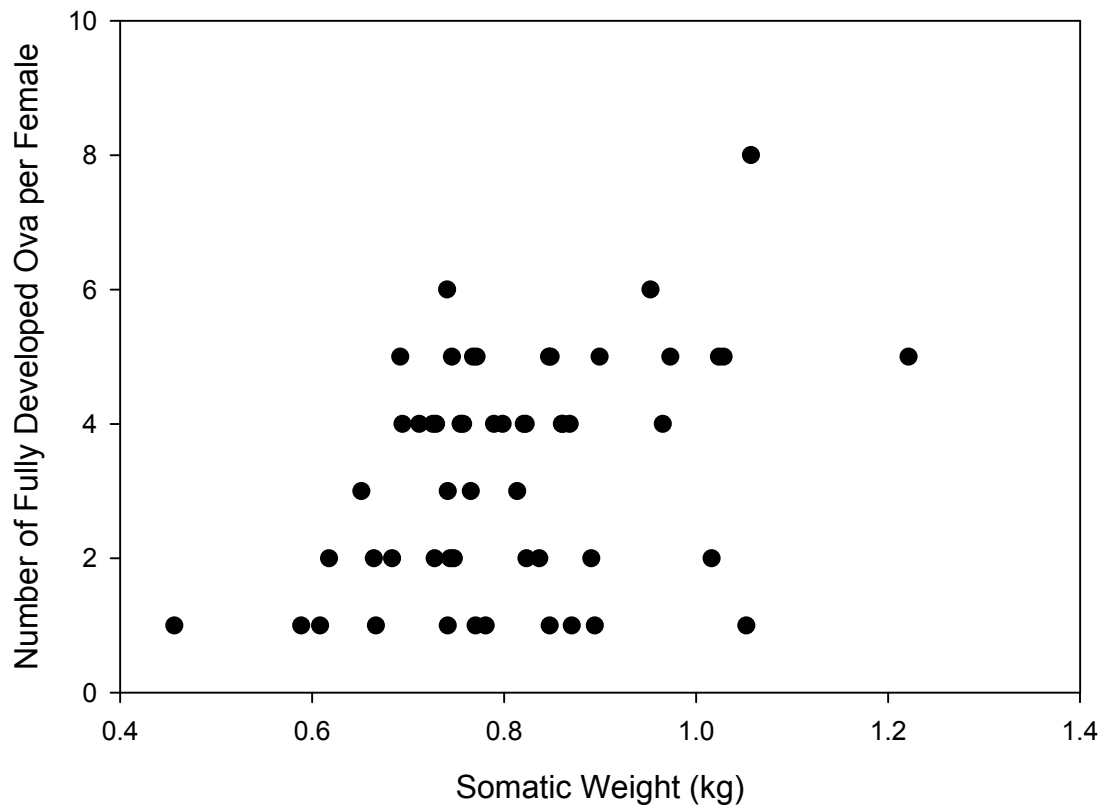


Figure 21. Number of fully developed ova (20 mm diameter or greater) per reproductively active adult female, as a function of somatic body weight.

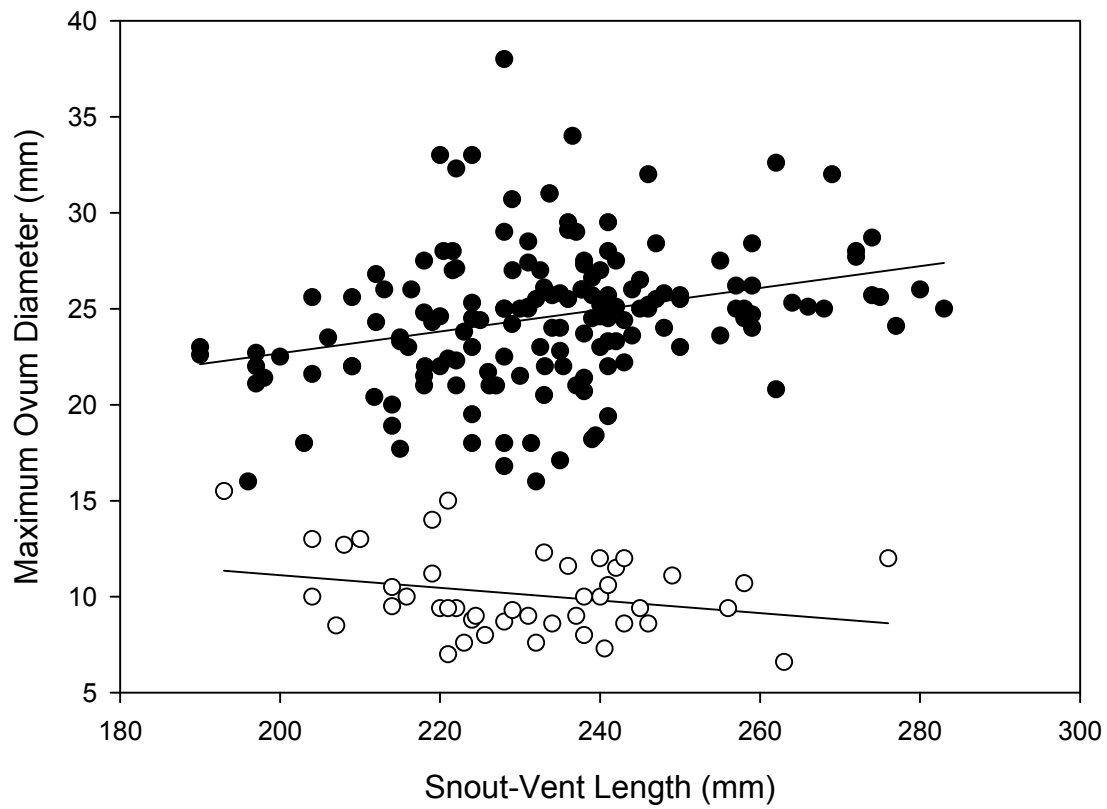


Figure 22. Maximum ovum diameter per adult female as a function of snout-vent length. Filled circles represent reproductively active individuals (those with maximum ovum diameter of 16 mm or greater), and open circles represent inactive individuals (those with maximum ovum diameter of less than 16 mm).

Chapter 2

Abundance and distribution

Introduction

Chimaeroids worldwide are captured incidentally in commercial, recreational, and artisanal fisheries. Several chimaeroids are targeted by commercial fishermen, including the cockfish, *Callorhynchus callorhynchus*, off Argentina (Di Giacomo and Perier 1991), the elephantfish, *C. milii*, off New Zealand (Francis 1998), and the St. Joseph, *C. capensis*, off South Africa (Freer and Griffiths 1993b). *Callorhynchus milii* stocks off New Zealand were declared severely overfished in 1986, but seem to be recovering (Francis 1998). There is not currently a directed fishery for *Hydrolagus colliei*, but fishery mortality is incurred through bycatch and discard. Increasing interest in the meat and liver oil of chimaeroids, for use as machine lubricant and human dietary supplements (Brennan and Gormley 1999; Hardy and Mackie 1971), indicates that more chimaeroid species may be directly harvested in the near future. As coastal and pelagic fish stocks decrease, commercial fleets began fishing at increasing depths to obtain greater yields (Pauly et al. 2003), increasing the likelihood of chimaeroid bycatch (Compagno and Musick 2005).

Despite the rising interest in chimaeroid fisheries (Brennan and Gormley 1999), there are few data regarding population status. The International Union for Conservation of Nature Shark Specialist Group (IUCN-SSG) lists the status of all chimaeroid species as data deficient, and stresses the need for life history information for this group (Didier 2005). There is only limited information on the impacts of fishing on chimaeroid populations (Francis 1997; Francis 1998), as no formal population assessments have been conducted.

Hydrolagus colliei is ecologically important on soft substrates of the outer shelf and upper slope off coastal California, and the outer shelf of northern Baja California (Allen 2006), based on relative abundance. It is one of the ten most abundant groundfishes along the United States West Coast, between ~ 50 and 500 m depth (Keller et al. 2006). In the nearshore waters of the Pacific Northwest it is a more substantial component of the demersal ecosystem, as the most abundant groundfish in Puget Sound, Washington (Palsson 2002), and in the transboundary waters of Washington and British Columbia (Palsson et al. 2004). Despite the potential ecosystem impact of *H. colliei* as predator and prey because of its sheer abundance, nothing is known of its vulnerability to fishing mortality.

Previous authors have hypothesized that *H. colliei* performs movements at multiple temporal scales (Mathews 1975; Quinn et al. 1980). Mathews (1975) suggested that *H. colliei* in the northern Gulf of California underwent a seasonal migration. Quinn et al. (1980) found evidence of seasonal movements and diel migrations in Puget Sound. If these behaviors are typical of *H. colliei* populations, their susceptibility to depletion by fisheries may be increased, as they would be more easily captured in great numbers.

I test the hypothesis that *H. colliei* populations along the U.S. West Coast have decreased during the years 1977 to 2006. Fishing effort or oceanographic productivity regimes may have caused past changes in population size. The hypothesis that distribution varies with sex and ontogeny is tested, providing insight into how behavioral ecology may increase the potential for population depletion. Natural mortality is estimated using a measure of reproductive output, and age at maturity is estimated using

life history theory. Thus, inference is made to the resilience of the population to fishing mortality.

Materials and Methods

Temporal and spatial trends in abundance were tested using data from the NOAA Fisheries, Alaska Fisheries Science Center (AFSC), triennial trawl survey of groundfish abundance from 1977 to 2004. The triennial survey varied in northern and southern extent among years, therefore, analyses were restricted to the latitudinal range that was surveyed in all sampling periods (36.5° to 48.5° N). Within this region, trawls were conducted at 55 to 500 m bottom depth. Sample sites were selected randomly within depth and latitude strata ($n = 4,215$; Fig. 1A). Surveys were conducted from mid-July through September, with the exception of 2001, which was conducted from June through August (Weinberg et al. 2002), and 2004, conducted from late May through July. Survey vessels were chartered commercial trawlers with high-opening Nor-eastern otter trawl nets, with rubber bobbin roller gear. Mesh size was 13 cm in trawl body, with a 9 cm mesh codend fitted with a 3 cm liner (Weinberg et al. 1984). Tow duration was 30 min, with a speed of ~ three knots, or 5.6 km/h (Gunderson and Sample 1980). Trawls were conducted during daylight hours (Weinberg et al. 1984). Catch-per-unit-effort (CPUE, in terms of no./km² sampled) was calculated per tow by dividing the number of individuals captured by the product of mean net width and distance fished. There were forty-two hauls in which the catch of *H. colliei* was recorded only in kg. For these hauls the number of individuals per tow was estimated by dividing the kg per tow by the average individual mass in kg (calculated from all other hauls). Hauls identified as having little

or no bottom contact were removed from the analysis following the guidelines of Zimmermann et al. (2003).

Catch-per-unit-effort was standardized with generalized linear models (GLMs), using the ‘Delta-GLM’ function (Dick 2006) in R (version 2.4.1 for Windows). Because the percentage of trawls with a non-zero ratfish catch varied from 32 to 62%, depending on depth (Fig. 2), a delta-GLM approach was appropriate. The basis for the delta-GLM approach was pioneered by Aitchison (1955) and Pennington (1983), and the method was later modified to compare the relative abundance of fish populations through time (Lo et al. 1992; Stefansson 1996). The delta-GLM technique uses one GLM to estimate the probability of a positive observation using the Bernoulli probability density function and a logit link function, and a separate GLM to estimate the mean of positive observations. An index of abundance is then derived as the product of the year effects from the two models. Preliminary comparisons among candidate error distributions (lognormal, gamma, and inverse gaussian) for the positive data (following Dick 2004) provided support for the use of the lognormal distribution. This error distribution, therefore, was used for the positive GLM throughout subsequent analytical steps.

Selection of explanatory variables and model structure was performed using Akaike’s Information Criterion (AIC, Akaike 1973). This information criterion was more appropriate for model choice than hypothesis testing (likelihood ratio tests, or drop-in-deviance-tests), because it provided a penalty term for the number of model parameters (Akaike 1974; Burnham and Anderson 2002; Sakamoto et al. 1986), allowed comparison of non-nested models (Hilborn and Mangel 1997), and was more robust for analyses of large datasets (Dick 2004). Additionally, drop-in-deviance-tests are only

analogous to a likelihood ratio test when the dispersion parameter is equal to one, which is not the case for the normal and gamma distribution (Venables and Ripley 2002). The AIC was used instead of the Bayesian Information Criterion (BIC, Schwartz 1978) because it is more biologically realistic, considering the large amount of variance unexplained by the “best” model (Burnham and Anderson 2002), and because the number of potential explanatory variables was small (depth, latitude, and year). AIC scores were compared among candidate models with backwards stepwise variable selection. Akaike weights were calculated for each model, following Burnham and Anderson (2002):

$$w_i = \frac{\exp(-0.5\Delta_i)}{\sum_{r=1}^R \exp(-0.5\Delta_r)}$$

where Δ_i is the difference between the AIC scores of the i th model and the model with the minimum AIC value, and R is the number of models compared. Using Bayesian ideas, Akaike weights can be interpreted as estimates of the probability that model i is the ‘best’ of all included candidate models (Burnham and Anderson 2002). To facilitate clear interpretation of results, the model structure selected by AIC for the binomial GLM also was used for the positive GLM, even when the “best” model differed between GLMs.

When the model was conducted with data from the entire survey region, models with interactions of either year and latitude or year and depth resulted in the lowest AIC scores. To avoid these interactions, which would interfere with the interpretation of abundance by year (Maunder and Punt 2004), the data were modeled as three separate regions: the continental slope (250 to 500 m depth) from 36.5° to 48.5° N latitude ($n = 742$), and southern (36.5° to 39.5° N; $n = 678$) and northern (39.5° to 48.5° N; $n = 2,795$)

sections of the outer continental shelf and upper slope (50 to 250 m depth). These geographic delineations are biologically significant, representing prominent bathymetric (shelf break) and oceanographic (Cape Mendocino) transitions. Because of insufficient sampling in greater depths during the years 1980 to 1992, the presence of interactions between year and depth could not be tested for in the full slope model. A model with truncated years (only 1977, and 1995 to 2004; Table 1A), therefore, was fitted to verify the absence of a significant year and depth interaction. Variance estimates for the year effect were generated with a jackknife routine to compare standardized abundances among years. A two-step partitioning cluster analysis (Cope and Punt in review), incorporating intra-year variance in abundance, was used to identify stock structure by grouping model regions with similar inter-annual abundance trends.

A separate delta-GLM was created to examine the effects of coastal morphology and oceanography on the spatial distribution of *H. colliei* abundance. It was possible to include the entire latitudinal range in this model because years were lumped into three groups (1977 to 1986, 1989 to 1992, and 1995 to 2004), based on changes in sampling design through time (Zimmermann et al. 2003). Variance in the latitude effect was generated with a jackknife routine to determine spatial patterns of abundance. Standard regression diagnostics were performed for the final models to check for model misspecification and heteroscedascity (Maunder and Punt 2004; McCullagh and Nelder 1989; Ortiz and Arocha 2004).

Data from the NOAA Fisheries, Northwest Fisheries Science Center (NWFSC), West Coast Groundfish Survey (WCGS) were used to analyze more recent abundance trends from 2003 to 2006. Survey methods are summarized from Keller et al. (2006), as

follows. Standard Aberdeen-style otter trawl nets were used, with 14 cm mesh in the trawl body, and a 13 cm mesh codend with a 5 cm mesh liner. Footrope was composed of rubber bobbin rollers and 25 cm dropper chains. Tow duration was ~ 15 min at ~ 2.2 knots or 4.1 km/h. Tows were conducted during daylight hours only. Surveys were performed as two passes from the North to South between late May and mid October, with the exception of the 2003 survey, which began in late June. Sample sites were selected randomly within depth and latitude strata. Tows were conducted from 25 to 1,428 m, but the maximum depth of *H. colliei* capture was 711 m.

For the purposes of comparison, CPUE was calculated as the number of individuals per km² using the same technique and spatial constraints as the triennial trawl dataset ($n = 1,234$; Fig. 1B). These constraints are logical, since the proportion of tows in which ratfish were captured was minimal (0.03) between 500 m, the maximum trawl depth of the triennial trawl survey, and 913 m, the maximum reported depth range for ratfish. Tows conducted at depths greater than 500 m, therefore, were excluded from abundance estimates. Similar measures also were taken to calculate standardized abundance indices with a delta-GLM. The best fitting models as determined with AIC, however, consistently contained interaction effects between year and depth and/or year and latitude, regardless of the binning structure applied to explanatory variables. Because the presence of interactions between spatial and temporal variables confounds the interpretation of the delta-GLM year index as an indicator of temporal trends (review in Maunder and Punt 2004), the CPUE data were simply expressed as the geometric mean per region of the triennial trawl models. For ease of comparison, the ratio of the relative abundances estimated by the WCGS and the triennial trawl survey for the year 2004 was

used to standardize the WCGS results. The geometric mean CPUE from each year and region of the WCGS were rescaled to the GLM-standardized triennial trawl abundances by dividing the WCGS values by x , where $x = [2004 \text{ WCGS geometric mean CPUE}] \div [2004 \text{ GLM-standardized triennial trawl CPUE}]$.

Length-frequencies from the 2005 and 2006 NWFSC surveys ($n = 682$ tows with non-zero catch; Fig. 3) were graphed separately for each sex and geographical region. Regions were defined as the two latitudinal regions from the delta-GLM, and two southern regions, north (34.5° to 36.5° N) and south (32.6° to 34.5° N) of Point Conception. Tow depths were 53 to 571 m, and categorized into 100 m bins. To determine the size selectivity of the survey, length-frequencies were recoded as proportions of the number of individuals captured in the size class most represented in the catch. Selectivity was then calculated by fitting a logistic equation to those data:

$$S(L) = \frac{1}{1 + e^{-(a+b*L)}}$$

Where $S(L)$ is the proportion of representation of size class L in the catch, compared with the fully selected size, and parameters a and b are estimated iteratively. From this two-year dataset, sex ratio for the entire survey area was analyzed for departure from a 1:1 relationship using a Chi-square test. Linear least-squared regression was used to test for differences in sex ratio with depth, with all locations pooled. ANCOVA was used to test for latitudinal differences in the effect of depth on sex ratio, with mean proportion of males captured per tow as the dependent variable, latitude as the main effect, and depth as the covariate.

Qualitative observations of *H. colliei* distribution were made by video analysis of visual submersible surveys conducted during August and September of 2001 and 2002, at

Cordell Bank, California, by the Cordell Bank National Marine Sanctuary (CBNMS).

Total size of each individual was recorded with paired lasers. Habitat type was recorded following the classification scheme of Greene et al. (1999).

Natural Mortality

Natural mortality was estimated as a function of reproductive output (Gunderson 1997):

$$M = 1.79 * GSI$$

Where M is the instantaneous natural mortality rate and GSI is the estimated annual reproductive output. A proxy for GSI was used to appropriately represent the life history of the ratfish (after Matta 2006):

$$GSI_{egg} = \frac{\text{average maximum ovum mass} * \text{annual fecundity}}{\text{average mature female somatic mass}}$$

Where average maximum ovum mass was estimated from a subset ($n = 12$) of individuals with mature ova (diameter > 20 mm), and annual fecundity was estimated from observed laboratory parturition rates (see chapter 1 of this thesis for details). From this estimate of natural mortality, an estimate of age at first maturity was produced, using a rearrangement of the relationship provided by Charnov (1993):

$$\alpha = 2 \div M$$

Where α is age at first maturity, and M is natural mortality.

Results

Selectivity and the Distribution of ontogeny and sex

For the years 2005 and 2006 combined, for the entire survey area, the proportion of males in the catch (0.47) was significantly less than the expected value of 0.5 ($\chi^2 = 25.3898$, $df = 1$, $p < 0.001$). In a spatially explicit context, there was a trend for decreasing proportion of males with depth ($t = 5.701$, $df = 678$, $p < 0.001$). This trend, however, was not consistent for all latitudes (ANCOVA: factor = depth*latitude, $F = 1.689$, $df = 15, 648$, $p = 0.049$; Fig. 4).

The size selectivity function indicated that individuals were not fully selected until at least adult size (Fig. 5). The selectivity is likely not related to the gear, however, because the codend mesh size was small enough to capture all ratfish, if present. If the latter is true, size selectivity is essentially equal to one, but small individuals were underrepresented in the size-frequency distribution because of sample site allocation, therefore, this selectivity will be hereafter referred to as “survey selectivity”.

Length-frequency distribution appeared to vary with depth and latitude. There was a general trend of large individuals being increasingly prevalent with decreasing depth, with the discrepancy becoming more noticeable with increasing latitude (Fig. 6). Trends in the shape of the distributions were similar for each sex. Absolute positions of distributions were not compared between sexes, as females attain larger size than males.

Dense congregations of *H. colliei* were observed in the vicinity of Cordell Bank (located ~ 40 km off the California coast at 38°1'42" N, 123°26'41" W). They were patchily distributed, occurring in aggregations on the shelf break and slope around the bank. Occasionally these aggregations were size-specific. Adult ratfish were observed

on the slope, at a depth of 200 to 300 m. Juvenile (possibly young-of-the-year, or YOY) ratfish were located on the shelf break and upper slope, between 150 and 250 m. In two consecutive years, a single transect on mud or mixed mud habitat revealed at least 50 individuals of only ~ 20 cm TL. Hundreds of *H. colliei* egg cases were found in the troughs of large sand waves (~ one meter high), 60 m deep, on the continental shelf on the eastern side of the bank.

Natural Mortality

Using the natural mortality estimation method from Gunderson (1997), with the Matta (2006) modification, M was estimated at 0.17 to 0.26, given the range of fecundity estimates. The estimated range of M provides an expected age at first maturity of 7.8 to 11.6 years.

Spatial and Temporal Abundance Trends

The models that best predicted the probability of catching at least one ratfish, and the catch rate, varied among regions (Table 1). The slope model with truncated years indicated the absence of a year and depth interaction (Table 1A), therefore, the slope model with all years included (and no year and depth interaction) was used for inferring temporal abundance trends. The models selected to create temporal and spatial indices of abundance are as follows:

- 1) Slope: year, latitude (2 degree bins), depth (62 m bins)
- 2) Northern shelf and upper slope: year, latitude (1 degree bins), depth (50 m bins),
depth * latitude
- 3) Southern shelf and upper slope: year, latitude (1 degree bins), depth (67 m bins),
depth * latitude
- 4) Entire survey region: year (1977 to 1986, 1989 to 1992, 1995 to 2004), latitude
(0.5 degree bins)

The models fit the positive data reasonably well (see appendix), with R^2 values of 0.201, 0.125, 0.151, and 0.111, respectively. Cluster analysis indicated that the temporal abundance trends were similar between the slope, and northern shelf and upper slope populations ($Sil = 0.95$), but differed for the southern shelf and upper slope population. The slope model indicated a consistent increase in abundance since 1995, with the exception of 2001 (Fig. 7A). The same trend was even more dramatic in the northern shelf and upper slope region (Fig. 7B). Abundance trends in the southern shelf and upper slope region were not as straightforward, with increasing abundance from 1977 to 1986, and lesser abundance thereafter, with the exception of a large peak in 1995 (Fig. 7C).

The model created to determine spatial trends in abundance included only the main effects of two explanatory variables: year (grouped), and latitude (0.5 degree bins). Standardized abundance (Fig. 8) was greater off Cape Flannery (48.0 to 48.5° N), Monterey Bay (36.5 to 37.0° N), and just south of Cape Mendocino (40.0 to 40.5° N). Abundance was less near the Columbia River Plume (44.5 to 45.5° N), between Cape

Mendocino and Cape Blanco (40.5 to 42.0° N), and just south of San Francisco Bay (37.0 to 37.5° N).

Discussion

Selectivity and the Distribution of ontogeny and sex

The phenomenon of sexual segregation by depth occurs in many elasmobranch populations (e.g. Compagno et al. 1991). In this study, sex ratio became more skewed toward females with depth across most of the geographic range, similar to the pattern observed for the black dogfish, *Centroscyllium fabricii* (Yano 1995) and the marbled catshark, *Galeus arae* (Bullis 1967). The reasons for this type of sexual segregation remain unknown. This result, however, may be an artifact of size selectivity of sampling (Fig. 5). Survey catch may be biased toward females, because males reach a smaller size at maturity and lesser maximum size than females.

Visual analysis of length-frequency distributions indicated that the prevalence of large individuals decreased with depth (Fig. 6). This trend, however, may be an artefact of sampling design, as the number of trawl samples decreased with depth. The length-frequencies of deeper areas, therefore, may not be representative of the true size structure.

Ontogenetic segregation by habitat type can be inferred from the size selectivity of the survey, wherein only adults were sufficiently sampled. Absolute biomass estimates derived from the triennial trawl survey would therefore be an underestimate. The disproportionately lesser number of juveniles in the catch indicated that they may be associated with rocky habitats that are not easily sampled with trawl gear. Visual

observations of aggregations of juveniles on soft-bottom habitats around Cordell Bank provide evidence against the latter hypothesis, perhaps indicating that the dearth of juveniles in the catch may be caused by vertical movements. Submersible observations at Stonewall Bank revealed an abundance of ratfish at night, but an absence during the day (Hixon and Tissot 1992), providing more evidence for the phenomenon of vertical movements.

The presence of aggregations of egg cases and juveniles near the shelf break, adjacent to Cordell Bank, indicate that this may be a nursery area for *H. colliei*. Egg case deposition also has been observed on Daisy Bank, ~ 56 km west of Newport, Oregon (Mark Hixon, pers. comm.). These observations indicate offshore banks may be nursery areas for *H. colliei*, as they are for many species of rockfish (Pearcy et al. 1989).

The wave formations in the sandy habitat where the egg cases were found would indicate that there are high-velocity currents propagating near the seafloor in this region. Aggregations of egg-cases of the catsharks *Apristurus brunneus* and *Parmaturus xaniurus* have also been found at the shelf break and upper slope interface in regions with strong seafloor currents (Flammang 2005). The shelf break is a nursery area for many species, including *Scyliorhinus retifer* (Able and Flescher 1991). Ridges with strong currents are nursery areas for some deep-sea teleosts and cephalopods (Drazen et al. 2003). Flammang (2005) indicated that the currents were needed to provide oxygenated water for egg cases.

Alternative reasons for the selective deposition of egg cases into sand troughs may be to reduce egg case mortality by avoiding predator-dense habitats, and to prevent passive transport of the unborn offspring to less favorable habitats. There also may be

increased food abundance for juveniles near offshore banks, but Heupel et al. (2007) noted that chondrichthyan nursery areas typically function more to decrease early life history mortality than to increase food availability. The existence of nursery areas may increase the vulnerability of the species to population depletion by potentially increasing the mortality of immature individuals (through fisheries catch), the most important vital rate contributing to population growth in chondrichthyans (Cortes 2002; Frisk et al. 2005).

Natural Mortality

The estimated natural mortality of 0.17 to 0.26 is slightly less than the median of 0.27 calculated from 55 species of elasmobranchs (review in Frisk et al. 2005). The estimated age at first maturity of 7.8 to 11.6 was similar to, if not slightly greater than, the female-specific median of 8 years calculated using 68 shark populations (review in Cortes 2000). It should be noted, however, that estimates for *H. colliei* were indirectly derived, and should be interpreted with caution.

Spatial and Temporal Abundance Trends

Populations on the slope and the northern region of the shelf and upper slope have greatly increased since 1998. No such increase, however, was observed for the southern shelf and upper slope population. Probable causes of this geographic variation are climate and differential fishing mortality.

Temporal trends in abundance of many U.S. West Coast groundfishes have been attributed to fluctuations in fishing mortality, with landings used as a proxy for this

factor. Levin et al. (2006) reported changes in the benthic fish assemblage off the U.S. West Coast, with abundances of many rockfish species decreasing, and all flatfish and chondrichthyan species increasing. Size at maturity, maximum size, and individual growth rate, were also associated with population growth rate. Abundance trends were inversely associated with landings, indicating that fishing mortality was a contributing factor to decreasing population size of rockfishes.

To assess the temporal and spatial effects of fishing on *H. colliei* populations, U.S. West Coast groundfish landings were compared with the spatially explicit abundance trends. Annual landings from all gear types in the U.S. West Coast groundfish fisheries increased steadily from 1985 to 1989, then remained above 200,000 mt before decreasing in 2002 and 2003 to record minima since accounting began by the Pacific Fishery Management Council (PFMC) Groundfish Management Team in 1981 (Fig. 9; PacFIN 2008). Beginning in 2003, the PFMC enacted new management procedures, most notably closing specific depth zones of the continental shelf to trawling and reducing catch limits of certain species. With fishing effort concentrated on the deeper waters of the continental slope and outer shelf, groundfish landings have since increased, before a decline in 2007. These trends in fishing effort, inferred by landings, do not coincide with *H. colliei* abundance trends. Fishing mortality, therefore, is not the primary factor regulating *H. colliei* abundance in space or time.

Levin et al. (2006) reported on the influence of harvest on population size, but concurrent climate influences were not addressed. A strong El Niño occurred between 1997 and 1998, and a shift to a cold regime of the Pacific Decadal Oscillation (PDO) may have occurred around the same time. These cold regimes provide more nutrient-rich

water to the California Current System (CCS), promoting greater primary productivity, which may increase the abundance of benthic epifauna and infauna that *H. colliei* prey upon (Johnson and Horton 1972). Increased food availability may allow *H. colliei* population size to increase during cold regimes.

The increased abundance in the slope population in 1983 and 1998, relative to adjacent survey years, indicated that El Niño conditions may cause *H. colliei* populations to move to deeper waters. Exceptionally strong El Niño events occurred between 1982 and 1983, and 1997 and 1998. El Niño events cause a depression in depth of the surface mixed layer (Simpson 1984; Zimmerman and Kremer 1984; Zimmerman and Robertson 1985). The mixed layer contains nutrient depleted, warm water during such anomalies (Eppley et al. 1979; Jackson 1977; Zimmerman and Kremer 1984). These movements, therefore, likely are caused by a depression of the thermocline and nutricline.

Hydrolagus colliei has a shallow depth distribution, relative to other chimaeroids. Within the latitudinal extent of the range surveyed, they were most prevalent at depths of 150 to 400 m (Fig. 2). As previously hypothesized (Dean 1906), their abundance decreased with depth at higher latitudes, but this relationship gradually degraded toward the lower latitudes (Fig. 10), perhaps explaining the model interactions between depth and latitude. This pattern is a common biogeographical phenomenon of many marine species, and typically is attributed to the bathymetric distribution of thermal isoclines. Tolimieri and Levin (2006), however, found that although bottom temperature decreases with depth and latitude on the U.S. West Coast, spatial variation of fish assemblage structure was not fully explained temperature alone. Assemblage structure within the depths 200 to 500 m changed in the vicinity of Cape Mendocino and Point Conception, a

similar pattern to that of nearshore fishes (SCCWRP 1973), with less drastic shifts around Cape Blanco and the Columbia River plume.

Intraspecific population structure of *H. colliei* may be produced by physical factors similar to those which structure demersal fish communities, as they seem to share some geographical boundaries. Anomalous lesser and greater densities were observed across all depths at specific latitudinal regions (Fig. 8). Such anomalies may be caused by variability in the strength of currents at the seafloor, seafloor habitat and relief, prey abundance, or aggregative behavior. Regions with greater ratfish abundance (36.5 to 37.0°, 40 to 40.5°, 48.0 to 48.5° N) corresponded with the prominent coastal physical features of Monterey Bay, Cape Mendocino, and Cape Flannery. These areas are exceedingly productive, as their coastal morphology increases the amount of localized upwelling, therefore increasing the rate of primary productivity.

Increased primary productivity at the sea surface may provide more nutrients to benthic infauna and epifauna, thus providing a greater abundance of prey for *H. colliei*, which feed primarily on shrimp (*Pandalus* sp. and *Crago* sp.), echinoderms (*Brisaster* sp.), and gastropod mollusks (Johnson and Horton 1972). The lesser density of *H. colliei* between Cape Mendocino and Cape Blanco (40.5 to 42.0° N) may be caused by lesser food abundance relative to these adjacent highly productive upwelling regions formed by the two coastal promontories (NOAA 2008). Lesser *H. colliei* abundances near the Columbia River plume (~45.0° N), and just south of San Francisco Bay (~37.5° N), cannot be explained as easily.

This pattern of decreased abundance is somewhat counterintuitive, because these are areas of great runoff, therefore, one would expect increased abundance of their

benthic macrofaunal prey, as coastal runoff contains greater nutrient levels than coastal marine waters (Bakun 1996). Eutrophic plumes with high sediment loads, however, can create anoxic conditions on the seafloor, which can cause population depletion of benthic invertebrates (Baden et al. 1990) and fishes (Møllgaard and Nielsen 1990).

Additionally, there may be strong currents on the seafloor in these regions, as evidenced by large sand waves at the mouth of San Francisco Bay (Barnard et al. 2006), perhaps deterring the relatively small-bodied ratfish. Combes and Daniel (2001) reported that maximum sustained swimming speed of *H. colliei* was only 0.15 ms^{-1} , consequently, they may not be able to inhabit areas with strong currents for protracted time periods.

The latitudinal population structure may indicate the presence of intraspecific phylogenetic barriers. *Hydrolagus colliei* should be expected to display strong population structure because it has no embryonic dispersal, and unknown levels of juvenile and adult dispersal. Combes and Daniel (2001), however, noted that flexibility of the pectoral fins of *H. colliei* allows for increased efficiency, which indicates that adult dispersal potential could be greater than previously thought. Cape Mendocino is an intraspecific phylogeographic break for some fishes (Cope 2004; Dawson et al. 2001). Anomalously lesser ratfish abundance just north of this coastal promontory, combined with the evidence of differing temporal abundance trends within populations to the north and south, indicates that it may play a similar role for this species.

Conclusions

The life history, movement patterns, and aggregative behavior of *H. colliei* indicate that it may be vulnerable to population depletion by excess fisheries mortality.

Temporal abundance trends, however, indicate that their population size has increased significantly within the last decade. It is unclear whether this increase was caused by the success of fisheries management policy, or shifting regimes of oceanographic productivity increasing their abundance and/or availability to fishing gear. It is evidence, nonetheless, of the resilience of this species to increased mortality from anthropogenic and environmental sources. The paradigm that all chondrichthyans are particularly susceptible to exploitation, therefore, may not apply to chimaeroids.

Literature Cited

- Able KW, Flescher D (1991) Distribution and habitat of chain dogfish, *Scyliorhinus retifer*, in the Mid Atlantic bight. *Copeia* 1: 231-234
- Aitchison J (1955) On the distribution of a positive random variable having a discrete probability mass at the origin. *Journal of the American Statistics Association* 50: 901-908
- Akaike H (1973) Information theory and an extension of the maximum likelihood principle. In: Petrov BN, Csaki F (eds) *Proceedings of the 2nd international symposium on information theory*. Publishing House of the Hungarian Academy of Sciences, Budapest, pp 268-281
- Akaike H (1974) A new look at the statistical model identification. *IEEE Transactions on Automatic Control* AC-19: 716-723
- Allen MJ (2006) Continental shelf and upper slope. In: Allen MJ, Pondella DJ, II, Horn MH (eds) *The Ecology of Marine Fishes: California and Adjacent Waters*. University of California Press, Berkeley, CA
- Baden SP, Loo LO, Pihl L, Rosenberg R (1990) Effects of eutrophication on benthic communities including fish: Swedish west coast. *Ambio* 19: 113-122
- Bakun A (1996) *Patterns in the ocean: ocean processes and marine population dynamics*. University of California Sea Grant (in cooperation with Centro de Investigaciones Biologicas de Noroeste, La Paz, Baja California Sur, Mexico), San Diego, California, USA
- Barnard PL, Hanes DM, Rubin DM, Kvitek RG (2006) Giant sand waves at the mouth of San Francisco Bay. *Eos, AGU* 87: 285, 289

- Brennan MH, Gormley TR (1999) The quality of under-utilised deep-water fish species. Teagasc Research Report 22 (Project Armis No. 4560)
- Bullis HRJ (1967) Depth segregations and distribution of sex-maturity groups in the marbled catshark, *Galeus arae*. In: Gilbert PW, Mathewson RF, Rall DP (eds) Sharks, Skates, and Rays. The Johns Hopkins Press, Baltimore, pp 141-148
- Burnham KP, Anderson DR (2002) Model Selection and Multimodel Inference: A Practical Information-Theoretic Approach. Springer-Verlag, New York
- Charnov EL (1993) Life History Invariants: Some Explorations of Symmetry in Evolutionary Ecology. Oxford University Press, Inc., New York
- Combes SA, Daniel TL (2001) Shape, flapping and flexion: wing and fin design for forward flight. *The Journal of Experimental Biology* 204: 2073-2085
- Compagno LJV, Ebert DA, Cowley PD (1991) Distribution of offshore demersal cartilaginous fish (Class Chondrichthyes) off the west coast of Southern Africa, with notes on their systematics. *South African Journal of Marine Science* 11: 43-139
- Compagno LJV, Musick JA (2005) Deepwater species. In: Fowler SL, Cavanaugh RD, Camhi M, Burgess GH, Cailliet GM, Fordham SV, Simpfendorfer CA, Musick JA (eds) Sharks, rays and chimaeras: the status of the chondrichthyan fishes. Status Survey. IUCN/SSC Shark Specialist Group. IUCN, Gland, Switzerland and Cambridge, UK, pp 216-217
- Cope JM (2004) Population genetics and phylogeography of the blue rockfish (*Sebastes mystinus*) from Washington to California. *Canadian Journal of Fisheries and Aquatic Sciences* 61: 332-342

- Cope JM, Punt AE (in review) Drawing the lines: Resolving fishery management units with simple fisheries data. *Canadian Journal of Fisheries and Aquatic Sciences*
- Cortes E (2000) Life history patterns and correlations in sharks. *Reviews in Fisheries Science* 8: 299-344
- Cortes E (2002) Incorporating uncertainty into demographic modeling: Application to shark populations and their conservation. *Conservation Biology* 16: 1048-1062
- Dawson MN, Staton JL, Jacobs DK (2001) Phylogeography of the tidewater goby, *Eucyclogobius newberryi* (Teleostei, Gobiidae), in coastal California. *Evolution* 55(6): 1167-1179
- Dean B (1906) Chimaeroid fishes and their development. Carnegie Institute Publication, Washington, D.C.
- Di Giácomo EE, Perier MR (1991) Evaluación de la biomasa y explotación comercial de pez gallo (*Callorhynchus Callorhynchus*) en el golfo San Matías, Argentina. *Frente Maritimo* 9: 7-13
- Dick EJ (2004) Beyond 'lognormal versus gamma': discrimination among error distributions for generalized linear models. *Fisheries Research* 70: 351-366
- Dick EJ (2006) Delta-GLM. Version 1.7.2, Programmed in R version 2.2 for Windows
- Didier DA (2005) Order chimaeriformes, chimaeras. In: Fowler SL, Cavanaugh RD, Camhi M, Burgess GH, Cailliet GM, Fordham SV, Simpfendorfer CA, Musick JA (eds) *Sharks, rays and chimaeras: the status of the chondrichthyan fishes. Status survey*. IUCN/SSC Shark Specialist Group, IUCN, Gland, Switzerland and Cambridge, UK

- Drazen JC, Goffredi SK, Schlining B, Stakes DS (2003) Aggregations of egg-brooding deep-sea fish and cephalopods on the gorda escarpment: a reproductive hot spot. *Biological Bulletin* 205: 1-7
- Eppley RW, Renger EH, Harrison WG (1979) Nitrate and phytoplankton production in Southern California Coastal Waters. *Limnology and Oceanography* 24: 483-494
- Flammang BE (2005) Distribution and reproductive ecology of deep-sea catsharks (Chondrichthyes: Scyliorhinidae) of the eastern North Pacific. M.S. Thesis, Moss Landing Marine Laboratories
- Francis MP (1997) Spatial and temporal variation in the growth rate of elephantfish (*Callorhinchus milii*). *New Zealand Journal of Marine and Freshwater Research* 31: 9-23
- Francis MP (1998) New Zealand shark fisheries: development, size and management. *Marine and Freshwater Research* 49: 579-591
- Freer DWL, Griffiths CL (1993) The fishery for, and general biology of, the St. Joseph *Callorhinchus capensis* (Dumeril) off the southwestern Cape, South Africa. *South African Journal of Marine Science* 13: 63-74
- Frisk MG, Miller TJ, Dulvy NK (2005) Life histories and vulnerability to exploitation of elasmobranchs: inferences from elasticity, perturbation and phylogenetic analyses. *Journal of Northwest Atlantic Fishery Science* 35: 27-45
- Greene GH, Yoklavich MM, Starr RM, O'Connell VM, Wakefield WW, Sullivan DE, McRea Jr. JE, Cailliet GM (1999) A classification scheme for deep seafloor habitats. *Oceanologica Acta* 22: 663-678

- Gunderson DR (1997) Trade-off between reproductive effort and adult survival in oviparous and viviparous fishes. *Canadian Journal of Fisheries and Aquatic Sciences* 54: 990-998
- Gunderson DR, Sample TE (1980) Distribution and abundance of rockfish off Washington, Oregon, and California during 1977. *Marine Fisheries Review* 42: 2-16
- Hardy R, Mackie PR (1971) Observations on the chemical composition and toxicity of ratfish (*Chimaera monstrosa*). *Journal of the Science of Food and Agriculture* 22: 382-388
- Heupel MR, Carlson JK, Simpfendorfer CA (2007) Shark nursery areas: concepts, definition, characterization and assumptions. *Marine Ecology Progress Series* 337: 287-297
- Hilborn R, Mangel M (1997) *The Ecological Detective: Confronting Models with Data*. Princeton University Press, Princeton, NJ
- Hixon MA, Tissot BN (1992) Fish Assemblages of Rocky Banks of the Pacific Northwest [Stonewall Bank]. A final report supplement by the Department of Zoology of Oregon State University for the U.S. Department of the Interior, Minerals Management Service Pacific OCS Office, Camarillo, CA
- Jackson GA (1977) Nutrients and production of giant kelp, *Macrocystis pyrifera*, off southern California. *Limnology and Oceanography* 22: 979-995
- Johnson AG, Horton HF (1972) Length-weight relationship, food habits, parasites, and sex and age determination of the ratfish, *Hydrolagus colliei* (Lay and Bennett). *Fishery Bulletin* 70: 421-429

- Keller AA, Horness BH, Tuttle VJ, Wallace JR, Simon VH, Fruh EL, Bosley KL, Kamikawa DJ (2006) The 2002 U.S. West Coast upper continental slope trawl survey of groundfish resources off Washington, Oregon, and California: Estimates of distribution, abundance, and length composition. U.S. Department of Commerce, NOAA Technical Memorandum, NMFS-NWFSC-75
- Levin PS, Holmes EE, Piner KR, Harvey CJ (2006) Shifts in a Pacific Ocean fish assemblage: the potential influence of exploitation. *Conservation Biology* 20: 1181-1190
- Lo NCH, Jacobson ID, Squire JL (1992) Indices of relative abundance from fish spotter data based on delta-lognormal models. *Canadian Journal of Fisheries and Aquatic Sciences* 49: 2515-2526
- Mathews CP (1975) Note on the ecology of the ratfish, *Hydrolagus collei*, in the Gulf of California. *California Fish and Game* 61: 47-53
- Matta EM (2006) Aspects of the life history of the Alaska skate, *Bathyraja parmifera*, in the eastern Bering Sea. M.S. Thesis, University of Washington, Seattle
- Maunder MN, Punt AE (2004) Standardizing catch and effort data: a review of recent approaches. *Fisheries Research* 70: 141-159
- McCullagh P, Nelder JA (1989) *Generalized Linear Models*. Chapman and Hall, New York
- Mellergaard S, Nielsen E (1990) Fish disease investigations in Danish coastal waters with special reference to the impact of oxygen deficiency. *ICES C.M. E6*: 1-21
- NOAA CP (2008) Sea-viewing Wide Field-of-view Sensor (SeaWiFS) Sea Surface Chlorophyll-a Concentration, West U.S., 0.036 degree latitude resolution. Data

- courtesy of NASA/GSFC/DAAC, GeoEye. Data accessed through the OceanWatch server http://las.pfeg.noaa.gov/oceanWatch/oceanwatch_safari.php, developed at the Environmental Research Division, Southwest Fisheries Science Center, National Marine Fisheries Service, NOAA.
- Ortiz M, Arocha F (2004) Alternative error distribution models for standardization of catch rates of non-target species from a pelagic longline fishery: billfish species in the Venezuelan tuna longline fishery. *Fisheries Research* 70: 275-297
- PacFIN (2008) PFMC Port Group Report: Groundfish Landed-catch (Metric tons) for All Gears. <http://www.psmfc.org/pacfin/pfmc.html>. Accessed January 7, 2008.
- Palsson WA (2002) Survey-based stock trends for Puget Sound groundfishes: Monitoring the road to recovery. Puget Sound Research 2001. Puget Sound Action Team, Olympia, Washington
- Palsson WA, Beam J, Hoffmann S, Clarke P (2004) Fish without borders: trends in the status and distribution of groundfish in the transboundary waters of Washington and British Columbia. In: Droscher TW, Fraser DA (eds) Proceedings of the 2004 Georgia Basin/Puget Sound Research Conference
- Pauly D, Alder J, Bennett E, Christensen V, Tyedmers P, Watson R (2003) The future of fisheries. *Science* 302: 1359-1361
- Pearcy WG, Stein DL, Hixon MA, Pikitch EK, Barss WH, Starr RM (1989) Submersible observations of deep-reef fishes of Heceta Bank, Oregon. *Fishery Bulletin* 87: 955-965
- Pennington M (1983) Efficient estimators of abundance, for fish and plankton surveys. *Biometrics* 39: 281-286

- Quinn TP, Miller BS, Wingert RC (1980) Depth distribution and seasonal and diel movements of ratfish, *Hydrolagus coliei*, in Puget Sound, Washington. Fishery Bulletin 78: 816-821
- Sakamoto Y, Ishiguro M, Kitagawa G (1986) Akaike Information Statistics. KTK Scientific Publishers, Tokyo, and D. Reidel Publishing, Dordrecht
- SCCWRP (1973) The ecology of the Southern Californian bight: implications for water quality management. El Segundo, California. Southern California Coastal Water Research Project, Technical Report 104
- Schwartz G (1978) Estimating the dimension of a model. Annals of Statistics 6: 461-464
- Simpson JJ (1984) El Niño-induced onshore transport in the California current during 1982-1983. Geophysical Research Letters 11: 241-242
- Stefansson G (1996) Analysis of groundfish survey abundance data: combining the GLM and delta approaches. ICES Journal of Marine Science 53: 577-588
- Tolimieri N, Levin PS (2006) Assemblage structure of eastern Pacific groundfishes on the U.S. continental slope in relation to physical and environmental variables. Transactions of the American Fisheries Society 135: 317-332
- Venables WN, Dichmont CM (2004) GLMs, GAMs and GLMMs: an overview of theory for applications in fisheries research. Fisheries Research 70: 319-337
- Weinberg KL, Wilkins ME, Dark TA (1984) The 1983 Pacific west coast bottom trawl survey of groundfish resources: estimates of distribution, abundance, age and length composition. U.S. Department of Commerce, NOAA Technical Memorandum NMFS F/NWC-70

- Weinberg KL, Wilkins ME, Shaw FR, Zimmerman FR (2002) The 2001 Pacific West Coast bottom trawl survey of groundfish resources: Estimates of distribution, abundance, and length and age composition. U.S. Department of Commerce, NOAA Technical Memorandum NMFS-AFSC-128
- Yano K (1995) Reproductive biology of the black dogfish, *Centroscyllium fabricii*, collected from waters off western Greenland. Journal of the Marine Biological Association of the U.K. 75: 285-310
- Zimmerman RC, Kremer JN (1984) Episodic nutrient supply to a kelp forest ecosystem in southern California. Journal of Marine Research 42: 591-604
- Zimmerman RC, Robertson DL (1985) Effects of El Niño on local hydrography and growth of the giant kelp, *Macrocystis pyrifera*, at Santa Catalina Island, California. Limnology and Oceanography 30: 1298-1302
- Zimmermann M, Wilkins ME, Weinberg KL, Lauth RR, Shaw FR (2003) Influence of improved performance monitoring on the consistency of a bottom trawl survey. ICES Journal of Marine Science 60: 818-826

Table 1. Model selection criteria for each delta-GLM, sorted by AIC score of the binomial fit. Final models are in bold.

Model structure	df	Binomial			Lognormal		
		AIC	Δ AIC	Akaike weights	AIC	Δ AIC	Akaike Weights
<i>(A) Slope with years truncated</i>							
Year + Latitude + Depth + Year:Latitude + Depth:Latitude + Year:Depth	59	733.44	24.34	0.00	945.45	25.60	0.00
Year + Latitude + Depth + Year:Latitude + Depth:Latitude	47	719.94	10.84	0.00	926.37	6.52	0.04
Year + Latitude + Depth + Depth:Latitude	27	714.62	5.52	0.06	925.80	5.95	0.05
Year + Latitude + Depth	12	709.10	0.00	0.94	919.85	0.00	0.92
Latitude + Depth	8	740.02	30.92	0.00	939.60	19.75	0.00
Latitude	5	761.50	52.40	0.00	947.70	27.85	0.00
1	1	797.60	88.50	0.00	966.30	46.45	0.00
<i>(B) Slope</i>							
Year + Latitude + Depth + Year:Latitude + Depth:Latitude	76	963.92	18.57	0.00	1225.29	17.65	0.00
Year + Latitude + Depth + Depth:Latitude	32	946.98	1.63	0.31	1212.24	4.60	0.09
Year + Latitude + Depth	17	945.35	0.00	0.69	1207.64	0.00	0.91
Latitude + Depth	8	978.92	33.57	0.00	1221.18	13.54	0.00
Latitude	5	997.10	51.75	0.00	1232.00	24.36	0.00
1	1	1031.00	85.65	0.00	1256.00	48.36	0.00
<i>(C) Northern shelf and upper slope</i>							
Year + Latitude + Depth + Year:Latitude + Depth:Latitude + Year:Depth	143	3611.35	30.91	0.00	4329.52	53.57	0.00
Year + Latitude + Depth + Year:Latitude + Depth:Latitude	116	3591.95	11.51	0.00	4305.10	29.15	0.00
Year + Latitude + Depth + Depth:Latitude	44	3580.44	0.00	1.00	4286.91	10.96	0.00
Year + Latitude + Depth	20	3631.00	50.56	0.00	4275.95	0.00	1.00
Latitude + Depth	11	3748.00	167.56	0.00	4304.20	28.25	0.00
Latitude	8	3776.00	195.56	0.00	4308.00	32.05	0.00
1	1	3876.00	295.56	0.00	4383.00	107.05	0.00
<i>(D) Southern shelf and upper slope</i>							
Year + Latitude + Depth + Year:Latitude + Depth:Latitude + Year:Depth	53	854.99	31.17	0.00	882.09	26.84	0.00
Year + Latitude + Depth + Year:Latitude + Depth:Latitude	35	839.04	15.22	0.00	861.88	6.63	0.02
Year + Latitude + Depth + Depth:Latitude	17	823.82	0.00	0.80	856.55	1.30	0.33
Year + Latitude + Depth	13	826.57	2.75	0.20	855.25	0.00	0.64
Latitude + Depth	4	877.20	53.38	0.00	872.70	17.45	0.00
Latitude	2	873.20	49.38	0.00	872.00	16.75	0.00
1	1	921.30	97.48	0.00	868.50	13.25	0.00
<i>(E) Entire survey area with years grouped</i>							
YearGrouped + Latitude + YearGrouped:Latitude	71	5521.10	2.50	0.22	6355.88	20.45	0.00
YearGrouped + Latitude	25	5518.60	0.00	0.78	6335.43	0.00	1.00
Latitude	23	5623.30	104.70	0.00	6353.50	18.07	0.00
1	1	5839.00	320.40	0.00	6522.00	186.57	0.00

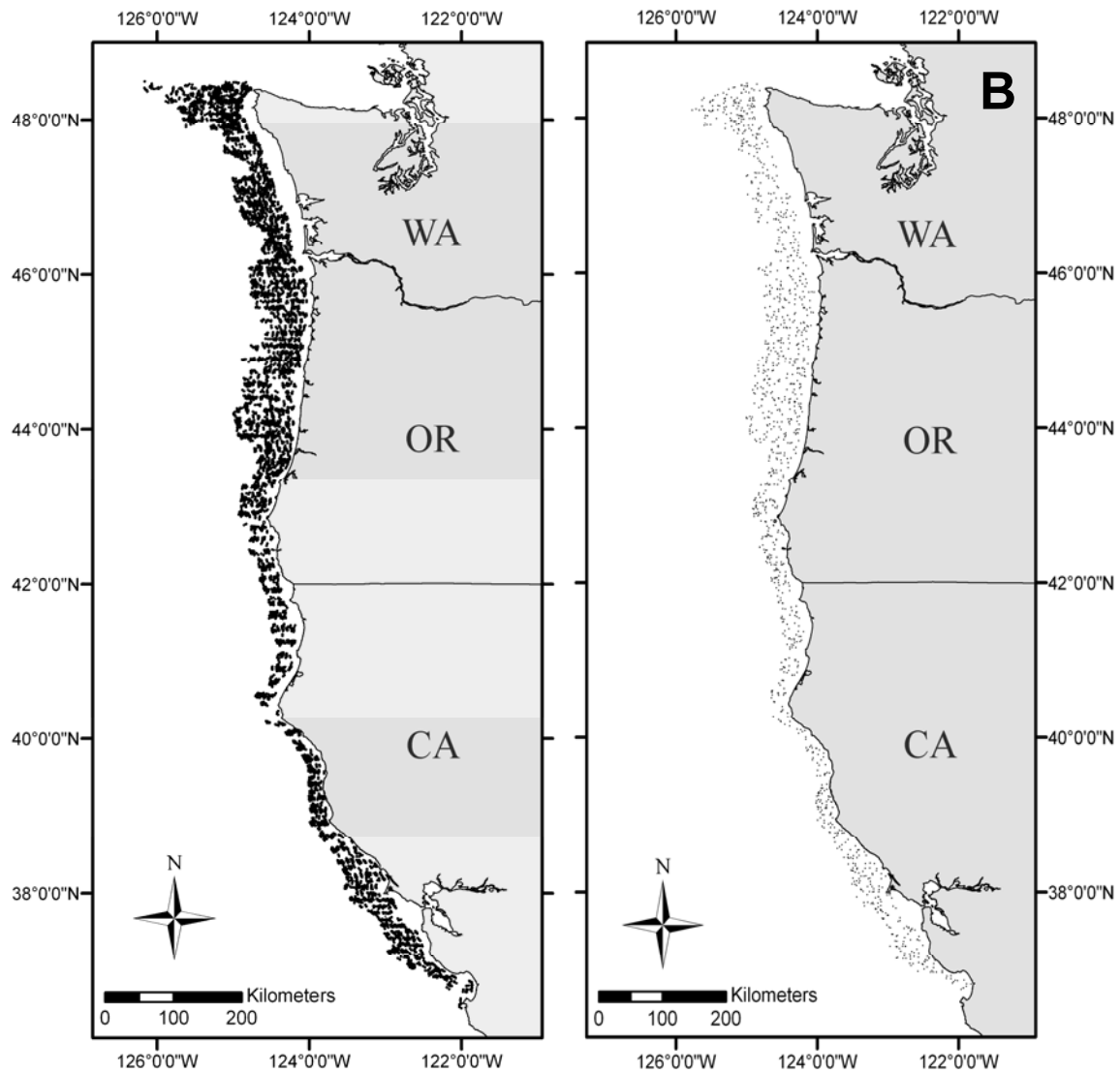


Figure 1. Start-of-haul locations for (A) the AFSC triennial trawl surveys (1977 to 2004), and (B) the NWFSC West Coast Groundfish Surveys (2003 to 2006). Samples shown here are those restricted to the latitudinal range used for abundance analysis (36.5° to 48.5° N).

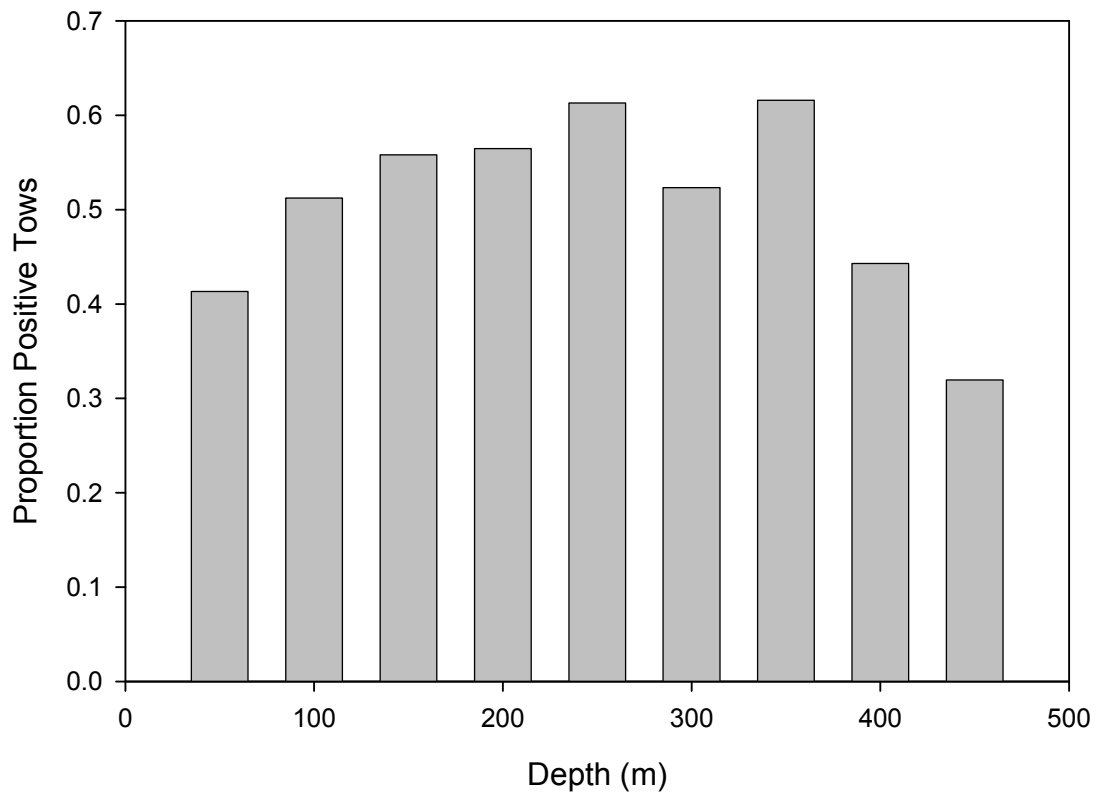


Figure 2. Proportion of positive tows by 50 m depth bin (each bin comprises 50 m from the given x-axis label).

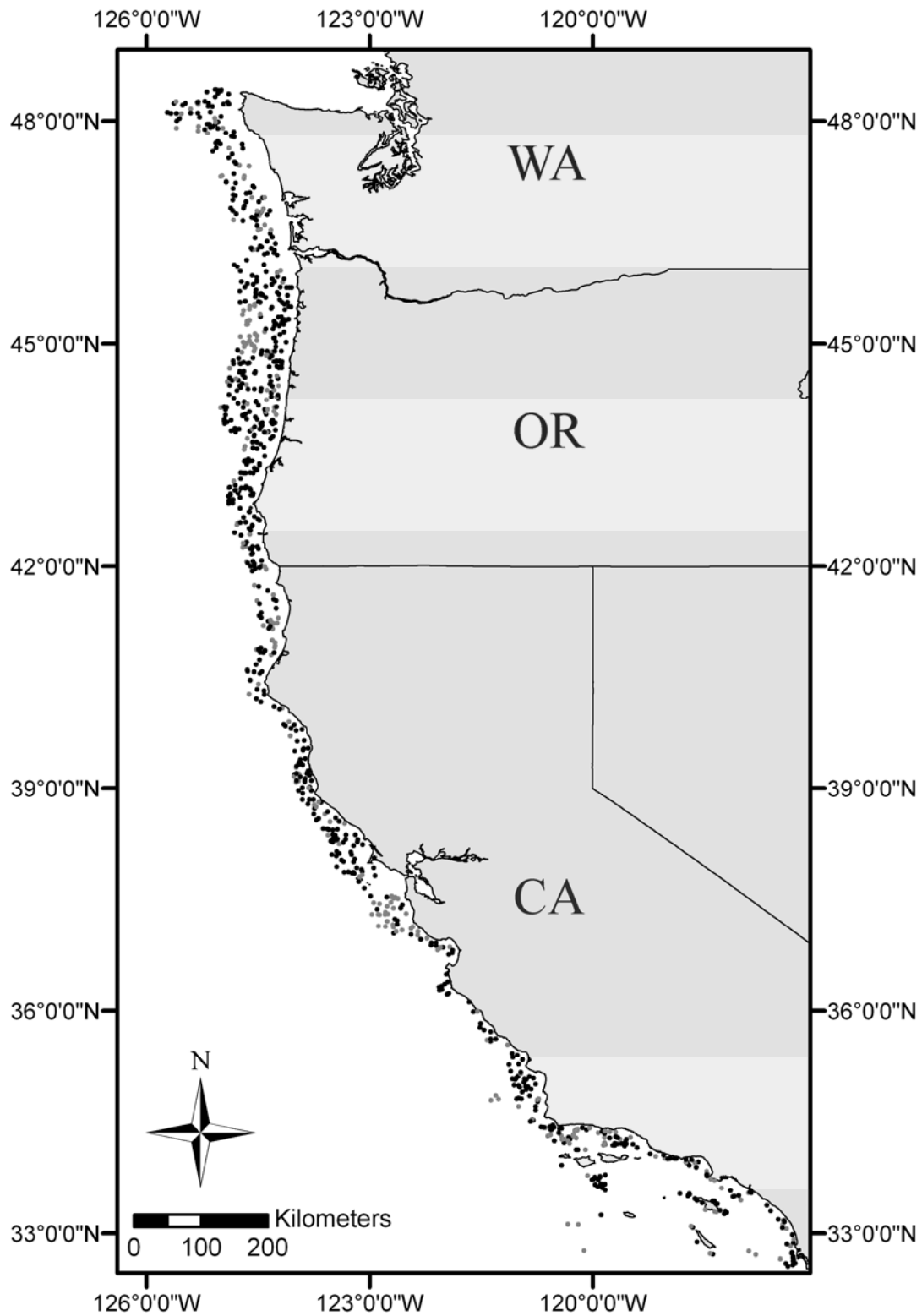


Figure 3. Start-of-haul locations for the 2005 and 2006 NWFSC West Coast Groundfish Surveys. Hauls with zero catch are in grey and those with positive catch are in black.

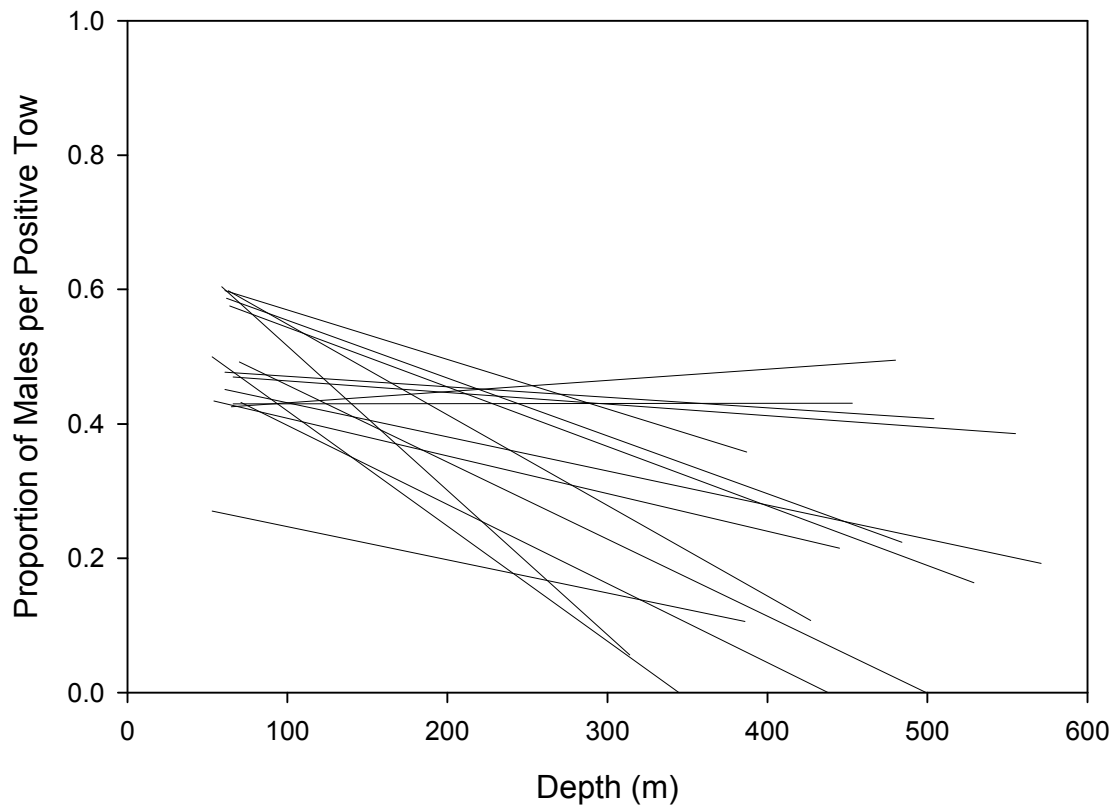


Figure 4. Proportion of male ratfish by depth. Linear regression lines are shown for each degree of latitude, but raw data are not shown for the sake of clarity.

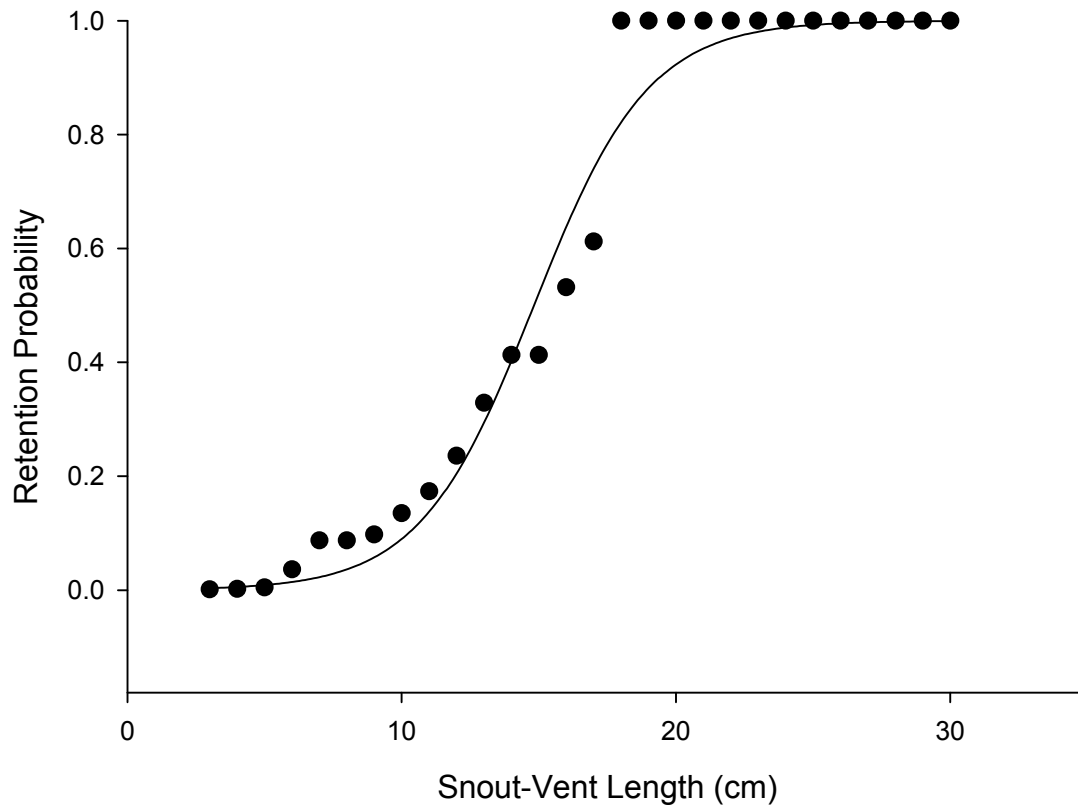


Figure 5. Survey selectivity function for the NWFSC West Coast Groundfish Survey, from the years 2005 and 2006 ($n = 7,020$).

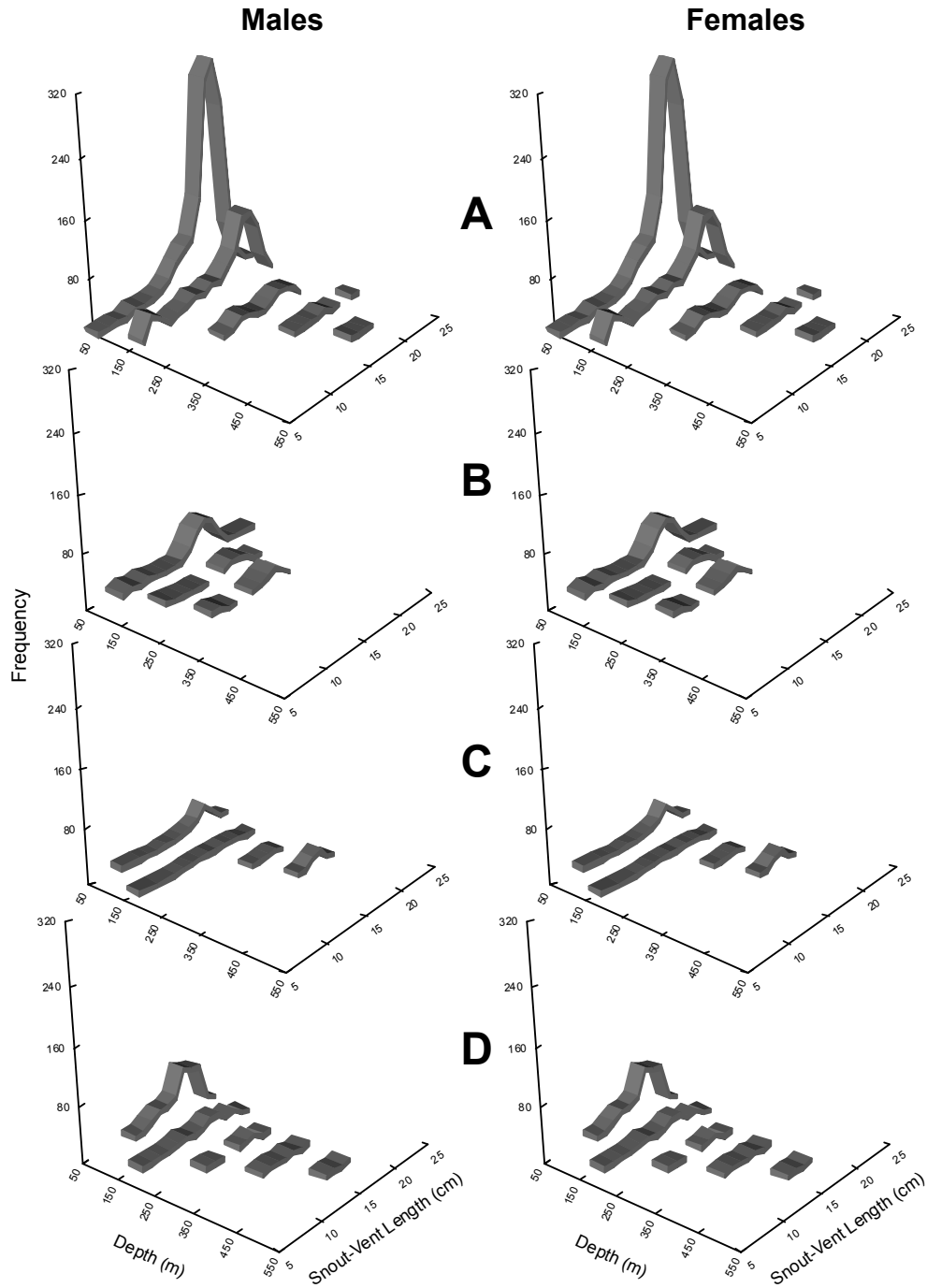


Figure 6. Length-frequencies by depth for males and females between the latitudinal regions (A) 39.5° to 48.5° N, (B) 36.5° to 39.5° N, (C) 34.5° to 36.5° N, and (D) 32.6° to 34.5° N.

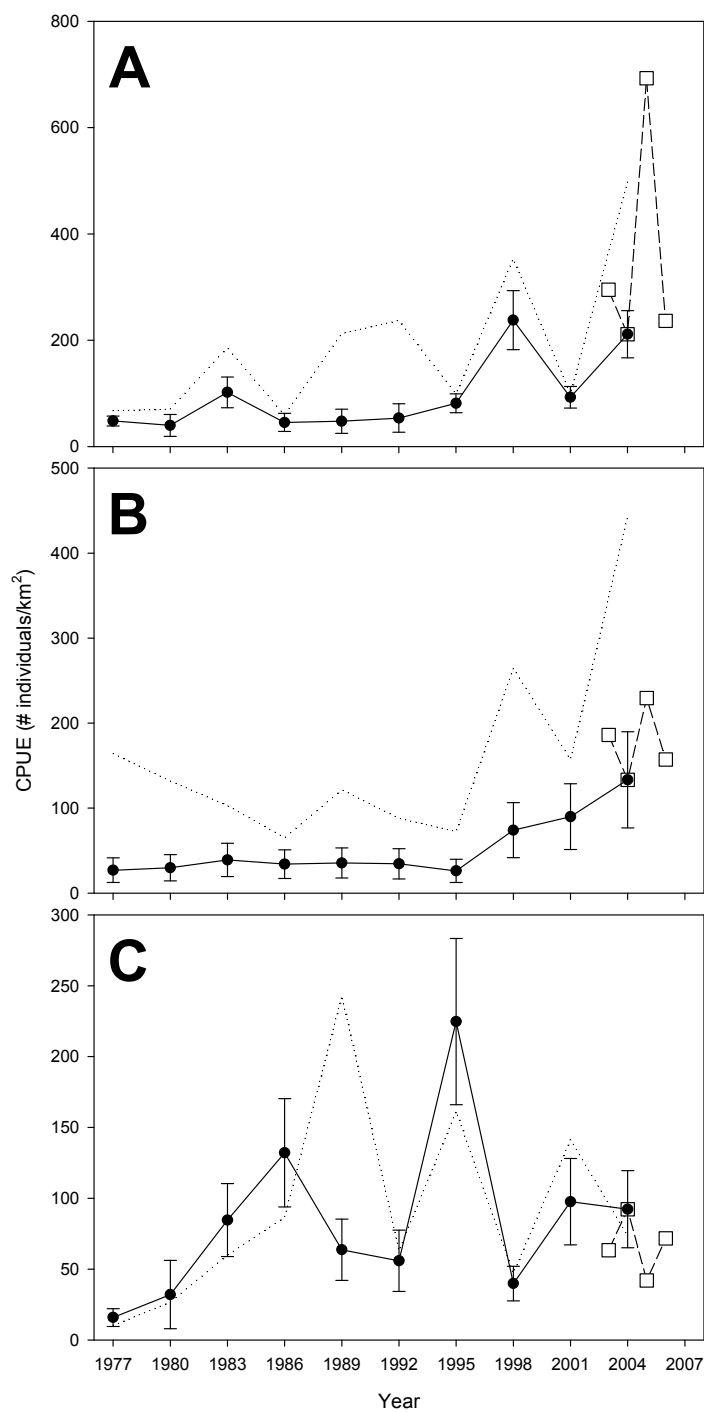


Figure 7. GLM-standardized CPUE estimates from the continental slope (250 to 500 m depth) between the latitudes of 36.5° to 48.5° N (A), the continental shelf and upper slope (50 to 250 m depth) between the latitudes of 39.5° to 48.5° N (B), and 36.5° to 39.5° N (C). Error bars represent SEs. Dotted lines represent the geometric mean CPUE. Open squares represent geometric mean CPUE from the NWFSC survey, standardized by the GLM-standardized 2004 triennial trawl CPUE.

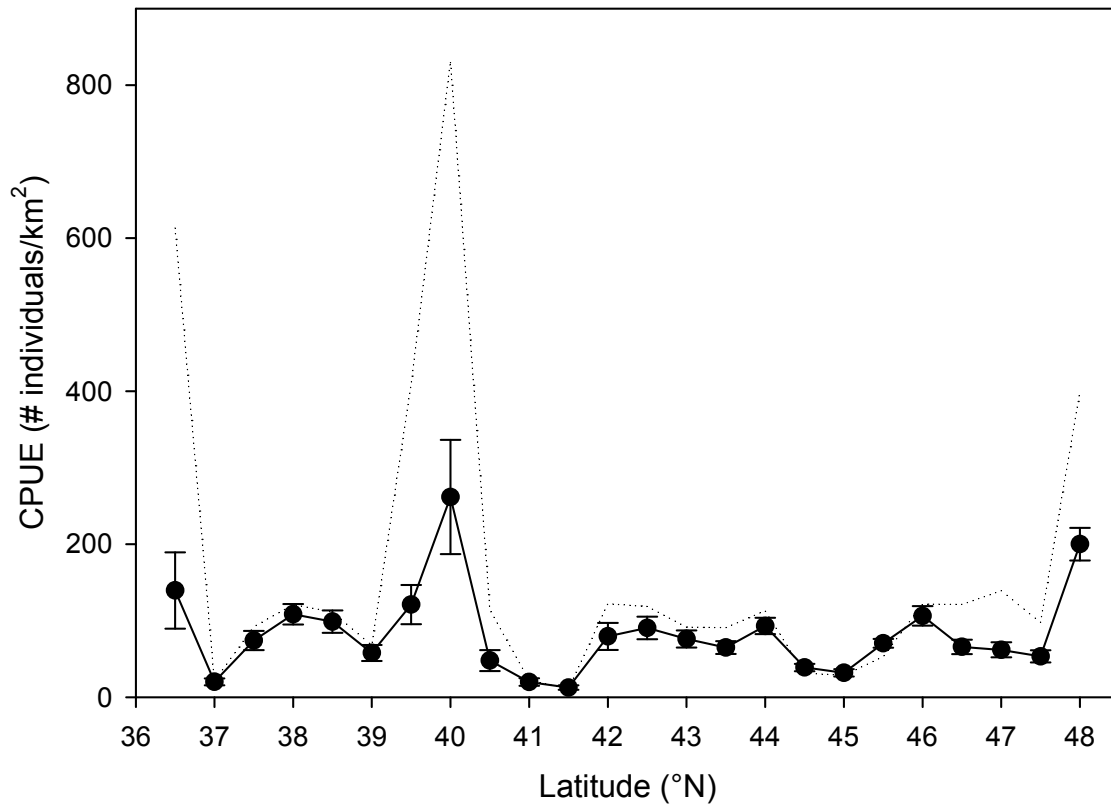


Figure 8. Standardized CPUE estimates for the entire survey area by 0.5° latitude bin (each bin comprises 0.5° north from the given x-axis label). Error bars represent SEs. A dotted line represents the geometric mean CPUE.

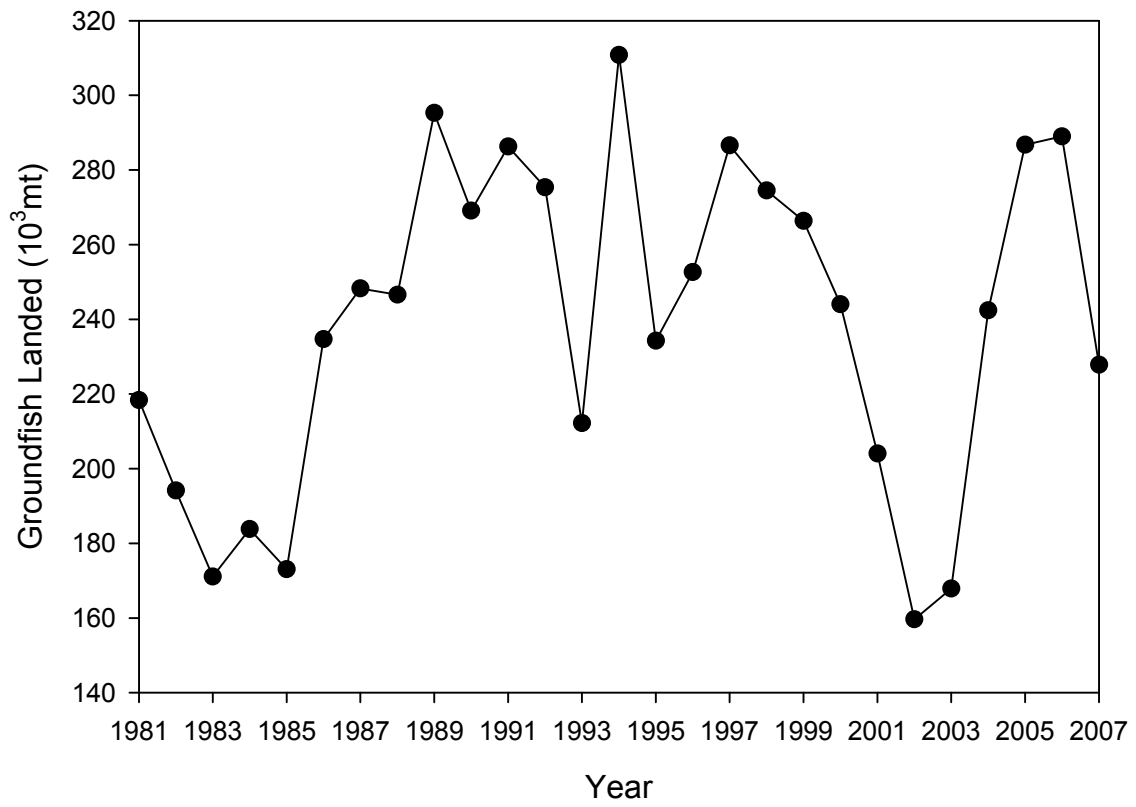


Figure 9. Groundfish landings off California, Oregon, and Washington from 1981 to 2007 (PacFIN 2008).

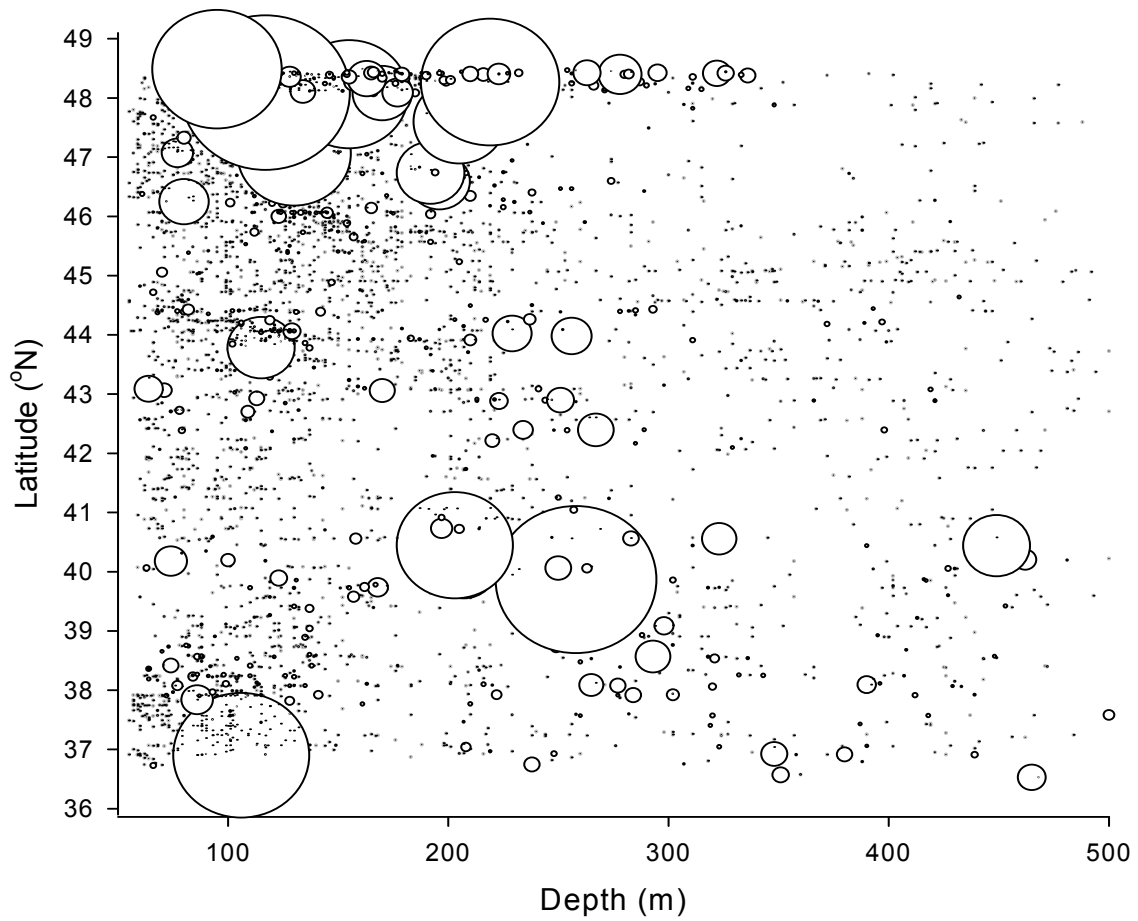


Figure 10. Bubble plot of raw CPUE data by depth and latitude. Size of the bubbles correspond to the relative CPUE, with zero catches in gray.

Appendix: Generalized linear model diagnostic graphs

In each of the following figures, individual models are identified by a letter scheme, where:

A = slope

B = northern shelf and upper slope

C = southern shelf and upper slope

D = entire survey region with years grouped

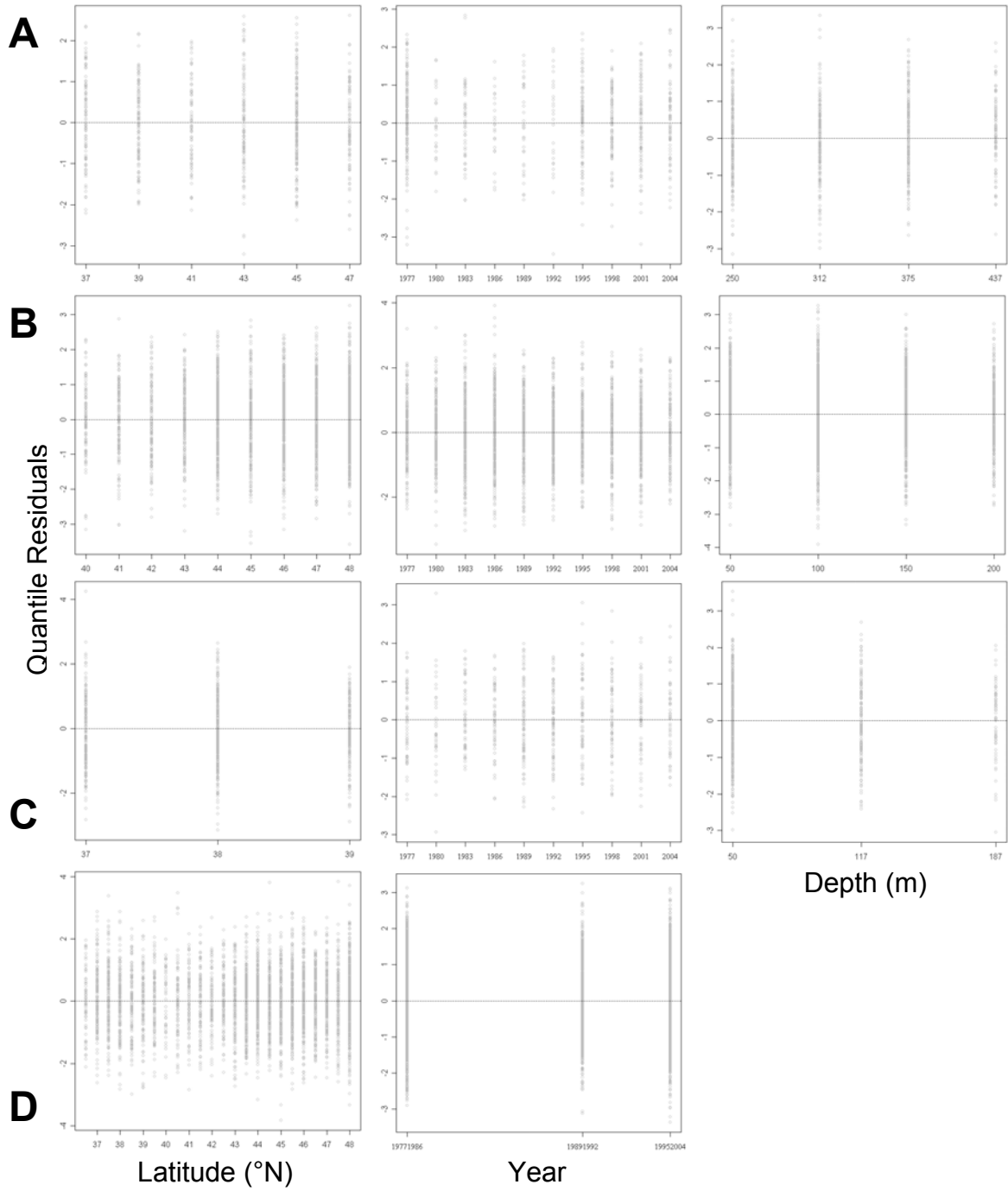


Figure 1. Quantile residuals against each explanatory variable for the binomial GLMs. Dotted line indicates the null pattern.

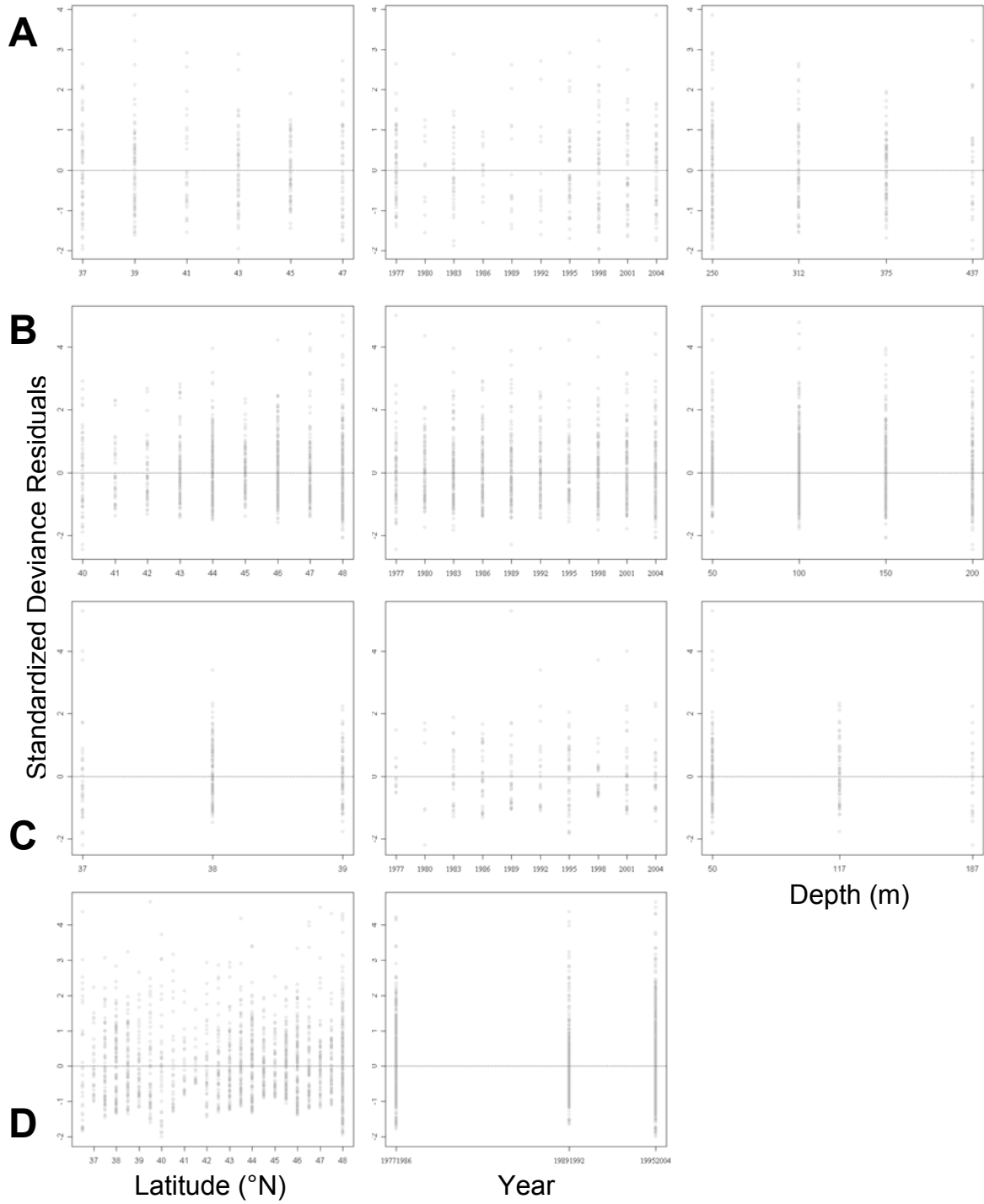


Figure 2. Standardized deviance residuals against each explanatory variable for the positive GLMs. Dotted line indicates the null pattern.

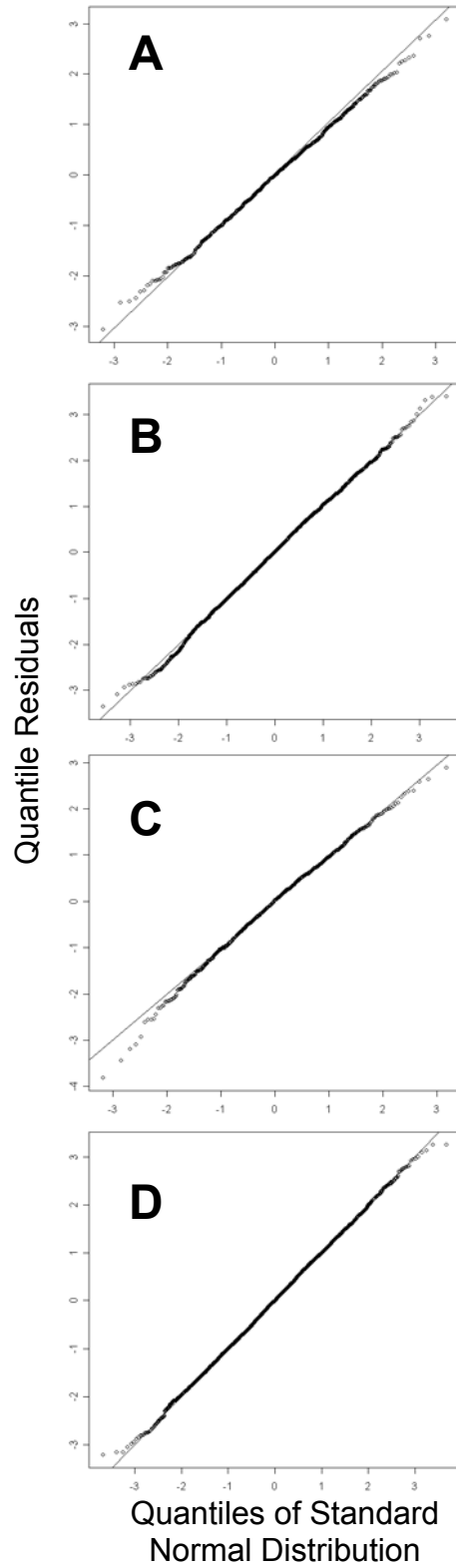


Figure 3. Quantile-quantile plots of the quantile residuals from the binomial GLMs, with a line fit through the first and third quantiles.

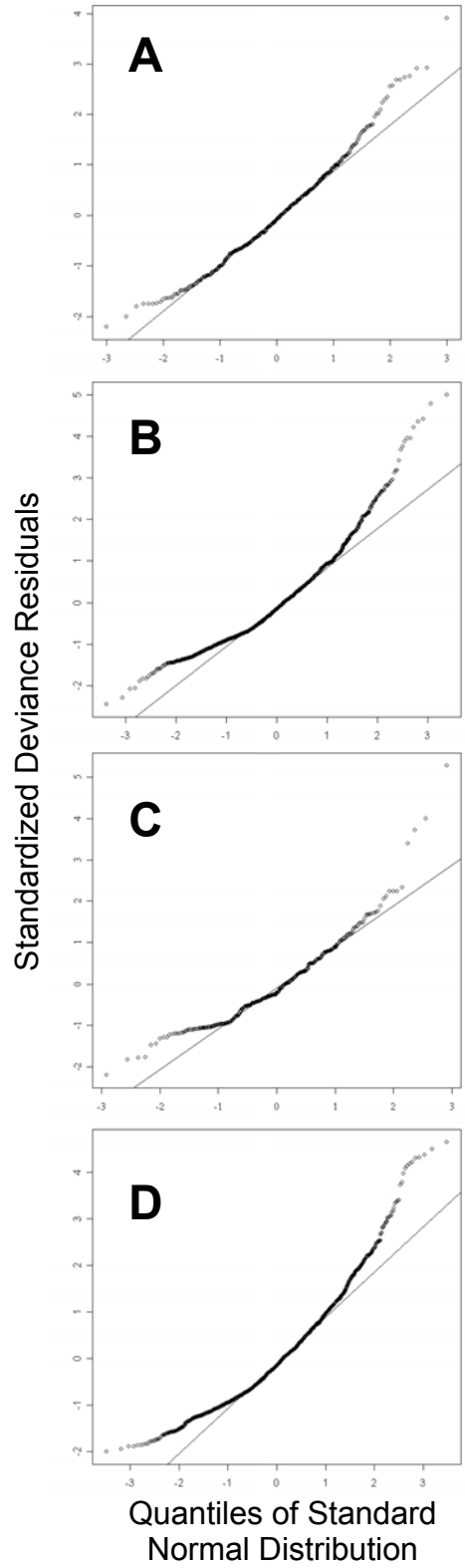


Figure 4. Quantile-quantile plots of the standardized deviance residuals from the binomial GLMs, with a line fit through the first and third quantiles.

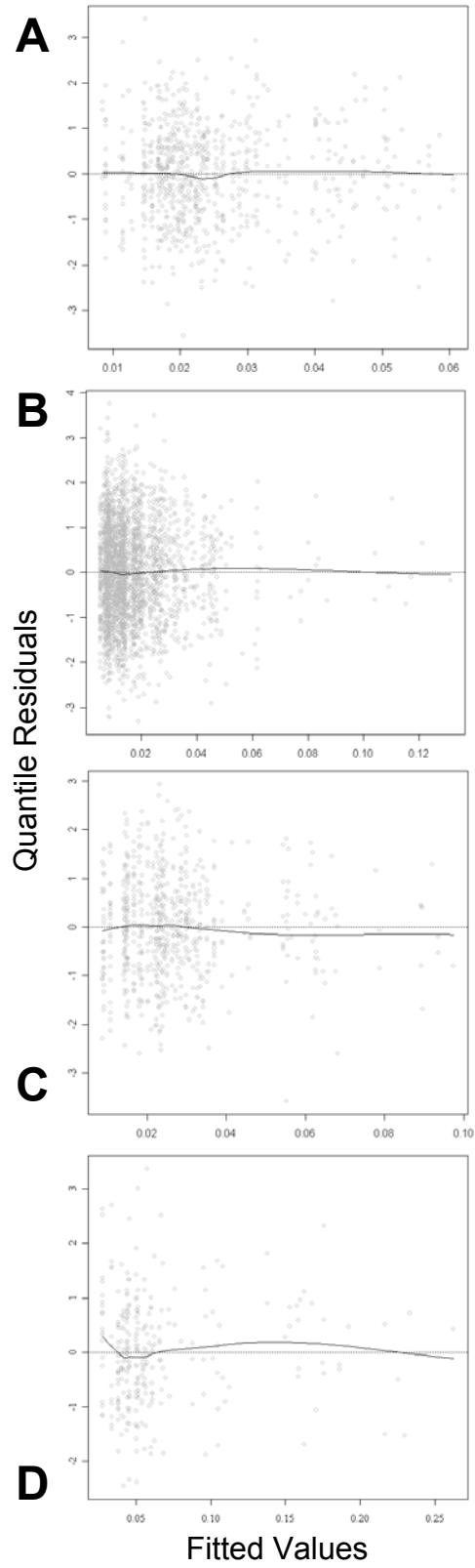


Figure 5. Quantile residuals against fitted values for the binomial GLMs, with a Loess smoother (span = 2/3). Dotted line indicates the null pattern.

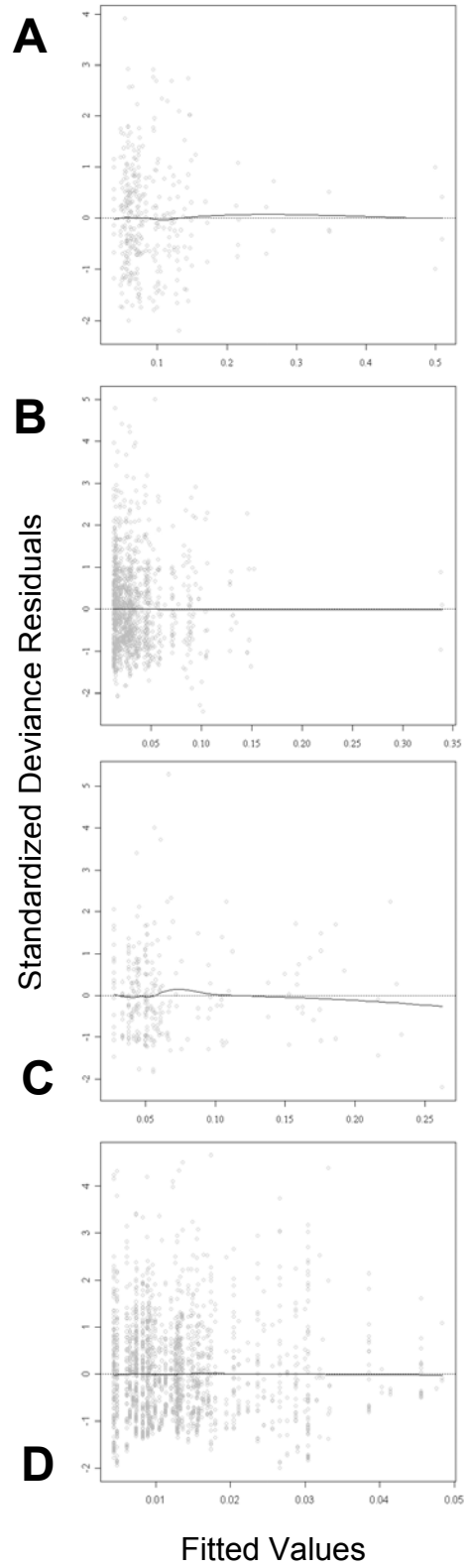


Figure 6. Standardized deviance residuals against fitted values for the positive GLMs, with a Loess smoother (span = 2/3). Dotted line indicates the null pattern.

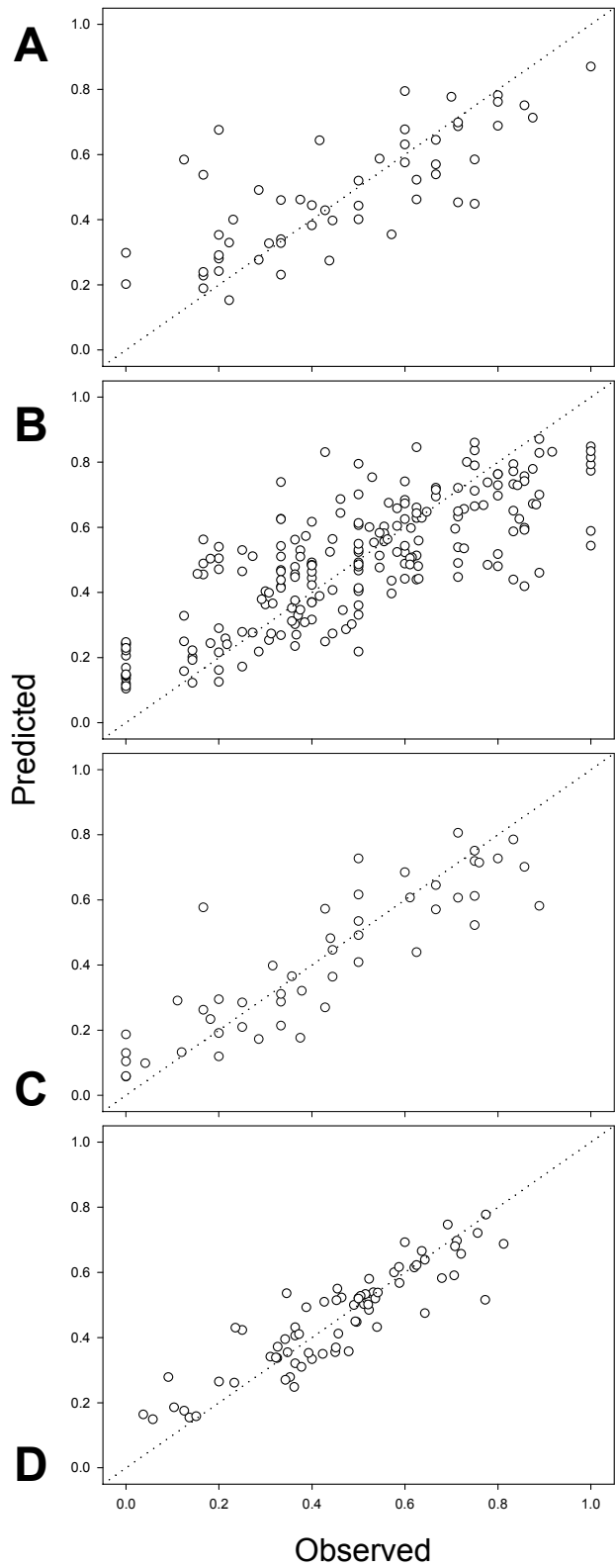


Figure 7. Proportion of positive tows predicted by the binomial model against the proportion of positive tows observed. Cells with less than five observations were excluded from the analysis. Dotted line is a 1:1 reference.

Chapter 3

Assessment of the dorsal-fin spine for chimaeroid (Holocephali: Chimeriformes) age estimation

Introduction

Knowledge of fish age and growth characteristics is necessary for stock assessment and development of successful management or conservation plans. Few researchers have attempted to age chimaeroids (Calis et al. 2005; Freer and Griffiths 1993a; Johnson and Horton 1972; Moura et al. 2004; Sullivan 1977), and none have convincingly validated their age estimates. Researchers have primarily used the dorsal-fin spine as the ageing structure, because vertebral centra, commonly used to age other chondrichthyans, are poorly calcified in holocephalans (personal observation, Johnson and Horton 1972; Ridewood 1921). In *Hydrolagus colliei*, the number of transverse ridges of vomerine tooth plates increases with body size, therefore has been proposed as a promising ageing structure (Johnson and Horton 1972; Simmons and Laurie 1972).

These ridges may be ephemeral, however, as they are likely formed by a combination of deposition and erosion of the ever-growing tooth plates (Didier et al. 1994), a process which may be extremely rapid (Ward and Grande 1991). These ridges may be serially replaced, leading to underestimation of lifetime growth and age (Didier and Rosenberger 2002). Modal analyses of length-frequency distribution, and eye lens diameter and weight may be used to determine the age structure of chimaeroids (Francis 1997; Francis and Maolagáin unpublished), but are likely only useful for verification of ageing from a hard part composed of calcium phosphate or dentine (Cailliet and Goldman 2004).

The dorsal-fin spine may have been derived from modifications of individual (Goodrich 1909) or multiple scales (Patterson 1965), but its derivation remains controversial (Maisey 1979). Halstead and Bunker (1952) indicated that the spine stem is composed of vasodentine, and the interior is a pulp cavity occupied by a cartilaginous rod

enveloped by a layer of areolar connective tissue. Halstead and Bunker (1952) described the spine as having a thin outer layer of integument, consisting of an outer avascular epidermis of squamous epithelium, and an inner vascularized dermis of fibrous connective tissue. An enamel layer, which is present in dorsal-fin spines of squaloid sharks, has not been identified in the chimaeroid dorsal-fin spine (Goodrich 1909; Halstead and Bunker 1952).

Based on the growth of elasmobranch dorsal-fin spines, researchers have assumed the chimaeroid spine grows primarily by secretions of cells in the spine lumen that deposit dentine on the inner surface of the spine (Holden and Meadows 1962). This type of growth would create conical growth zones stacked on top of one another, each new growth zone displacing the previous growth zones distally. Chimaeroid dorsal-fin spines have only one inner and outer layer of dentine (Calis et al. 2005), and there is debate among authors whether elasmobranch dorsal-fin spines have two or three dentine layers (review in Clarke and Irvine 2006). Early squaloid researchers interpreted opaque and translucent band pairs within the inner layer of dorsal-fin spines as dentine growth increments deposited with consistent, annual periodicity (Kaganovskaia 1933), but this was only validated for *Squalus acanthias* (Campana et al. 2006; McFarlane and Beamish 1987; Tucker 1985).

I test the hypothesis that the dorsal-fin spine of *H. colliei* is a reliable structure for age estimation. To aid interpretation of spine growth, the internal structure of the spine was compared with hard parts used for age determination of other fishes. Knowledge of *H. colliei* age and growth dynamics is necessary to determine its vulnerability to fishing

mortality, currently applied as discard mortality from the commercial groundfisheries of the eastern North Pacific.

Materials and Methods

Age and Growth Determination

The dorsal-fin spine was the primary structure evaluated for age estimation of *H. colliei*. Dorsal-fin spines were excised from each individual and stored frozen.

Transverse (perpendicular to axis of spine) sectioning of the spine has produced the best results for ageing in other chimaeroids (Calis et al. 2005; Francis and Maolagáin unpublished; Freer and Griffiths 1993a; Sullivan 1977), however, I also attempted longitudinal sectioning to visualize the entire zone of dentine deposition. For a subset of spines, transverse and longitudinal sections were collected from a single spine for direct comparison of growth bands. Dorsal-fin spine terminology follows Clarke and Irvine (2006).

To locate the appropriate region on the spine to extract transverse sections, morphometric measurements of dried dorsal-fin spines were recorded to the nearest mm (after Calis et al. 2005). Not all measurements were consistent, however, as many individuals had obvious wear of the spine tip. To address this problem, past researchers created a correction factor, using the linear relationship of spine width at fixed positions on the longitudinal axis of unworn spines (Sullivan 1977). After correcting spine lengths, and sectioning and analyzing a representative sample of spines for growth increments, the best sectioning position for ageing was determined by the distance from the actual or theoretical unworn spine tip. In this study, the validity of using lateral spine width as a

proxy for the distance from the spine tip was tested with ANCOVA, using width as the dependent variable, individual as a random independent factor, and distance from the spine tip as a covariate. In the first phase of this sampling, width was measured microscopically at multiple fixed distances from the spine tip (following Sullivan 1977), then later at multiple random distances. These two datasets produced the same results when tested separately, so data were combined for the final test. In the early stages of experimentation, spines were sectioned throughout the ageable region to establish the lateral spine width and distance from spine tip that contained a cross section of all dentine deposits to prevent underestimation of age. At least six sections were taken from each specimen, with section thickness varying from 0.1 to 0.6 mm, selected to include the optimal range in previous studies (Calis et al. 2005; Francis and Maolagáin unpublished; Freer and Griffiths 1993a).

Before sectioning, spines were embedded in a polyester casting resin, which was allowed to harden for 24 h. Sections were cut using a Buehler Isomet low-speed saw with diamond-impregnated blade. Subsequently sections were polished with 1200- grit sandpaper to remove saw scratches and create a smooth surface. Sections were mounted on a microscope slide for enumeration of growth bands. Transmitted, reflected, and polarized light were used in microscopic analysis of the spine to determine the optimal lighting method for discerning growth bands. Several dorsal-fin spines were embedded, stained with Harris hematoxylin, and sectioned on a microtome for histological analysis using the methods of Natanson et al. (2007). To determine whether growth bands were indicative of somatic growth, band counts were plotted against snout-vent length (SVL) and total body mass.

Hard parts used in ageing must grow in proportion to body size to be considered an adequate ageing structure. Therefore, SVL was compared with several morphometric measurements of the dorsal-fin spine to test the assumption of a positive relationship between body size and dorsal-fin spine size. Each relationship was modelled with the linear or non-linear regression function that produced the best fit.

The hypothesized annual periodicity of growth band deposition was tested with direct validation by chemical marking with oxytetracycline (OTC). Three captive ratfish, held at the Vancouver Aquarium, were injected with a 25 mg kg⁻¹ body weight dose (Holden and Vince 1973) of OTC. After one year of growth, dorsal-fin spines were removed, sectioned, and viewed under reflected ultraviolet light. Care was taken to minimize the intensity and duration of sample exposure to ambient light to avoid degradation of the fluorescent properties of OTC.

Computed Tomography

Precise and accurate age estimation was challenging because of the lack of information about spine structure and development. The traditional technique of microscopic examination of thin-sectioned spines provides limited inference, as among-individual variation in the distribution of growth increments may prevent precise age estimation and validation. Radiological resources, therefore, were used to elucidate the physiological parameters of interest. Simple x-ray technology was insufficient, however, because of the small focal size necessary to resolve features on the scale of tens of microns. Analyses also were hampered by attempts to visualize a 3-dimensional object in a 2-dimensional projection. These problems were addressed by using computed

tomography to visualize the dorsal-fin spine with 3-dimensional imaging. Computed tomography (CT) is a radiological imaging technique that is analogous to a 3-dimensional x-ray. This study used micro-computed tomography (μ CT), which is the same method as CT, but with greatly decreased voxel size (increased resolution). All scans were 16-bit gray scale, with 6 micron isotropic voxel size. This technique is the state-of-the-art in high-resolution, 3-dimensional imaging of dense structures, yet this study is the first to use μ CT for age determination.

For comparative purposes, μ CT scans also were performed on ageing structures commonly used in other organisms. Structures included the dorsal-fin spine and vertebra of spiny dogfish (*Squalus acanthias*), vertebra and caudal thorn of rougtail skate (*Bathyraja trachura*), and otolith of Patagonian toothfish (*Dissostichus eleginoides*). The vertebra and neural arch of *H. colliei* also were scanned to determine their potential as ageing structures.

Results

Growth

Longitudinal sectioning was not successful in elucidating all growth increments. Longitudinal bands were only observed in two out of six spines, and only once were the band counts similar between longitudinal and transverse sections. Histological methods were not successful in producing sections with visible growth bands.

The length from base to tip (total spine length or TSL) of unworn dorsal-fin spines increased linearly with SVL ($t = 34.041$, $df = 19$, $p < 0.001$, $R^2 = 0.984$; Fig. 1A). The distance from spine tip to the apex of the pulp cavity (apex spine length or ASL)

increased linearly with SVL ($t = 7.817$, $df = 19$, $p < 0.001$, $R^2 = 0.760$; Fig. 1B).

Similarly, the lateral spine width at the apex of the pulp cavity (apex pulp cavity diameter, or APC) increased linearly with SVL ($t = 8.082$, $df = 19$, $p < 0.001$, $R^2 = 0.772$; Fig. 1C).

Lateral spine width along the longitudinal axis of the spine was not a consistent indicator of distance from the spine tip. The relationship between distance from spine tip and spine width varied among individuals (ANCOVA: factor = spine length*individual, $F = 2.807$; $df = 27$; $p = 0.001$; Fig. 2). Therefore, it is not possible to assure that transverse sections are collected at the same position among individuals, relative to growth zones.

Transverse sections viewed with incandescent transmitted light revealed much about the internal structure of the spine's dentine portions. The anterior dentine portion was composed of trabecular dentine (Fig. 3A), overlying the outer and inner concentric laminar dentine layers of the stem (Fig. 3B). The orientation of the canaliculi (the network of dentritic vessels within the dentine) indicated the inner dentine layer was deposited centripetally, and the outer dentine layer was deposited centrifugally. In the anterior dentine portion, dentine is deposited centripetally around each vascular canal.

Standard incandescent transmitted and reflected light failed to reveal clear growth increments in transverse sections. However, when viewed with transmitted light combined with a polarizing filter, zones of dark and light alternating bands were observed within the inner dentine layer (Fig. 4). These bands were most apparent in 0.4 mm thick sections. The greatest number of bands was found in sections 8.8 to 9.4 mm from the spine tip, near the apex of the pulp cavity.

The number of band pairs observed in the inner dentine layer was not a good predictor of body size. There was a trend indicating that the number of bands increased with SVL and total mass, but there was great variability (Fig. 5). No attempts were made to model the relationship because of the small sample size and the great inherent uncertainty.

Validation attempts by injection with OTC were inconclusive. The substance was not incorporated into the dorsal-fin spine dentine. Irregular patterns of fluorescence were observed in the soft tissues of the spine exterior and vascular canals, but they cannot be attributed to OTC injection.

Physiology of Hard Parts

As expected, mineral density gradients, potentially representing discrete growth zones, were observed in the hard parts of elasmobranch and teleost specimens. Such density gradients were observed in the second dorsal-fin spine (Fig. 6A) and vertebra (Fig. 6B) of *S. acanthias*. Scans of the spine revealed three large bands, representing the inner and outer dentine layers, separated by the trunk primordium (Maisey 1979). The enamel and dentine of the cap was distinguishable on the posterior-lateral edge.

Mineral density gradients were observed in the vertebra (Fig. 7A) and caudal thorns (Fig. 7B) of *B. trachura*. Micro-CT scans from the otolith of *D. eleginoides* also revealed well-defined density gradients (Fig. 8). These gradients were distributed in patterns consistent with their interpretation as growth zones from observations using light microscopy.

Mineral density gradients were not observed in the *H. colliei* dorsal-fin spine (Fig. 9). Numerous vascular canals were observed on the anterior and posterior edges of the spine. The canals connected the spine lumen to the spine exterior. Canals were present at irregular intervals along the majority of the spine's length, but were more concentrated toward the tip.

The vertebra and neural arch (Fig. 10) of *H. colliei* were poorly calcified. Vertebral centra were entirely absent from two of the three μ CT scans, and visible only as translucent streaks in the other. The neural arch had very thin walls, with greater density in the interior of the wall than the exterior.

Discussion

Growth

The vertebral centra and neural arch of *H. colliei* were poorly calcified, therefore, likely useless as structures for age determination. Encouraging results had been obtained from the use of neural arches for aging the bluntnose sixgill shark, *Hexanchus griseus* (McFarlane et al. 2002), but this is not the case for *H. colliei*. The dorsal-fin spine does show some promise as a structure for ageing, as it grows continuously with body size. TSL, ASL, and APC increased linearly with SVL, providing clear interpretation of the relationship between spine growth and body size. The fit of TSL on SVL was particularly good, and provides support for the use of dorsal-fin spines for ageing. Variation among individuals in the relationship between spine width at length from the spine tip, however, indicated that the technique of transverse sectioning may confound age determination.

Previous researchers hypothesized the optimal point of transverse sectioning was a set distance from the spine tip. To test this hypothesis, researchers measured lateral spine width at varying distances from the spine tip for many individuals. With individuals pooled, spine width was regressed on spine length, typically with a fairly good fit (e.g. Sullivan 1977). Based on that evidence, spine width was used to determine appropriate distance from tip for transverse sectioning. An ANCOVA, however, indicated that there was significant among-individual variation in the length to width relationship. Width, therefore, is *not* a good indicator of the point where all growth zones can be viewed. This means that it is not possible to section at the same point on every spine, relative to the growth zones. Thus, this type of spine growth, observed with this technique of sectioning, precludes the use of validation tools such as marginal increment analysis and edge analysis (e.g. Guillart-Furio 1998). These complications further impede accurate and precise age estimation using the dorsal-fin spine.

The greatest band pair counts were in transverse sections near the apex of the pulp cavity. This point, however, can be as far as 16 mm from the spine tip, whereas the length of the entire spine can be as short as 13 mm. In older individuals, there may be no transverse plane at which all growth zones overlap. This would lead to underestimation of age. Underestimation of ages using internal growth bands also occurred in the ageing of squaloid dorsal-fin spines, perhaps because of lack of formation of additional growth zones in older individuals (Irvine et al. 2006a; Irvine et al. 2006b), or because growth zones were indistinguishable with advanced age (Irvine et al. 2006a). The results of this study indicate age estimates using the dorsal-fin spine of chimaeroids were prone to imprecision, or even bias, based on the region of transverse section.

Age validation attempts with laboratory grow-outs of OTC-injected *H. colliei* failed. The OTC was not incorporated internally, similar to observations of the chain dogfish, *Scyliorhinus retifer* (Lisa Natanson, NOAA Fisheries, Southeast Fisheries Science Center, pers. comm.). The fluorescence observed in the soft tissues of the spine could not have been caused by OTC, as it becomes absent from circulation within four months of injection in elasmobranchs (Tanaka 1990). The fluorescence in the soft tissues must be caused by a naturally-occurring substance.

Physiology of Hard Parts

Vascular canals were observed in the anterior and posterior edges of the *H. colliei* dorsal-fin spine, connecting the spine lumen with the spine exterior. This indicates that the vascular system of the chimaeroid dorsal-fin spine functions similarly to elasmobranch dorsal-fin spines *sensu* Maisey (1979). Arterial blood is supplied to the spine by small blood vessels leading distally within the loose connective tissue of the spine lumen. These vessels exit the spine lumen anteriorly and posteriorly through vascular canals that penetrate the stem. Veins in the anterior dentine portion and its associated dermis lead proximally to the spine base.

The dorsal-fin spine is not composed of vasodentine as proposed by Halstead and Bunker (1952). Instead, the inner, and perhaps outer, dentine layers are composed of orthodentine (Patterson 1965; Schaeffer 1977), as in elasmobranch dorsal-fin spines (Maisey 1979). The anterior dentine portion, and perhaps the posterior-lateral dentine portions, are likely composed of osteodentine (Patterson 1965), or a similar substance of unknown definition (Maisey 1979). This composition and orientation of growth surfaces

confirms that the bands observed in the inner dentine layer may indeed be indicative of incremental growth. However, the periodicity with which these zones are formed may not be consistent, which would explain the poor relationship between band pair number and body size. This phenomenon of inconsistent periodicity of band pair formation also has been observed in Pacific angel shark (*Squatina californica*) vertebrae (Cailliet et al. 1983; Natanson and Cailliet 1990).

Growth may not occur on all depositional surfaces of the spine throughout ontogeny. Halstead and Bunker (1952) observed odontoblasts (the cells which produce dentine) on the inner surface of the stem in spines from young individuals only, indicating that dentine deposition in the inner dentine layer may cease once a particular age or size is achieved. This observation may have been confounded by taking transverse sections too close to the spine base, yet it still calls into question the utility of the inner dentine layer as a complete growth record.

The lack of density gradients observed in *H. colliei* dorsal-fin spines is likely a real phenomenon, not an artifact of CT scanning (e.g. beam hardening). The alternating bands observed with polarized light may be transitions between zones of the spine with differing proteinaceous fiber orientation, instead of many extremely thin layers of dentine deposited in bands of alternating thickness (e.g. calcium deposition in teleost otoliths or elasmobranch vertebrae). The mere presence of varying fiber orientation, opposed to mineral density gradients, decreases the likelihood that the bands observed represent a record of growth with consistent periodicity. This provides some tentative evidence that *H. colliei* may have aseasonal growth.

Conclusions

Future research is necessary before chimaeroid dorsal-fin spines can be used for age estimation. Subsequent studies should continue attempting description of spine structure and growth using alternative techniques, including histology. Validation is needed to evaluate the accuracy of past and future chimaeroid age estimates. Alternative validation methods will need to be employed, as this study refutes the applicability of marginal increment analysis, edge analysis, and chemical marking with OTC. Until the periodicity of growth is validated, the hypothesis of aseasonal growth remains plausible and it should not be assumed that age is quantifiable by standard techniques.

Literature Cited

- Cailliet GM, Goldman KJ (2004) Age determination and validation in chondrichthyan fishes. In: Carrier JC, Musick JA, Heithaus MR (eds) Biology of sharks and their relatives. CRC Press, Boca Raton, FL, pp 399-448
- Cailliet GM, Martin LK, Kusher D, Wolf P, Welden BA (1983) Techniques for enhancing vertebral bands in age estimation of California elasmobranchs. In: Prince E, Pulos L (eds) Proceedings of the international workshop on age determination of oceanic pelagic fishes: tunas, billfishes, and sharks, pp 157-165
- Calis E, Jackson EH, Nolan CP, Jeal F (2005) Preliminary age and growth estimates of the rabbitfish, *Chimaera monstrosa*, with implications for future resource management. e-Journal of Northwest Atlantic Fisheries Science 35
- Campana SE, Jones C, McFarlane GA, Myklevoll S (2006) Bomb dating and age validation using the spines of spiny dogfish (*Squalus acanthias*). Environmental Biology of Fishes 77
- Clarke MW, Irvine SB (2006) Terminology for the ageing of chondrichthyan fish using dorsal-fin spines. Environmental Biology of Fishes 77: 273-277
- Didier DA, Rosenberger LJ (2002) The spotted ratfish, *Hydrolagus colliei*: notes on its biology with a redescription of the species (Holocephali: Chimaeridae). California Fish and Game 88: 112-125
- Didier DA, Stahl BJ, Zangerl R (1994) Development and growth of compound tooth plates in *Callorhinchus milii* (Chondrichthyes, Holocephali). Journal of Morphology 222: 73-89

- Francis MP (1997) Spatial and temporal variation in the growth rate of elephantfish (*Callorhinchus milii*). *New Zealand Journal of Marine and Freshwater Research* 31: 9-23
- Francis MP, Maolagáin CÓ (unpublished) Development of ageing techniques for dark ghost shark (*Hydrolagus novaezelandiae*). National Institute of Water and Atmospheric Research
- Freer DWL, Griffiths CL (1993) Estimation of age and growth in the St. Joseph *Callorhinchus capensis* (Dumeril). *South African Journal of Marine Science* 13: 75-81
- Goodrich ES (1909) A treatise on zoology. Adam and Charles Black, London
- Guillart-Furio J (1998) Contribution to the knowledge of the biology and taxonomy of the deepsea shark, *Centrophorus granulosus* (Bloch and Schneider, 1801) (Elasmobranchii, Squalidae) in the Balearic Sea (western Mediterranean). Ph.D. Thesis
- Halstead BW, Bunker NC (1952) The venom apparatus of the ratfish, *Hydrolagus colliei*. *Copeia* 3: 128-138
- Holden MJ, Meadows PS (1962) The structure of the spine of the spur dogfish (*Squalus acanthias* L.) and its use for age determination. *Journal of the Marine Biological Association of the U.K.* 42: 179-197
- Holden MJ, Vince MR (1973) Age validation studies on the centra of *Raja clavata* using tetracycline. *Journal du Conseil* 35: 13-17
- Irvine SB, Stevens JD, Laurenson LJB (2006a) Comparing external and internal dorsal-spine bands to interpret the age and growth of the giant lantern shark, *Etmopterus*

- baxteri* (Squaliformes: Etmopteridae). Environmental Biology of Fishes 77: 253-264
- Irvine SB, Stevens JD, Laurenson LJB (2006b) Surface bands on deepwater squalid dorsal-fin spines: an alternative method for ageing the golden dogfish *Centroselachus crepidater*. Canadian Journal of Fisheries and Aquatic Sciences 63: 617-627
- Johnson AG, Horton HF (1972) Length-weight relationship, food habits, parasites, and sex and age determination of the ratfish, *Hydrolagus colliei* (Lay and Bennett). Fishery Bulletin 70: 421-429
- Kaganovskaia S (1933) A method of determining the age and the composition of the catches of the spiny dogfish (*Squalus acanthias* L.). Bulletin Far-East Br Acad Sci USSR 1(3):5-6 (translated from Russian by W.E. Ricker). Fisheries Research Board of Canada, Translation Series 281(1):5-6
- Maisey JG (1979) Finspine morphogenesis in squalid and heterodontid sharks. Zoological Journal of the Linnean Society 66: 161-183
- McFarlane GA, Beamish RJ (1987) Validation of the dorsal spine method of age determination for spiny dogfish. The Iowa State University Press, Iowa
- McFarlane GA, King JR, Saunders MW (2002) Preliminary study on the use of neural arches in the age determination of bluntnose sixgill sharks (*Hexanchus griseus*). Fishery Bulletin 100: 861-864
- Moura T, Figueiredo I, Machado PB, Gordo LS (2004) Growth pattern and reproductive strategy of the holocephalan *Chimaera monstrosa* along the Portuguese

- continental slope. *Journal of the Marine Biological Association of the United Kingdom* 84: 801-804
- Natanson LJ, Cailliet GM (1990) Vertebral growth zone deposition in Pacific angel sharks. *Copeia* 1990: 1133-1145
- Natanson LJ, Sulikowski JA, Kneebone JR, Tsang PC (2007) Age and growth estimates for the smooth skate, *Malacoraja senta*, in the Gulf of Maine. *Environmental Biology of Fishes*
- Patterson C (1965) The phylogeny of the chimaeroids. *Philosophical Transactions of the Royal Society of London, Series B* 249: 101-219
- Ridewood WG (1921) On the calcification of the vertebral centra in sharks and rays. *Philosophical Transactions of the Royal Society of London, Series B* 210: 311-407
- Schaeffer B (1977) The dermal skeleton in fishes. In: Andrews SM, Miles RS, Walker AD (eds) *Problems in vertebrate evolution*. Academic Press, Inc., New York, NY, pp 25-52
- Simmons JE, Laurie JS (1972) A study of *Gyrocotyle* in the San Juan Archipelago, Puget Sound, U.S.A., with observations on the host, *Hydrolagus colliei* (Lay and Bennett). *International Journal for Parasitology* 2: 59-77
- Sullivan KJ (1977) Age and growth of the elephant fish *Callorhynchus milii* (Elasmobranchii: Callorhynchidae). *New Zealand Journal of Marine and Freshwater Research* 11: 743-755
- Tanaka S (1990) Age and growth studies on the calcified structures of newborn sharks in laboratory aquaria using tetracycline. In: Pratt Jr HL, Gruber SH, Taniuchi T (eds)

- Elasmobranchs as living resources: advances in the biology, ecology, systematics, and the status of the fisheries. NOAA Technical Report pp 189-202
- Tucker R (1985) Age validation studies on the spines of the spurdog (*Squalus acanthias*) using tetracycline. Journal of the Marine Biological Association of the U.K. 35: 641-651
- Ward DJ, Grande L (1991) Chimaeroid fish remains from Seymour Island, Antarctic Peninsula. Antarctic Science 3: 323-330

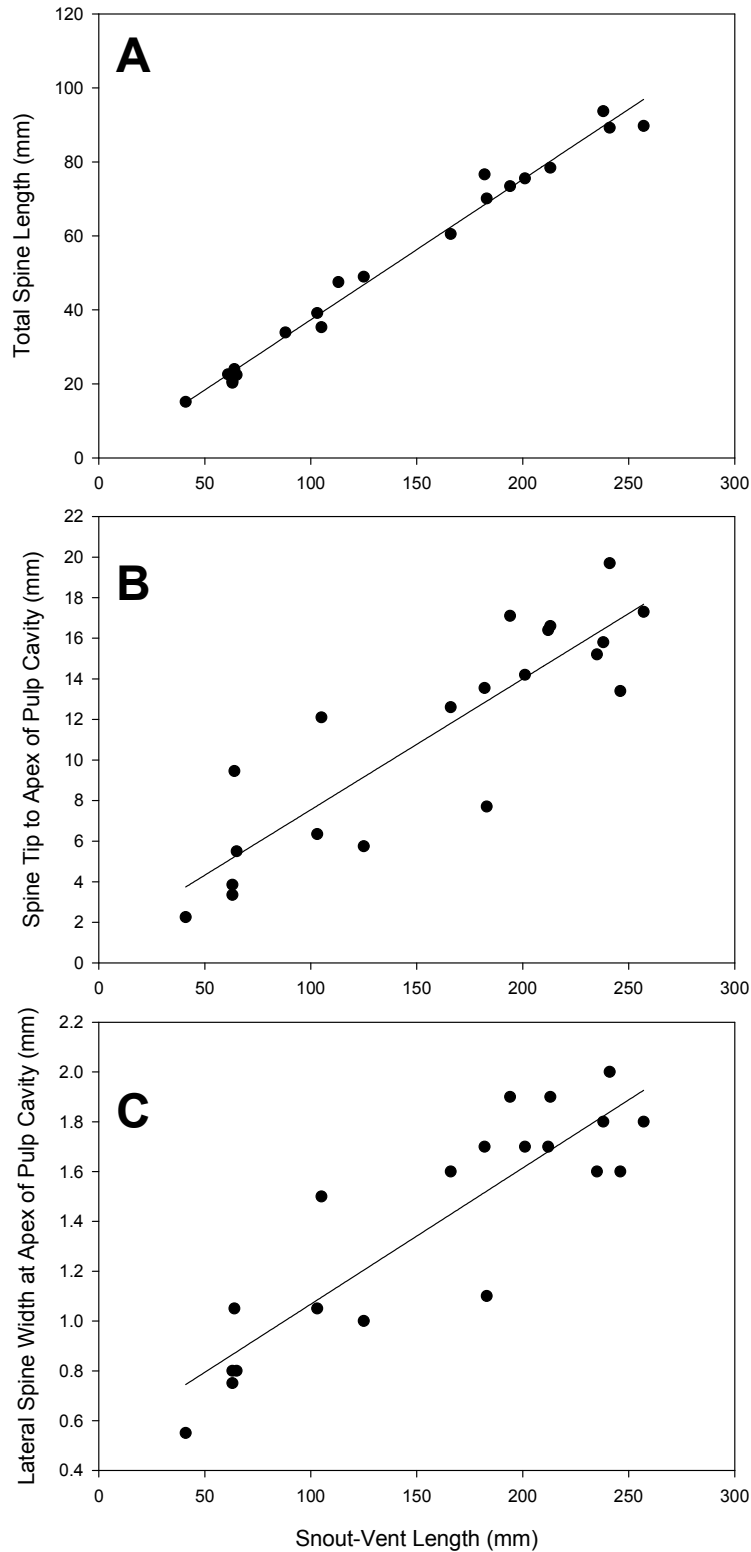


Figure 1. Comparison of snout-vent length to (A) total dorsal-fin spine length, (B) distance between the dorsal-fin spine tip and the apex of the pulp cavity, and (C) dorsal-fin spine width at the apex of the pulp cavity.

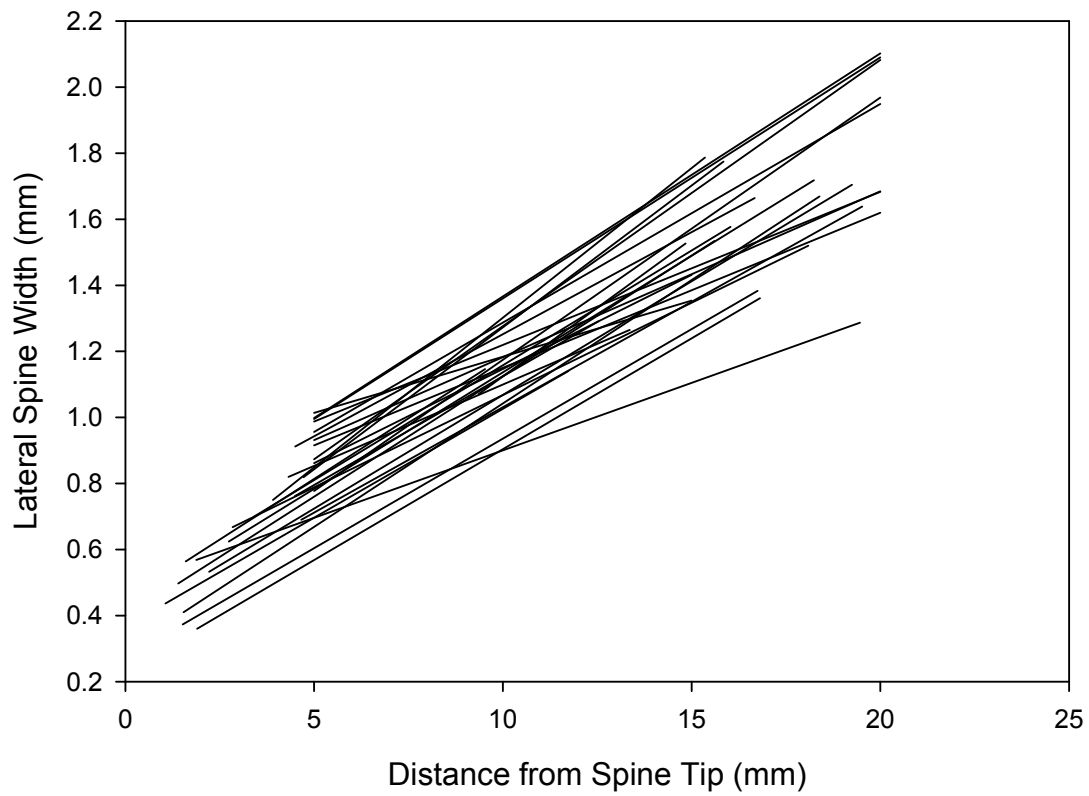


Figure 2. Comparison of distance from dorsal-fin spine tip and spine width among individuals ($n = 28$). Lines represent linear regressions for each individual.

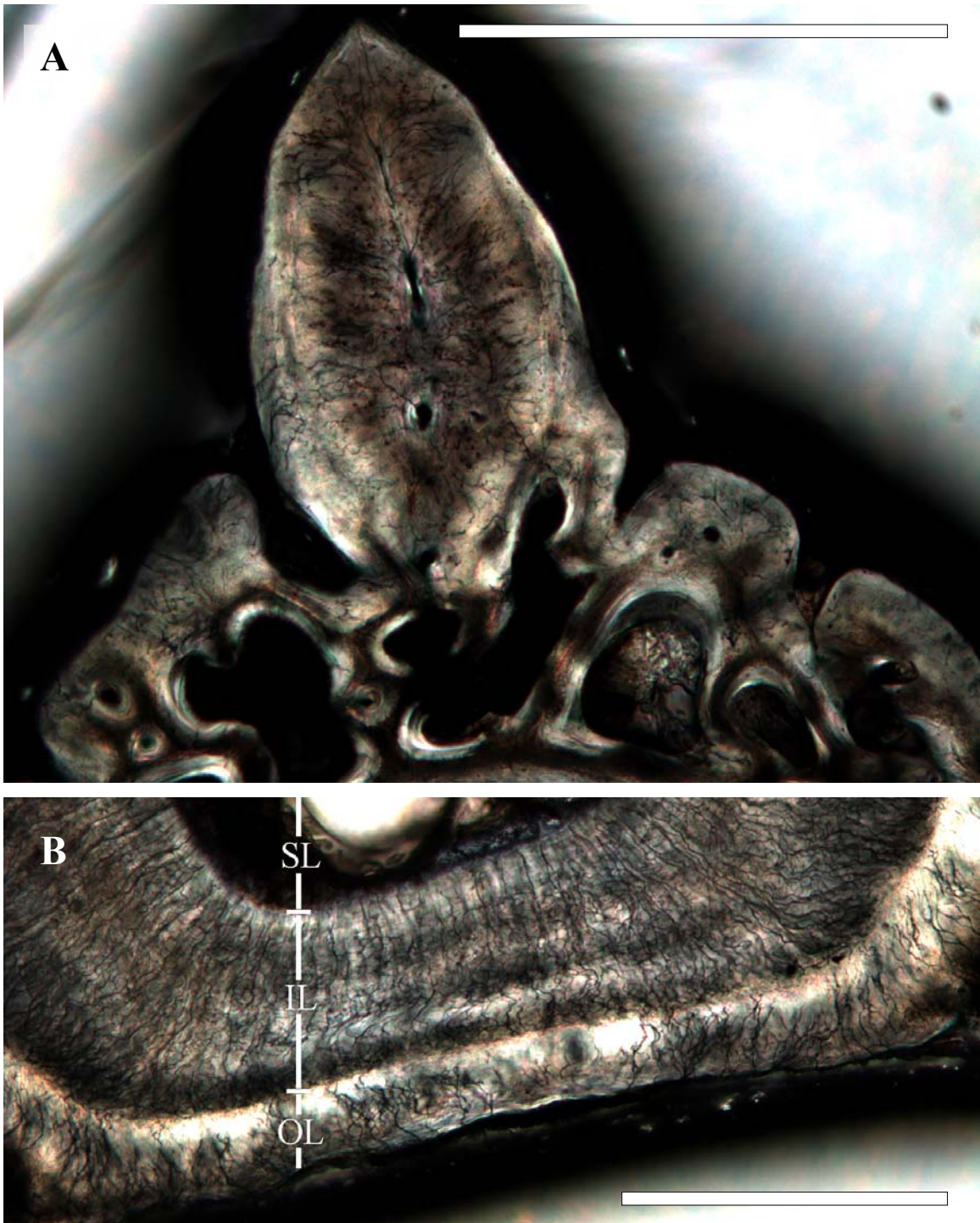


Figure 3. Photomicrograph of a transversely sectioned dorsal-fin spine (A) anterior dentine portion, and (B) posterior face, viewed with transmitted light. SL = spine lumen; IL = inner dentine layer; OL = outer dentine layer. Scale = 0.5 mm.

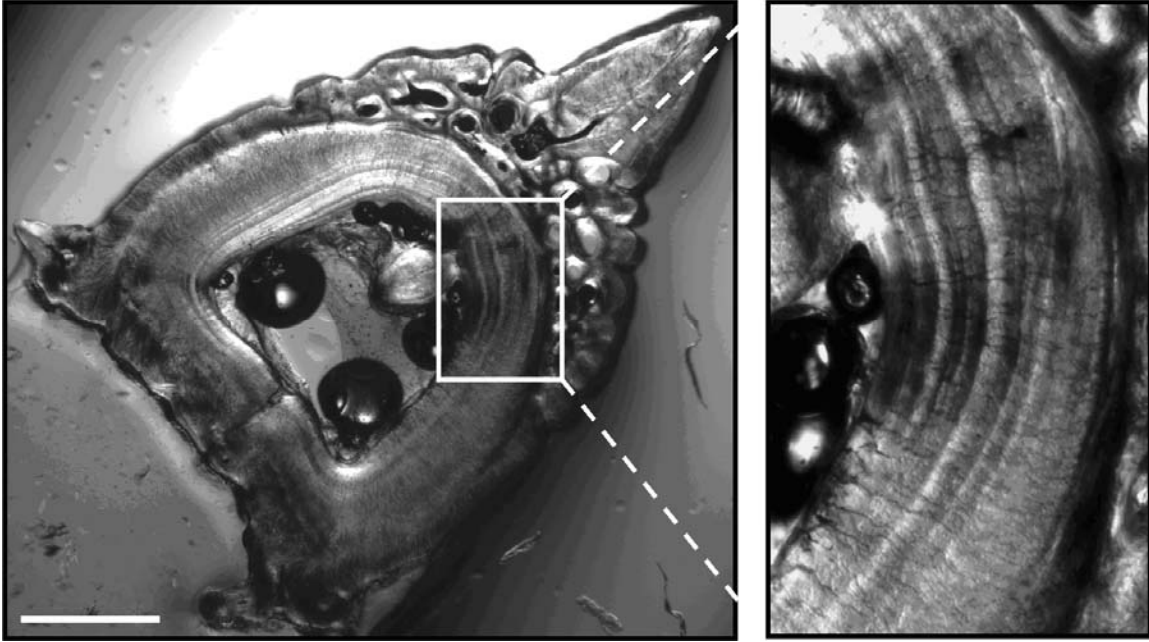


Figure 4. Photomicrograph of a transversely sectioned dorsal-fin spine viewed with polarized, transmitted light. Scale = 0.5 mm.

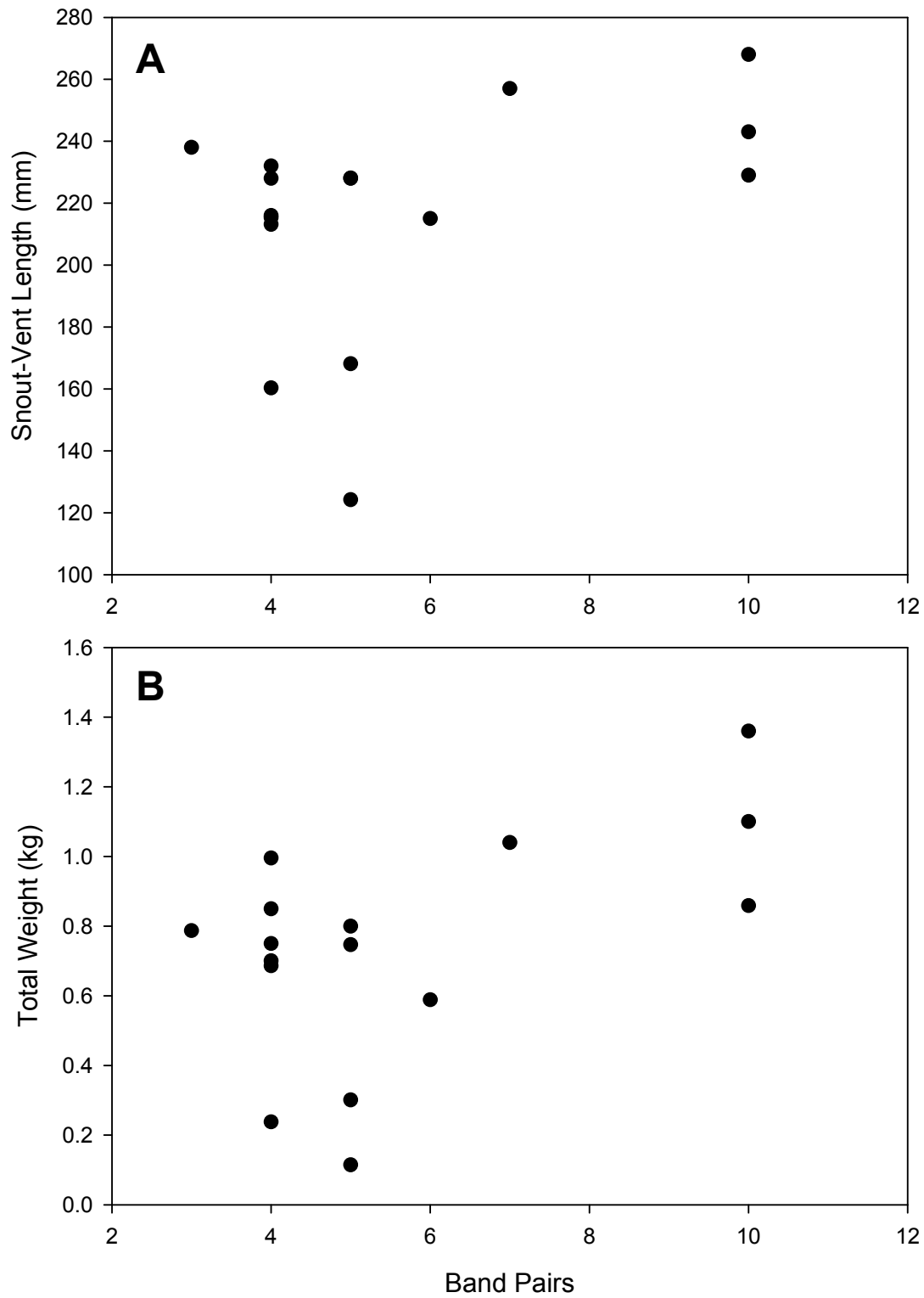


Figure 5. Comparison of the number of dorsal-fin spine band pairs to (A) snout-vent length, and (B) total mass for females ($n = 16$).

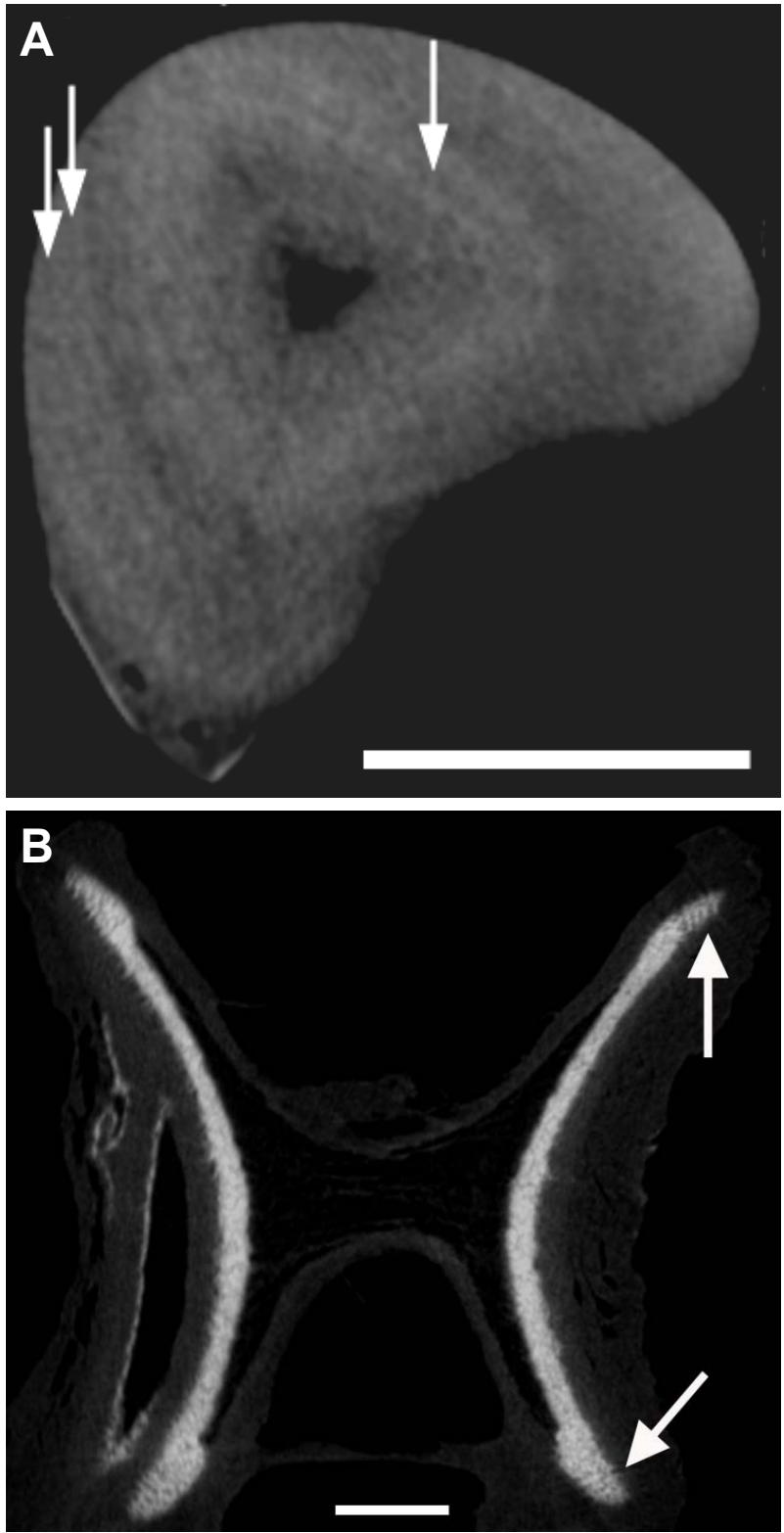


Figure 6. μ CT image of the (A) transverse plane of a second dorsal fin spine, and (B) the longitudinal plane of a vertebra from *S. acanthias*. Arrows indicate density gradients that may represent distinct growth zones. Scale = 0.5 mm.

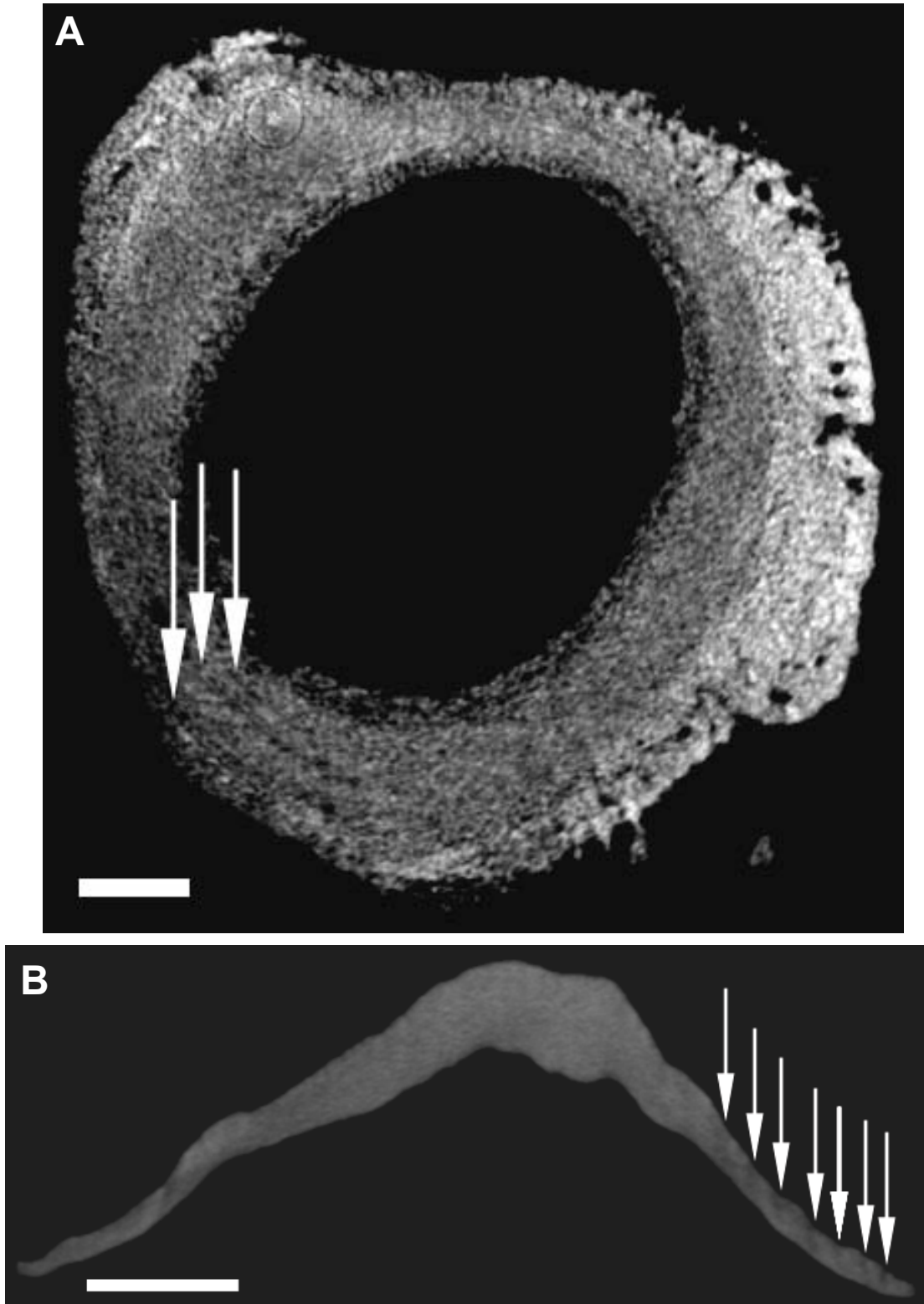


Figure 7. μ CT image of the (A) transverse plane of a vertebra, and (B) the longitudinal plane of a caudal thorn (just anterior to the thorn tip) from *B. trachura*. Arrows indicate density gradients that may represent distinct growth zones. Scale = 0.5 mm.

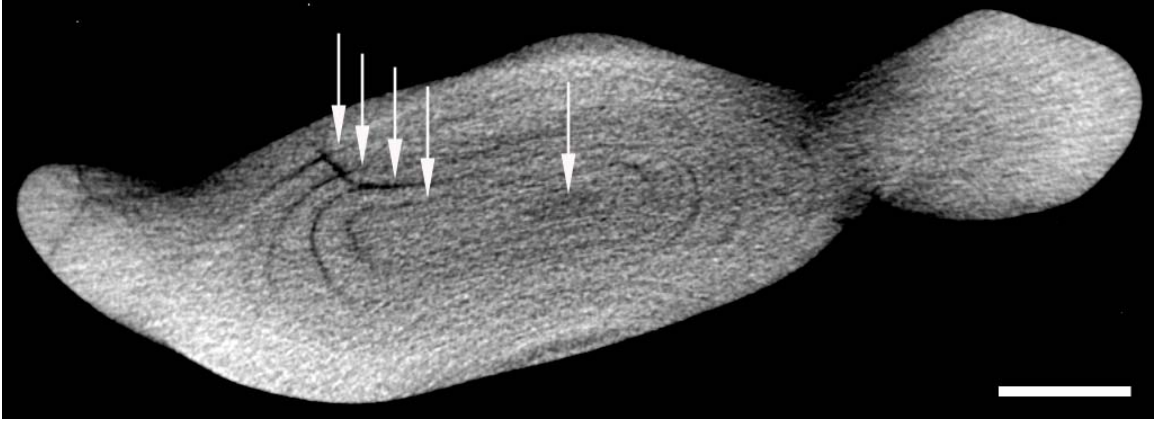


Figure 8. μ CT image of the transverse plane of a *D. eleginoides* otolith, just posterior to the focus. Arrows indicate density gradients that may represent distinct growth zones. Scale = 0.5 mm.

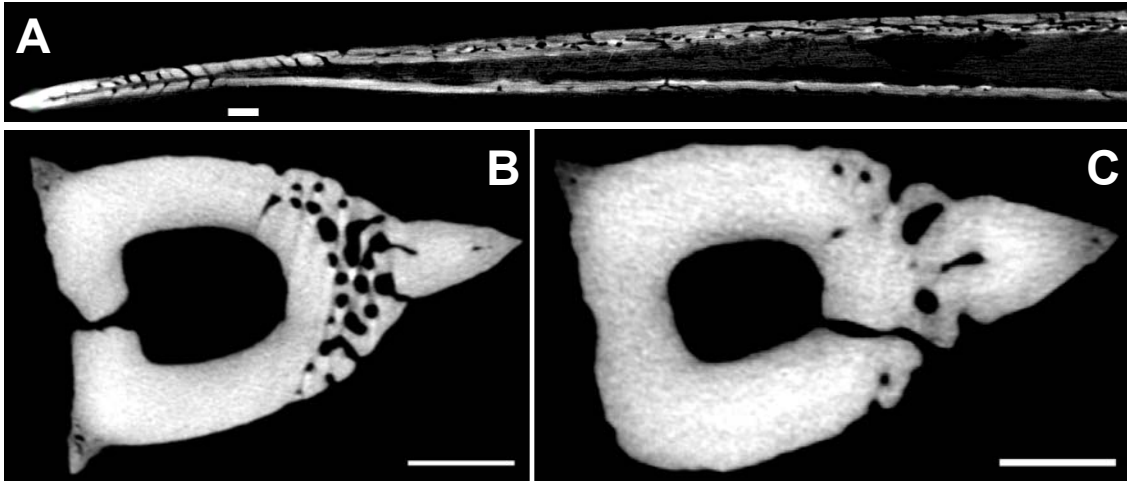


Figure 9. μ CT images of the *H. colliei* dorsal-fin spine, in the longitudinal (dorso-ventral) plane (A), and in the transverse plane, depicting dentine canals leading to the posterior (B) and anterior (C) spine exterior. Scale = 0.5 mm.

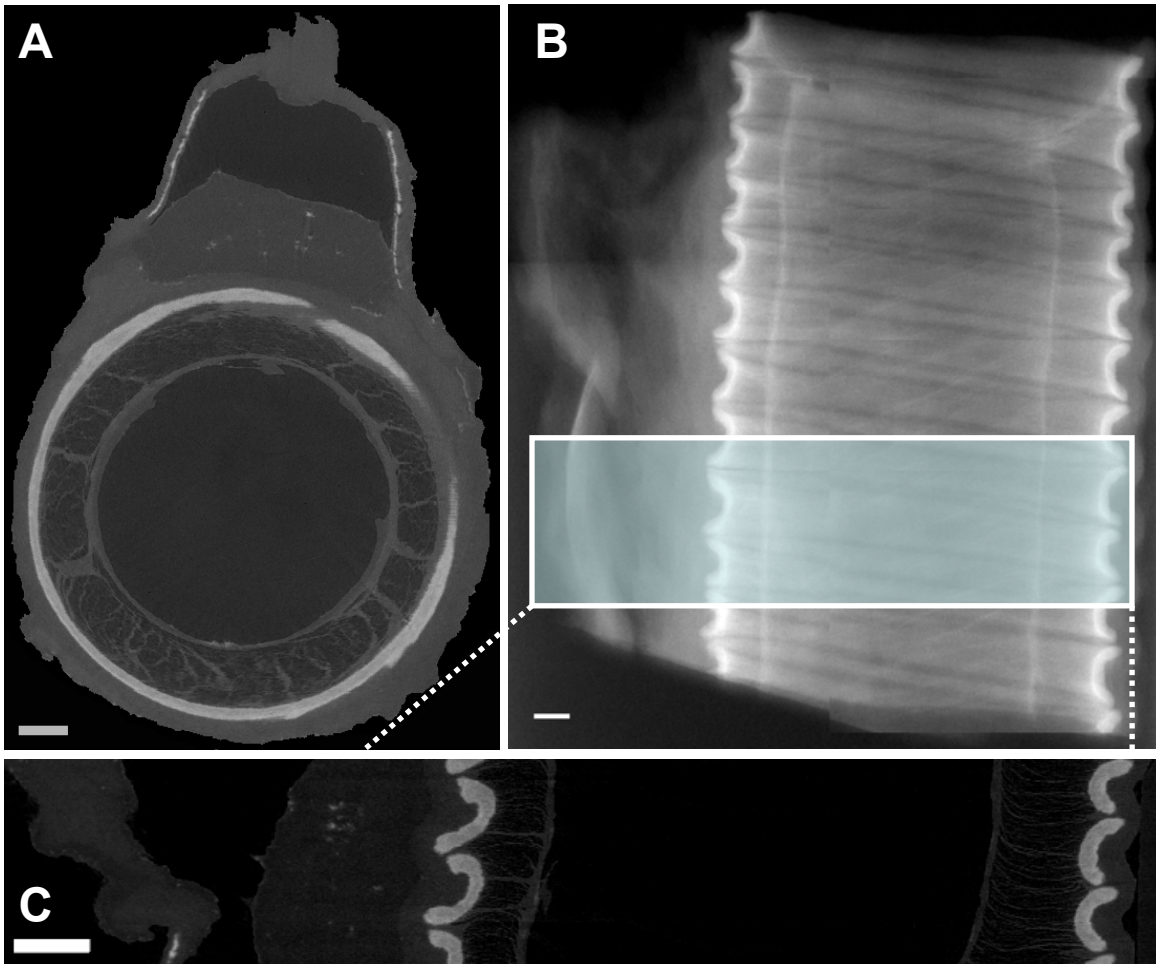


Figure 10. μ CT images of the *H. colliei* neural arch and vertebrae, from the transverse plane (A), and the longitudinal plane (B and C). Scale = 0.5 mm.